Managing Wind-based Electricity Generation and Storage

by

Yangfang Zhou

Submitted to the Tepper School of Business
in Partial Fulfilment of the Requirements for the Degree of

Doctor of Philosophy in
Management Of Manufacturing & Automation at
Carnegie Mellon University

Nov, 2012

Committee (in alphabetical order):

Professor Jay Apt
Professor Alan Scheller-Wolf (Co-chair)
Associate Professor Nicola Secomandi
Professor Stephen Smith (Co-chair)
Associate Professor Fallaw Sowell

To my dearest Grandma.

Acknowledgements

This thesis is not possible without the help of many great people.

I am deeply indebted to my co-advisor Alan for his wonderful guidance and support throughout my entire PhD life. He is always there for me whenever I need him, just as he is with any of his students. He has a magical knack for dismantling every big problem into small pieces and solving them one by one. Unintentionally, I have constantly challenged the limits of his patience, but I see none—not suggesting you should take this task.

Equally important, I will always be grateful for my co-advisor Steve, who gives me absolute freedom to do whatever I like, who helps me steer my research to the right direction, who has generously and honorably supported me for five years, and who always challenges me to achieve my full potential and stands by me when times are hard.

Also I would like to thank Nicola, a member of my committee, and a coauthor for every single essay that makes up this thesis. I learned enormously from him, from his academic rigor, from his down-to-earth approach, and from his great attention to details. In addition, I would like to thank Jay, who is extremely instrumental in guiding my research on energy. His insights have significantly improved this thesis. Also I would like to thank Fallaw, for agreeing to my almost-last-minute request to be on my committee, and for giving great suggestions.

I really appreciate many discussions with folks from the energy club at CMU, especially with Eric, Scott, Steve, Shira, Emily, Brandon, and Ryan. I also really appreciate the help of a great friend Liang for always being only a Skype away when I need to discuss research.

I am thankful for Lawrence, who made my PhD life in Tepper much more pleasant. I am also thankful to have met many friends at CMU: Michele, Elvin, Selva, Ying, Xin (both), Qihang, Ronghuo, Yingda, Emre, Ashiwini, Andrea, Andre, Negar, Xiao, Marsha, John, Maria, Benjamin, Amitabh, Jean, Laura, Zack, and Michael.

I would also like to particularly thank my parents and my brother for supporting me to pursue my dreams, and for tolerating my being half a planet away.

My special thanks goes to Arne, my best friend, and the sweetest guy that I have ever

known.

Lastly, anything I have now would be impossible without my dearest Grandma, a woman less than five feet tall with a permanent hump due to a childhood injury, a mother who shoulders the responsibility of a large family who in her seventies would still carry loads of fresh fruits and vegetables across mountains to sell in town just to make ends meet, a grandmother of not only my brother and me but also a grandmother to any kid in my village who needs help, and most importantly, my life instructor who never stepped into a classroom yet taught me many invaluable lessons that shaped who I am today. I am forever indebted to her for her boundless love.

Abstract

Among the many issues that profoundly affect the world economy every day, energy is one of the most prominent. Countries such as the U.S. strive to reduce reliance on the import of fossil fuels, and to meet increasing electricity demand without harming the environment.

Two of the most promising solutions for the energy issue are to rely on renewable energy, and to develop efficient electricity storage. Renewable energy—such as wind energy and solar energy—is free, abundant, and most importantly, does not exacerbate the global warming problem. However, most renewable energy is inherently intermittent and variable, and thus can benefit greatly from coupling with electricity storage, such as grid-level industrial batteries. Grid storage can also help match the supply and demand of an entire electricity market. In addition, electricity storage such as car batteries can help reduce dependence on oil, as it can enable the development of Plug-in Hybrid Electric Vehicles, and Battery Electric Vehicles. This thesis focuses on understanding how to manage renewable energy and electricity storage properly together, and electricity storage alone.

In Chapter 2, I study how to manage renewable energy, specifically wind energy. Managing wind energy is conceptually straightforward: generate and sell as much electricity as possible when prices are positive, and do nothing otherwise. However, this leads to curtailment when wind energy exceeds the transmission capacity, and possible revenue dilution when current prices are low but are expected to increase in the future. Electricity storage is being considered as a means to alleviate these problems, and also enables buying electricity from the market for later resale. But the presence of storage complicates the management of electricity generation from wind, and the value of storage for a wind-based generator is not entirely understood.

I demonstrate that for such a combined generation and storage system the optimal policy does not have any apparent structure, and that using overly simple policies can be considerably suboptimal. I thus develop and analyze a triple-threshold policy that I show to be near-

optimal. Using a financial engineering price model and calibrating it to data from the New York Independent System Operator, I show that storage can substantially increase the monetary value of a wind farm: If transmission capacity is tight, the majority of this value arises from reducing curtailment and time-shifting generation; if transmission capacity is abundant this value stems primarily from time-shifting generation and arbitrage. In addition, I find that while more storage capacity always increases the average energy sold to the market, it may actually decrease the average *wind* energy sold when transmission capacity is abundant.

In Chapter 3, I examine how electricity storage can be used to help match electricity supply and demand. Conventional wisdom suggests that when supply exceeds demand, any electricity surpluses should be stored for future resale. However, because electricity prices can be negative, another potential strategy of dealing with surpluses is to destroy them. Using real data, I find that for a merchant who trades electricity in a market, the strategy of destroying surpluses is potentially more valuable than the conventional strategy of storing surpluses.

In Chapter 4, I study how the operation and valuation of electricity storage facilities can be affected by their physical characteristics and operating dynamics. Examples are the degradation of energy capacity over time and the variation of round-trip efficiency at different charging/discharging rates. These dynamics are often ignored in the literature, thus it has not been established whether it is important to model these characteristics. Specifically, it remains an open question whether modeling these dynamics might materially change the prescribed operating policy and the resulting valuation of a storage facility. I answer this question using a representative setting, in which a battery is utilized to trade electricity in an energy arbitrage market.

Using engineering models, I capture energy capacity degradation and efficiency variation explicitly, evaluating three types of batteries: lead acid, lithium-ion, and Aqueous Hybrid Ion—a new commercial battery technology. I calibrate the model for each battery to manufacturers' data and value these batteries using the same calibrated financial engineering price model as in Chapter 2. My analysis shows that: (a) it is quite suboptimal to operate each battery as if it did not degrade, particularly for lead acid and lithium-ion; (b) reducing degradation and efficiency variation have a complimentary effect: the value of reducing both together is greater than the sum of the value of reducing one individually; and (c) decreasing degradation may have a bigger effect than decreasing efficiency variation.

Contents

List of Figures

List of Tables

Chapter 1

Introduction

Among the many issues that profoundly affect the world economy every day, energy is one of the most prominent. It is of strategic importance for countries such as the U.S. to reduce reliance on the import of fossil fuels; and it is of paramount importance that we meet our increasing electricity demand without harming the environment, or our own health and well-being.

Two of the most promising solutions for how we can safely meet our energy needs are to rely on renewable energy, and to develop efficient electricity storage.

(1) Renewable energy—such as wind energy and solar energy—is free yet abundant. For instance, wind energy alone, if harnessed at a 20% efficiency, can supply more than five times of all the world's energy needs (Lu et al. 2009). Renewable energy is environmentally friendly; it does not emit carbon dioxide. More than twenty-nine states in the U.S. have already established Renewable Portfolio Standards (DSIRE 2012b), which require a certain percentage of electricity to come from renewable energy: For instance, New York state requires that 15% of electricity consumption should come from renewable resources by 2015 (DSIRE 2012a). However, renewable energy is inherently intermittent and variable—as wind does not always blow and the sun does not always shine. To mitigate these issues, renewable energy can be coupled with electricity storage, such as grid-level industrial batteries.

(2) Other than supporting the growth of renewable energy, grid-level electricity storage can also help match the supply and demand of an entire electricity market. This is crucial, as electricity supply and demand must be matched in real time to ensure the integrity of the power grid. In addition, electricity storage such as car batteries can help reduce dependence

on oil, as it can facilitate the development of Plug-in Hybrid Electric Vehicles (PHEVs), and Battery Electric Vehicles (BEVs): In 2011, the transportation sector accounted for about 25% of the total carbon emission in the U.S. (EIA 2012). California is in the process of enacting laws to mandate a minimum amount of electricity storage for 2015 and 2020 (CPUC 2012).

For all of these reasons, renewable energy and electricity storage are two pillars that are likely to shape the world's energy future. This thesis focuses on understanding how to manage them properly, together, or electricity storage alone.

In Chapter 2, I will focus on studying the problem of managing renewable energy, specifically wind energy. Wind energy is booming worldwide: in the past decade, U.S. wind generation capacity has grown more than tenfold (Wiser and Bolinger 2010); similar growth has been seen in other countries as well.

Managing power generation from wind is conceptually straightforward: generate and sell as much electricity as possible when prices are positive, and do nothing otherwise. However, this strategy may dilute a wind farm's potential revenue because (i) it requires curtailing wind energy when it exceeds the capacity of the transmission line that connects the wind farm to the electricity market; (ii) this strategy also requires curtailment when prices are negative: negative prices are observed in almost every electricity market, often caused by the high cost of shutting down conventional power plants when electricity supply exceeds demand; and (iii) this strategy sells electricity when prices are positive but unfavorable, especially because wind in the U.S. tends to blow most strongly at night when electricity prices are typically low. Electricity storage is being considered as a means to alleviate curtailment and boost revenue, as it also enables buying electricity from the market for later resale. But the presence of storage complicates the management of electricity generation from wind, and the value of storage for a wind-based generator is not entirely understood.

I model the problem of managing a combined wind and storage system with transmission capacity as a Markov Decision Process (MDP). I demonstrate that for such a system the optimal generation and storage policy does not have any apparent structure, and that using overly simple policies can be considerably suboptimal. I thus develop and analyze a triple-threshold policy that I show to be near-optimal and practical to compute on realistic instances. This triple-threshold policy generalizes existing policy structures in the literature (Nascimento and Powell 2010, Secomandi 2010b).

Using a financial engineering price model and calibrating it to data from the New York Independent System Operator (NYISO), I show that storage can substantially increase the monetary value of an wind farm: If transmission capacity is tight, the majority of this value arises from reducing curtailment and time-shifting generation; if transmission capacity is abundant this value stems primarily from time-shifting generation and arbitrage. In addition, I find that while more storage capacity always increases the average energy sold to the market, it may actually decrease the average *wind* energy sold when the transmission capacity is abundant.

In Chapter 3 I examine how electricity storage can be used to help match electricity supply and demand. Conventional wisdom suggests that when supply exceeds demand, any electricity surpluses should be stored for future resale. However, because electricity prices can be negative, another potential strategy of dealing with electricity surpluses is to destroy them. I compare these two strategies of dealing with surpluses from the perspective of a merchant who trades electricity in a market. I do so by modeling the problem of managing an electricity storage facility at different round-trip efficiencies (the ratio of electricity discharged to that charged): a high round-trip efficiency represents the storage strategy; a low round-trip efficiency represents the destruction strategy (as the majority of the electricity is lost during the conversion process).

I find that the optimal policy to operate storage with prices that can potentially be negative has an elegant policy structure, which subsumes a classical result in Charnes et al. (1966). Using this structure in conjunction with the same price model as in Chapter 2, I find that the strategy of destroying surpluses is potentially more valuable than the conventional strategy of storing surpluses.

In Chapter 4 I study how the operation and valuation of electricity storage facilities can be affected by their physical characteristics and operating dynamics. Examples of such characteristics are the degradation of energy capacity over time, and the variation of round-trip efficiency at different charging/discharging rates. Such dynamics are often ignored in the literature (Graves et al. 1999, Sioshansi et al. 2009, Walawalkar et al. 2007); thus it has not been established whether it is important to model these dynamics in operating and valuing a storage facility. Specifically, in Chapter 4 I answer the following two questions: (Q1) How suboptimal is it to operate an actual battery as if it were ideal? (Q2) How much do practitioners overestimate the value of a battery if they use the value of operating an ideal battery optimally?

I answer these questions using a representative setting, in which a battery is utilized to trade electricity in an energy arbitrage market. I model the problem of managing a battery as an MDP. Using engineering models, I capture the dynamics of energy capacity degradation and efficiency variation explicitly for three types of batteries: lead acid, lithium-ion, and Aqueous Hybrid Ion—a new commercial battery technology. I calibrate the model for each battery to manufacturers' data and determine the value of each battery under an optimal policy using the same calibrated financial engineering price model as in Chapter 2 and 3. My analysis over a twenty-year horizon shows that: (a) it is quite suboptimal to operate each battery as if it did not degrade, particularly for lead acid and lithium-ion; but it does not matter much if one ignores efficiency variation; (b) reducing degradation and efficiency variation have a complimentary effect: the value of reducing both together is greater than the sum of the value of reducing each one individually; and (c) decreasing degradation may have a bigger effect than decreasing efficiency variation.

This thesis revolves around managing two promising solutions for meeting the world's energy needs in a sustainable way. In Chapter 2 I study how to manage wind power with electricity storage. My results give guidance to managers operating wind farms, and can serve as a basis for sizing a generation and storage system. In Chapter 3 I study different strategies of using electricity storage to help match electricity supply and demand. My results can inform policy makers about the need to assess the potential impact of different strategies of dealing with surpluses. In Chapter 4 I study how the operations and valuation of electricity storage could be affected by storage dynamics. The results not only demonstrate the importance of modeling dynamics, but also pinpoint the most promising area of focus to improve each battery. My modeling of battery dynamics can also be used to study the operation of electric car fleets and battery swapping stations. I conclude with future work in Chapter 5.

Chapter 2

Managing wind-based electricity generation in the presence of storage and transmission capacity

2.1 Introduction

The last decade has seen a boom in global wind-based electricity generation: since 2000, U.S. wind generation capacity has grown more than tenfold (Wiser and Bolinger 2010); similar growth has been seen in other countries as well. This global trend will probably continue for at least another decade or two, as many countries have enacted policies to promote wind energy (REN21 2010).

Managing wind energy generation is conceptually straightforward: generate and sell as much as possible when the price is positive (electricity prices can be negative), and do nothing otherwise. However, this policy may dilute a wind farm's revenue because of the following:

(i) This strategy requires curtailing wind energy when it exceeds the capacity of the transmission lines connecting wind farms (mostly remote) to electricity markets. Curtailment is a significant issue: in 2009, 17% of the wind power in the Electric Reliability Council of Texas

This chapter is a joint work with Alan Scheller-Wolf, Nicola Secomandi, and Stephen Smith; it is under the second round revision for the *MSOM Special Issue on the Environment.*

(ERCOT) was curtailed due to lack of transmission capacity (Wiser and Bolinger 2010). This bottleneck in transmission capacity is unlikely to disappear in the near future, as it takes much longer (about five years) to build transmission lines than to build wind farms (about one year; SECO 2011).

(ii) This strategy also leads to curtailment when electricity prices are negative. Negative prices have been observed in the New York Independent System Operator (NYISO 2011), ERCOT (ERCOT 2008), the Nordic Power Exchange (Sewalt and de Jong 2007), and the European Energy Exchange (Fanone and Prokopczuk 2010, Genoese et al. 2010). Negative prices may be caused by the high cost of ramping up and down conventional power plants: when electricity demand is low, these plant operators may try to avoid a costly shut-down by paying others to consume their excess power (Brandstätt et al. 2011, Genoese et al. 2010, Knittel and Roberts 2005, Nicolosi 2010, Sewalt and de Jong 2007).

(iii) This strategy may sell wind energy when prices are positive, but unfavorable. For instance, wind in the U.S. tends to blow most strongly at night, when electricity prices are typically low.

These problems can be alleviated by co-locating wind farms with electricity storage facilities, for instance, grid-level electricity batteries. Storage also enables buying electricity for future resale. However, the presence of storage complicates the management of a wind farm: the operator needs to decide periodically how much to generate, and how much to buy from the market, or to sell to the market from generation and/or inventory. In addition, the value of storage for a wind generator is not yet completely understood.

We investigate this problem of operating a wind-based electricity generation, storage, and transmission (WST) system. We model our problem as a finite-horizon MDP. We show that computing an optimal policy for this MDP does not have any apparent structure, while overly simple policies may be considerably suboptimal. We thus develop several heuristic policies that are easier to compute than an optimal policy. Our most effective policy has a triple-threshold structure, which can be exploited in computation: this policy requires two fewer dimensions of computation than an optimal policy, and thus is an order or magnitude faster to compute. Moreover, this heuristic is within 2% of optimality for a comprehensive range of system configurations in experiments using electricity price and wind energy models calibrated to data from NYISO.

Our experiments also quantify the monetary and energy values of storage when using our

triple-threshold policy (the energy value of storage captures how storage can change the energy flow rate in a WST system). We find that storage can substantially increase the monetary value of a WST system: For a typical scenario with tight transmission capacity, storage increases the monetary value of the system by 33.5%, of which 17% is due to reducing curtailment, 12% to time-shifting generation, and 4.5% to arbitrage. When the transmission capacity is less constraining, storage increases the monetary value of the system by 21%, of which 1.5% is due to reducing curtailment, 15% is due to time-shifting, and 4.5% to arbitrage.

Storage can thus greatly decrease the average wind energy curtailed (by 87% compared to the no-storage case) and increase the average energy that the system sells to the market (by 26% compared to the no-storage case) when transmission capacity is tight. However, with ample transmission capacity, adding storage may actually decrease the average *wind* energy sold, primarily because the benefit of reducing curtailment decreases, and is surpassed by the conversion loss at the storage facility.

Our results provide guidelines for practitioners to operate WST systems near optimally, and also can help them evaluate the merits of storage for wind farms. In addition, our work provides a basis for the sizing of storage facilities and transmission lines.

The rest of this chapter is organized as follows: we review the literature in §2.2. We present our MDP model in §2.3 and explore heuristics in §2.4. We discuss our framework for the valuation of storage in §2.5. We specify the price model and the wind energy model used in our numerical study in §2.6 and §2.7, respectively. We carry our numerical analysis in §2.8. We conclude and discuss future work in §2.9.

2.2 Literature Review

In the literature on wind-storage systems, Denholm and Sioshansi (2009) and Fertig and Apt (2011) consider the interplay of storage and transmission capacity: the former studies how to best locate storage when transmission capacity is binding; the latter studies the optimal sizing of storage and transmission capacity. In contrast, we develop policies to manage an existing WST system. Moreover, these papers evaluate the value of storage assuming price and wind energy are deterministic processes, while our paper captures the uncertainty of both, which is more realistic; we show that ignoring uncertainty may result in a significant loss of value.

Other related studies examine different uses of storage for wind farms. Brown et al. (2008)

focus on how to serve the load of an isolated system using wind generators and pump-hydro storage to minimize daily operating cost. Castronuovo and Lopes (2004) maximize the daily profit of a wind-hydro system in a market. Korpaas et al. (2003) consider a wind-storage system that serves load as well as trades in an electricity market. In contrast to this literature, we include transmission capacity and explore how it affects the value of storage.

Wu and Kapuscinski (2012) investigate how to curtail wind energy to minimize the total balancing cost of an electricity market (possibly in the presence of storage) from the point of view of an electricity market operator. In contrast, we study how to operate a single wind farm co-located with storage from the perspective of a wind farm manager. Xi et al. (2011) optimize the use of an electricity storage facility in both the electricity energy and ancillary markets; we consider the use of storage for a wind farm constrained by transmission capacity, investigating different operating policies, and assessing both the monetary and energy values of storage for such a system.

Another stream of work centers on how a wind-farm manager can use storage to make better bidding decisions in a forward market. Some papers assume price is deterministic, such as Bathurst and Strbac (2003) and Costa et al. (2008); others take price uncertainty into account, such as Gonzalez et al. (2008), Löhndorf and Minner (2010), and Kim and Powell (2011). Different from these papers, we do not consider bidding and assume any electricity offered to the market is accepted. This is realistic: many electricity markets in the U.S. treat wind generators as "must-run" in normal conditions (Wiser and Bolinger 2010); in addition, 38% of all the wind capacity developed in the U.S. in 2009 was sold through merchant/quasi-merchant projects "whose electricity sales revenue is tied to short-term contracted and/or wholesale spot electricity market prices" (Wiser and Bolinger 2010, p. 43). Furthermore, this literature ignores transmission capacity, an integral factor in the operation of remote wind farms, which we model.

As electricity can be viewed as a special type of inventory, our work is also related to the literature in inventory theory (see Zipkin 2000 and Porteus 2002). In this literature demand is the typical source of uncertainty, but supply can also exhibit randomness. In contrast, price and wind (supply) are the sources of uncertainty in our model.

This chapter is particularly related to the literature on commodity and energy storage. Cahn (1948) introduces the classic warehouse problem, for which Charnes et al. (1966) show

the optimality of a simple basestock policy. Rempala (1994) and Secomandi (2010b) extend this work to incorporate a limit on the rate at which the commodity can be injected into or withdrawn from storage. Other related work includes Boogert and de Jong (2008), Chen and Forsyth (2007), Lai et al. (2010a), Mokrian and Stephen (2006), Thompson et al. (2009), Wu et al. (2012), and Devalkar et al. (2011) (these authors also model the processing decision of a commodity processor; see Boyabatli et al., 2011 and Boyabatli, 2011 for related work). Different from these systems, our model has a random inflow, the wind energy.

Related settings with random inflow include hydropower generation (Nasakkala and Keppo 2008) and liquified natural gas (LNG) regasification (Lai et al. 2010b). These systems differ from ours in that they store their input (water or LNG), while our system stores the output (electricity). Thus, the operating policies of hydropower or LNG regasification systems in these papers feature only one sell-down threshold, which depends on model parameters, while our triple-threshold policy has additional store-up-to thresholds, which also depend on model parameters.

2.3 Model

We consider the problem of operating a WST system: a remote wind farm is co-located with a storage facility, both of which are connected to a wholesale market via a transmission line (Figure 2.1). The operator of this system can buy and sell electricity in this market (the transmission line is bi-directional). We assume that the WST system is small compared to the market, so the operator's decisions do not affect market prices. The operator makes trading decisions periodically over a finite horizon, specifically in time periods $t \in \mathscr{T} := \{1, \cdots, T\}$, where each period t is defined as the time interval $(t-1, t]$ (Figure 2.2). In terminal period $T+1$, any electricity left in the storage facility is worthless. It is easy to show that this assumption could be relaxed without changing the results.

Parameters. We assume the storage facility is finite in *energy* capacity and *power* capacity; without loss of generality, we normalize the energy capacity to one (energy unit). If we think of the storage facility as a warehouse for electricity, the *energy* capacity is analogous to the space of the warehouse; the *power* capacity is analogous to the maximum rate of adjusting the warehouse inventory. For the rest of this chapter and the whole thesis, any capacity should

Figure 2.1 System overview

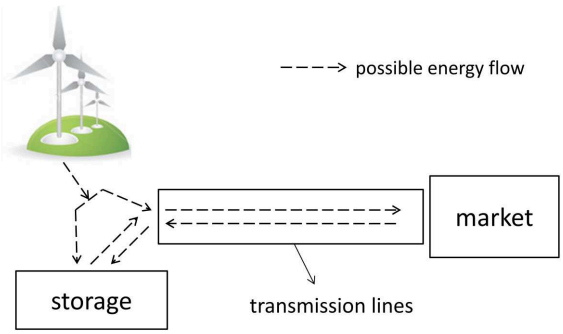

Figure 2.2 Order of events time line

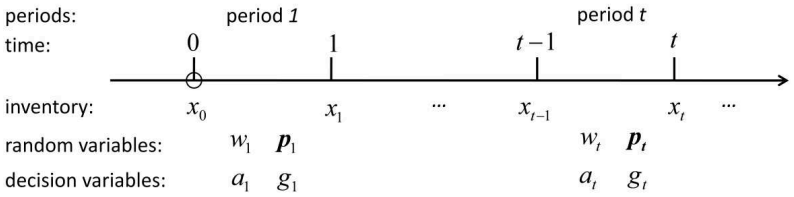

be interpreted as *power* capacity, unless specified otherwise. We use the following parameters:

- K_1, K_2: charging and discharging capacity (in energy units/period), respectively. $K_1 < 0 < K_2$.
- G, C: the generation and transmission capacity (in energy units/period), respectively. We assume that $G + K_2 \geq C$. This is realistic: since wind blows intermittently, it is reasonable to size the transmission capacity to be less than the sum of the wind farm's generation capacity and the storage discharging capacity so that the transmission line is better utilized (if $G+K_2 < C$, the transmission capacity is never constraining).
- α, β, η: efficiency of the storage facility in charging, discharging, and storing over one period, respectively; all three parameters are in (0, 1]. The round-trip efficiency is defined $\alpha \cdot \beta \cdot \eta$.
- τ: transmission efficiency, the ratio of the quantity of electricity flowing out of the transmission line to that flowing into this line, i.e., $1 - \tau$ is the ratio of loss in the line. We apply τ at the end of transmission in either direction.
- δ: risk-free discount rate (we use a risk-neutral valuation; Seppi, 2002), $0 < \delta < 1$.

State variables. A state variable with subscript t is known at time t, but unknown at earlier times, that is $0, 1, \cdots, t-1$ (Powell 2007, §5.2). At time $t-1$, the state S_{t-1} includes the following information:

- x_{t-1}: inventory of electricity (in energy units) in the storage facility at time $t-1$. The domain of this variable is $\mathscr{X} := [0, 1 \cdot \eta]$. The maximum inventory level is η because we assume that the storage loss happens at the end of each period.
- w_{t-1}: the maximum amount of available energy (in energy units) that the wind farm could produce in period $t-1$. $w_{t-1} = \min\{G, \text{the available wind energy in period } t-1\}$, where G is implicitly multiplied by one period.
- $\mathbf{p}_{t-1}$: price vector of electricity in period $t-1$ (\$/energy unit); each component of this vector is a factor in the price model in §2.6. We denote the sum of all the components in vector $\mathbf{p}_{t-1}$ by p_{t-1}, a scalar.

We thus define S_{t-1} as $(x_{t-1}, w_{t-1}, \mathbf{p}_{t-1})$. In particular, S_0 is the *given* initial state $(x_0, w_0, \mathbf{p}_0)$, where w_0 and $\mathbf{p}_0$ are the given wind and price in the initial stage, respectively.

Random variables. At time $t-1$, the random variables are

- w_t: the electricity that the wind farm can produce in period t; $w_t \in \mathscr{W} \subseteq \mathbb{R}^+$.
- $\mathbf{p}_t$: the price of electricity in period t; $\mathbf{p}_t \in \mathscr{P} \subseteq \mathbb{R}^n$, where n is the number of components in $\mathbf{p}_t$. Similarly, we denote p_t as the sum of all the components in $\mathbf{p}_t$.

These random variables are exogenous and may be correlated.

Sequence of events. We assume for each period $t \in \mathscr{T}$, the sequence of events is as follows (see also Figure 2.2):

1) The operator determines the joint inventory and generation action pair (a_t, g_t) contingent on the realization of the wind energy w_t for this period, where

- g_t: the quantity of electricity to generate in period t; $g_t \in \mathbb{R}^+$.
- a_t: the net inventory change in period t; $a_t \in \mathbb{R}$. If $a_t < 0$, a_t is the decrease in inventory due to selling; if $a_t \geq 0$, a_t is the increase in inventory due to generation and/or buying. It is easily shown that the option of simultaneously increasing and decreasing inventory is suboptimal.

2) Electricity flows through the system, incurring the loss in discharging (selling) or charging (generation and/or buying), as well as the loss in transmission.

3) The market price $\mathbf{p}_t$ is revealed, and the associated financial settlement is completed.

4) At the end of period t, a fraction $1-\eta$ of any resulting inventory is lost.

In practice, although the operator of a WST system makes trading decisions periodically (for instance, every hour in the real-time market in NYISO), the operator can change the wind generation by adjusting the angle of the wind turbine blades almost in real time, say every few seconds, based on current wind energy information. Our sequence of events is an approximation of this combined periodic trading and real-time adjustment. Specifically, we approximate the real-time adjustment by assuming that the operator *adapts* his decisions to the realized wind energy of the current period, so his decision pair $(a_t,\ g_t)$ is implemented *during* period t, rather than at the beginning of this period. But he does not observe $\mathbf{p}_t$ until period t is over.

Transition functions. The inventory level at time $t \geq 1$ is $x_t = \eta(x_{t-1} + a_t)$. The quantities w_{t-1} and $\mathbf{p}_{t-1}$ evolve to w_t and $\mathbf{p}_t$ according to two exogenous stochastic processes (we specify them in §2.6 and §2.7). We assume that the operator's decisions do not affect market price.

Immediate payoff function and constraints. Let $R(a_t, g_t, p_t)$ denote the immediate payoff function in period t of the triple (a_t, g_t, p_t), modeling either the purchasing cost or the selling revenue. The quantity sold or bought obeys different constraints in the following three cases:

- If $a_t < 0$, then the inventory decreases, which means that the total quantity sold is $(g_t - a_t\beta) \cdot \tau$. This quantity, before the transmission loss, cannot exceed the transmission capacity, so we have constraint C1: $g_t - a_t\beta \leq C$, where C is implicitly multiplied by one period.
- If $0 \leq a_t/\alpha \leq g_t$, the wind farm generates more electricity than it stores in the facility, which means that the operator sells the excess electricity to the market: $(g_t - a_t/\alpha) \cdot \tau$, which before the transmission loss cannot surpass the transmission capacity. This yields constraint C2: $g_t - a_t/\alpha \leq C$.
- If $a_t/\alpha > g_t$, more electricity is stored than is generated, which means that the operator buys the quantity $(a_t/\alpha - g_t)/\tau$ from the market. This quantity likewise cannot exceed the transmission capacity, yielding constraint C3: $(a_t/\alpha - g_t)/\tau \leq C$.

Thus, $R(a_t, g_t, p_t)$ is defined as follows:

$$R(a_t, g_t, p_t) := \begin{cases} p_t \cdot (g_t - a_t\beta) \cdot \tau, & \text{if } a_t < 0, \\ p_t \cdot (g_t - a_t/\alpha) \cdot \tau, & \text{if } 0 \le a_t \le g_t \cdot \alpha, \\ -p_t \cdot (a_t/\alpha - g_t)/\tau, & \text{if } a_t > g_t \cdot \alpha, \end{cases} \tag{2.1}$$

where the first two cases represent the selling revenue and the third case the purchasing cost. The feasible set of action pairs (a_t, g_t), denoted by $\Psi(x_{t-1}, w_t)$, is defined by the following constraints:

$$\begin{aligned} &\text{C1} : g_t - a_t\beta \le C, \text{ if } a_t < 0, \\ &\text{C2} : g_t - a_t/\alpha \le C, \text{ if } 0 \le a_t \le g_t \cdot \alpha, \\ &\text{C3} : (a_t/\alpha - g_t)/\tau \le C, \text{ if } a_t > g_t \cdot \alpha, \\ &\text{C4} : g_t \le w_t, \\ &\text{C5} : -x_{t-1} \le a_t \le 1 - x_{t-1}, \\ &\text{C6} : K_1 \le a_t \le K_2; \end{aligned}$$

C4 constrains the generation by the wind energy availability (note that this constraint implies that $g_t \le G$, as $w_t \le G$); C5 limits the inventory change by the energy available in the storage facility (left) and remaining storage *energy* capacity (right); and C6 incorporates the charging and discharging capacities (K_1 and K_2 are implicitly multiplied by one period).

Objective function. We formulate our problem as an MDP. Each stage of our MDP corresponds to one time period. A policy π is a mapping from any state S_t in any stage t to a feasible action pair (a_t, g_t). Let $A_t^\pi(S_t)$ denote the decision rule of policy π in period t, and let Π denote the set of all feasible policies. Our objective is to maximize the total discounted expected cash flows over all feasible policies:

$$\max_{\pi \in \Pi} \sum_{t=1}^{T} \delta^{t-1} \mathbb{E}\left[R(A_t^\pi(S_t), p_t) | S_0\right], \tag{2.2}$$

where the expectation $\mathbb{E}$ is taken with respect to risk-adjusted distributions of wind and price; recall that we use risk-neutral valuation (Seppi 2002).

For each time $t-1$ where $0 \leq t-1 \leq T$, we define $V^*_{t-1}(S_{t-1})$ as the optimal value function from time $t-1$ onward. In addition, set $V^*_T(S_T) := 0$, $\forall S_T$. For any time $t-1$ where $0 \leq t-1 < T$, $V^*_{t-1}(S_{t-1})$ satisfies

$$\begin{aligned} & V^*_{t-1}(S_{t-1}) \\ & = \mathbb{E}\left[\max_{(a_t,g_t)\in\Psi(x_{t-1},w_t)} \mathbb{E}\left[R(a_t,g_t,p_t) + \delta V^*_t(S_t)|w_t,\mathbf{p}_{t-1}\right] \middle| w_{t-1},\mathbf{p}_{t-1}\right] \\ & = \mathbb{E}\left[\max_{(a_t,g_t)\in\Psi(x_{t-1},w_t)} R(a_t,g_t,\mathbb{E}[p_t|w_t,\mathbf{p}_{t-1}]) + \delta\mathbb{E}\left[V^*_t(S_t)|w_t,\mathbf{p}_{t-1}\right] \middle| w_{t-1},\mathbf{p}_{t-1}\right], \end{aligned} \tag{2.3}$$

where the last equality in (2.3) follows from the fact that $R(\cdot)$ is linear in its third argument. Note that (2.3) reflects our sequence of events: the inner maximization assumes that the operator adapts his decisions to w_t, but $\mathbf{p}_t$ is unknown until time t.

The optimal policy of (2.3) is in general complex due to the possible non-concavity of the value functions in inventory, resulting from negative prices *and* efficiency loss (see Appendix A.1 for a detailed explanation). Therefore, we compute an optimal policy via dynamic programming on a discretized state space. Because computing such an optimal policy is time-consuming (see §2.8.2), we develop heuristics which are more efficient to compute.

2.4 Heuristics

In this section we discuss several heuristic policies for solving the MDP (2.3), and demonstrate why they require significantly less computational effort than the optimal policy. We arrive at the first heuristic by optimizing a modified version of this MDP in §2.4.1 and the second heuristic by optimizing a model without the buying option in §2.4.2. We briefly examine other heuristics in §2.4.3. We compare the computational effort required for all heuristics and an optimal policy in §2.4.4.

2.4.1 Triple-threshold policy

To obtain the heuristic in this subsection, we modify the immediate payoff function in the MDP (2.3) to include the $\max\{\mathbb{E}[p_t|w_t, \mathbf{p}_{t-1}], 0\}$ instead of $\mathbb{E}[p_t|w_t, \mathbf{p}_{t-1}]$ as follows:

$$\begin{aligned} & V_{t-1}^{H1}(S_{t-1}) \qquad (2.4)\\ =&\mathbb{E}\left\{\max_{(a_t,g_t)\in\Psi(x_{t-1},w_t)} R(a_t, g_t, \max\{\mathbb{E}[p_t|w_t, \mathbf{p}_{t-1}], 0\}) + \delta\mathbb{E}\left[V_t^{H1}(S_t)|w_t, \mathbf{p}_{t-1}\right]\middle| w_{t-1}, \mathbf{p}_{t-1}\right\}, \end{aligned}$$

where we designate the optimal value function with superscript $H1$ (representing "Heuristic 1"). Similarly, we designate the optimal actions for model (2.4) with superscript $H1$, and abbreviate $g_t^{H1}(x_{t-1}, w_t, \mathbf{p}_{t-1})$ and $a_t^{H1}(x_{t-1}, w_t, \mathbf{p}_{t-1})$ to g_t^{H1} and a_t^{H1}, respectively. The optimal policy of (2.4) is then used as a heuristic for the original MDP (2.3).

Note that (2.4) includes a special case when the conditional expected prices are always nonnegative. To avoid trivial cases, we make the following benign assumption:

Assumption 2.1. For any period $t \in \mathscr{T}$, $\mathbb{E}[|p_k||w_{t-1}, \mathbf{p}_{t-1}] < \infty$ for any $k \geq t$.

The absence of negative conditional expected prices, combined with the lack of inventory holding cost and salvage penalty in model (2.4), imply that the operator is always better off having more inventory. This gives rise to Lemma 2.1, which characterizes the monotonicity of the value functions in inventory in (2.4) (see its proof in Appendix A.2).

Lemma 2.1. *For any time $t-1$ where $0 \leq t-1 \leq T$, $V_{t-1}^{H1}(x_{t-1}, w_{t-1}, \mathbf{p}_{t-1})$ is non-decreasing in x_{t-1} given any w_{t-1} and $\mathbf{p}_{t-1}$.*

Lemma 2.1, together with how the immediate payoff function varies with the generation decision g_t, implies that in model (2.4) it is optimal to generate as much energy as possible. This is in Lemma 2.2, which is formally proved in Appendix A.3.

Lemma 2.2. *For each period $t \in \mathscr{T}$, the optimal generation action g_t^{H1} for model (2.4) is $g_t^{H1} = \min\{w_t, C + \min\{1 - x_{t-1}, K_2\}/\alpha\}$.*

Before we prove the optimal inventory policy structure for (2.4) in Proposition 2.2, we prove the concavity of $V_{t-1}^{H1}(x_{t-1}, w_{t-1}, \mathbf{p}_{t-1})$ in Proposition 2.1 (see Appendix A.4 for its proof).

Proposition 2.1. *For any time $t-1$ where $0 \leq t-1 \leq T$, it holds that $|V_{t-1}^{H1}(x_{t-1}, w_{t-1}, \mathbf{p}_{t-1})| < \infty$ and $V_t^{H1}(x_{t-1}, w_{t-1}, \mathbf{p}_{t-1})$ is concave in $x_{t-1} \in \mathscr{X}$ given any w_{t-1} and $\mathbf{p}_{t-1}$.*

Figure 2.3 Proposition 2.2: The arrow on the left denotes the level used in Figure 2.4

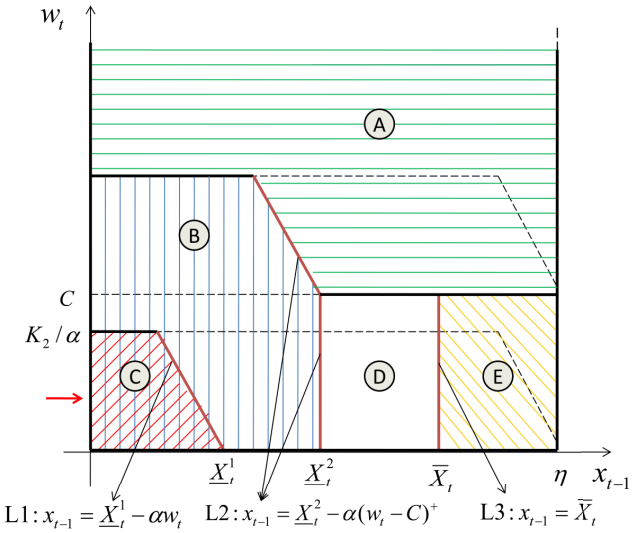

We now can establish the optimal inventory policy for (2.4), in Proposition 2.2 (the proof is in Appendix A.5). We define $x^+ := \max\{x, 0\}$ and $x^- := \min\{x, 0\}$.

Proposition 2.2. *For each period $t \in \mathscr{T}$, given any $w_t \in \mathscr{W}$ and $\mathbf{p}_{t-1} \in \mathscr{P}$, there exist three inventory levels $\underline{X}_t^1(w_t, \mathbf{p}_{t-1})$, $\underline{X}_t^2(w_t, \mathbf{p}_{t-1})$, and $\overline{X}_t(w_t, \mathbf{p}_{t-1})$ (simplified to $\underline{X}_t^1$, $\underline{X}_t^2$, and $\overline{X}_t$, respectively) where $\underline{X}_t^1 \le \underline{X}_t^2 \le \overline{X}_t$ such that a_t^{H1} is computed as follows (recall that $g_t^{H1} = \min\{w_t, C + \min\{1 - x_{t-1}, K_2\}/\alpha\}$):*

A) If either (1) $w_t \ge C + \min\{1 - x_{t-1}, K_2\}/\alpha$ or (2) $C \le w_t < C + \min\{1 - x_{t-1}, K_2\}/\alpha$ and $x_{t-1} > \underline{X}_t^2 - \alpha(w_t - C)^+$: $a_t^{H1} = \alpha(g_t^{H1} - C)^+$ (fill up);

B) If (1) $x_{t-1} + \alpha(w_t - C)^+ \le \underline{X}_t^2$ and $w_t < C + \min\{1 - x_{t-1}, K_2\}/\alpha$, but not (2) $w_t \le \min\{1 - x_{t-1}, K_2\}/\alpha$ and $x_{t-1} + w_t \cdot \alpha \le \underline{X}_t^1$: $a_t^{H1} = \min\{\underline{X}_t^2 - x_{t-1}, \alpha \cdot w_t, K_2\}$ (store up to $\underline{X}_t^2$);

C) If $w_t \le \min\{1 - x_{t-1}, K_2\}/\alpha$ and $x_{t-1} + w_t \cdot \alpha \le \underline{X}_t^1$: $a_t^{H1} = \min\{\underline{X}_t^1 - x_{t-1}, \alpha(C\tau + w_t), K_2\}$ (store up to $\underline{X}_t^1$);

D) If $w_t < C$ and $\underline{X}_t^2 \le x_{t-1} \le \overline{X}_t$: $a_t^{H1} = 0$ (do nothing);

E) If $w_t < C$ and $x_{t-1} > \overline{X}_t$: $a_t^{H1} = \max\{\overline{X}_t - x_{t-1}, (w_t - C)^-/\beta, K_1\}$ (sell down to $\overline{X}_t$).

Proposition 2.2 can be interpreted as follows. Given any point on the (x_{t-1}, w_t) plane, the optimal inventory action of policy $H1$ depends on the region into which this point falls: in region A) it is optimal to generate, sell, and store as much as possible; in region B) it is optimal to generate and store as much as possible to reach $\underline{X}_t^2$, and sell the rest; in region C) it is optimal to first generate and store, and then to buy as much as possible to reach

$\underline{X}_t^1$; in region D) it is optimal to keep the inventory level unchanged; i.e., to sell whatever is generated; and in region E) it is optimal to sell down as much as possible to reach inventory level $\overline{X}_t$.

Figure 2.3 demonstrates these five regions for a special case when the three thresholds ($\underline{X}_t^1$, $\underline{X}_t^2$, and $\overline{X}_t$) are not functions of w_t. This can occur, for instance, when the wind process for each period is independent, causing $\mathbb{E}\left[V_t^{H1}(S_t)|w_t, \mathbf{p}_{t-1}\right]$ in (2.4) to be independent of w_t. Note that the optimal actions still are functions of w_t, as spelled out in Proposition 2.2. For this special case, all curves that separate these regions are linear or piecewise linear, e.g., L1, L2, and L3 in Figure 2.3; however, for the general case where these three thresholds do depend on w_t, these three lines will not necessarily be linear or piecewise linear: their shapes depend on how $\underline{X}_t^1$, $\underline{X}_t^2$, and $\overline{X}_t$ are affected by the specific distribution of the wind and price process.

For $H1$, the most general structure of its optimal action is at the $\rightarrow$ in Figure 2.3, i.e., for any horizontal line on the (x_{t-1}, w_t) plane in Figure 2.3 such that $w_t < \min\{C, K_2/\alpha\}$. For such a case, we denote the optimal inventory action for the entire feasible inventory set $\mathscr{X}$ as follows, moving left to right:

$$a_t^{H1} = \begin{cases} \min\{\underline{X}_t^1 - x_{t-1}, \alpha(C \cdot \tau + w_t), K_2\}, & \text{if } x_{t-1} \in [0, (\underline{X}_t^1 - \alpha w_t)^+), \\ \min\{\underline{X}_t^2 - x_{t-1}, w_t \cdot \alpha, K_2\}, & \text{if } x_{t-1} \in [(\underline{X}_t^1 - \alpha w_t)^+, \underline{X}_t^2), \\ 0, & \text{if } x_{t-1} \in [\underline{X}_t^2, \overline{X}_t], \\ \max\{\overline{X}_t - x_{t-1}, (w_t - C)^-/\beta, K_1\}, & \text{if } x_{t-1} \in (\overline{X}_t, \eta]. \end{cases}$$

This is shown in Figure 2.4. For this case, the optimal action can be of four distinctive types: if $x_{t-1} < (\underline{X}_t^1 - \alpha w_t)^+$, generate and buy as much as possible to reach $\underline{X}_t^1$; if $(\underline{X}_t^1 - \alpha w_t)^+ \leq x_{t-1} \leq \underline{X}_t^2$, generate and store as much as possible to reach $\underline{X}_t^2$; if $\underline{X}_t^2 \leq x_{t-1} \leq \overline{X}_t$, maintain the same inventory level; if $x_{t-1} > \overline{X}_t$, sell to bring the inventory as close to $\overline{X}_t$ as possible. Because of these three inventory thresholds, we call the optimal policy the *triple-threshold* policy.

The existence of these three thresholds is due to the concavity of $V_{t-1}^{H1}(x_{t-1}, w_{t-1}, \mathbf{p}_{t-1})$ in x_{t-1}, in the presence of two efficiency losses: transmission loss ($\tau < 1$), and the loss in conversion ($\alpha \cdot \beta < 1$). As a result, the marginal values of the following types of action differ: storing one unit bought from the market; storing one unit from generation; and selling one

Figure 2.4 The optimal policy structure of the triple-threshold policy for the case $w_t < \min\{C, K_2/\alpha\}$

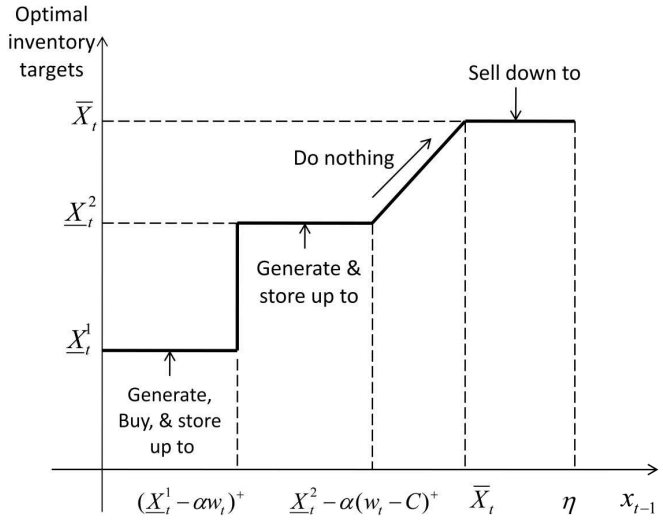

Figure 2.5 The optimal ending inventory level of the first period for Example 2.1

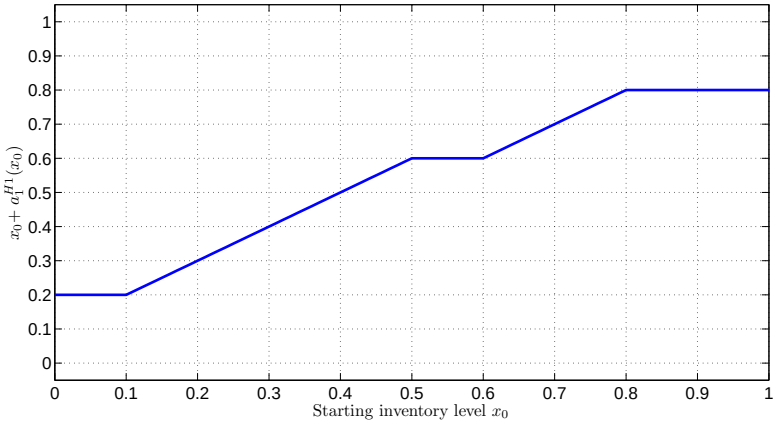

unit from the inventory. If $\tau = 1$, then $\underline{X}_t^1 = \underline{X}_t^2$, because the first two types of action have the same marginal value; if $\alpha \cdot \beta = 1$, then $\underline{X}_t^2 = \overline{X}_t$, because the last two types of action have the same marginal value. In the case $\tau = 1$, our optimal policy reduces to those shown in Secomandi (2010b).

Example 2.1. *This example illustrates the triple-threshold policy for a four-period model with a deterministic price and wind process: The price path is* $[0.25, 0.3, 3, 0.5]$*; the wind path is* $[0.1, 0.2, 0.1, 0.2]$*. Other related parameters are* $\alpha = \eta = 1$*,* $\beta = 0.5$*,* $\tau = 0.8$*,* $C = 0.3$*, and* $G = K_1 = K_2 = 1$*. Figure 2.5 plots the optimal ending inventory versus the starting inventory level in the first period; it displays a structure of three thresholds:* $\underline{X}_1^1 = 0.2$*,* $\underline{X}_1^2 = 0.6$*, and* $\overline{X}_1 = 0.8$ *(the derivation is available upon request).*

2.4.2 Dual-threshold policy and its variant

We now consider a heuristic that does not allow buying, even though conditional expected prices can be negative. In this model for each period $t \in \mathscr{T}$, the only difference from the original MDP (2.3) is in the feasible set: the new feasible decision set imposes the condition $a_t \leq g_t\alpha$, which is equivalent to removing constraint C3 from $\Psi(x_{t-1}, w_t)$.

Under this modification, the monotonicity of the value functions in inventory still holds, the proof of which is omitted because it is identical to that of Lemma 2.1. The optimal generation action for this case is as shown in the following lemma. For notation convenience, we use superscript $H2$ for the optimal actions and the optimal value function of this policy that does not admit buying.

Lemma 2.3. *For each period $t \in \mathscr{T}$, the generation action g_t^{H2} is determined as follows: If $\mathbb{E}[p_t|w_t, \mathbf{p}_{t-1}] < 0$: $g_t^{H2} = \min\{w_t, (1 - x_{t-1})/\alpha, K_2/\alpha\}$; if $\mathbb{E}[p_t|w_t, \mathbf{p}_{t-1}] \geq 0$: $g_t^{H2} = \min\{w_t, C + \min\{1 - x_{t-1}, K_2\}/\alpha\}$.*

Lemma 2.3 agrees with Lemma 2.2 when the conditional expected price is nonnegative: generate as much as possible. When the conditional expected price is negative, the optimal action of $H2$ is to sell nothing and generate as much as possible. Despite the possibility of negative conditional expected prices, the concavity of the value functions in inventory continues to hold due to the absence of the buying option, as stated in Proposition 2.3 (see Appendix A.7 for its proof):

Proposition 2.3. *For each time $t-1$ where $0 \leq t-1 \leq T$, it holds that $|V_{t-1}^{H2}(S_{t-1})| < \infty$ and $V_{t-1}^{H2}(x_{t-1}, w_{t-1}, \mathbf{p}_{t-1})$ is concave in $x_{t-1} \in \mathscr{X}$ given any $w_{t-1} \in \mathscr{W}$ and $\mathbf{p}_{t-1} \in \mathscr{P}$.*

With Proposition 2.3, we can prove the optimal inventory action of $H2$ in Proposition 2.4.

Proposition 2.4. *For every period $t \in \mathscr{T}$, the optimal inventory action is as follows: 1) if $\mathbb{E}[p_t|w_t, \mathbf{p}_{t-1}] < 0$: $a_t^{H2} = \alpha \min\{w_t, (1 - x_{t-1})/\alpha, K_2/\alpha\}$; 2) if $\mathbb{E}[p_t|w_t, \mathbf{p}_{t-1}] \geq 0$: the optimal inventory action is the same as in Proposition 2.2 except without region C).*

Proof: 1) this follows directly from Lemma 2.3; 2) the proof is straightforward from that of Proposition 2.2 and thus is omitted. □

Proposition 2.4 can be interpreted as follows: 1) if $\mathbb{E}[p_t|w_t, \mathbf{p}_{t-1}] < 0$, sell nothing and store as much as possible from generation; 2) if $\mathbb{E}[p_t|w_t, \mathbf{p}_{t-1}] \geq 0$, generate as much as

possible, and the inventory policy structure is a special case of the triple-threshold policy, a *dual-threshold* policy. This has two thresholds: generate-and-store-up-to and sell-down-to. Similar dual-threshold policies have also been found in other literature (Nascimento and Powell 2010, Secomandi 2010b). Similar to the triple-threshold policy, the two thresholds of the dual-threshold policy result from the conversion loss in the storage facility.

An improvement on this dual-threshold policy is to buy as much as possible when conditional expected prices are negative, and follow the dual-threshold policy otherwise.

2.4.3 Other heuristics

In this subsection, we describe three other heuristics that we use to benchmark the performance of the triple-threshold and dual-threshold policies.

Two-period policy. This heuristic makes decisions as if the problem were a two-period dynamic programming problem: for each period, the value of any inventory at the end of the *second* period is zero. Specifically for each stage t and each state, we find its action by solving a modified version of the MDP (2.3): we set $V_k(\cdot) = 0$ for all $k \in \mathscr{T}$, $k \geq t+2$ in (2.3). This action is then used as a heuristic action for the corresponding stage and state in (2.3).

Rolling horizon policy. This policy makes decisions by ignoring the uncertainty in the price and wind energy: for each state in each stage t, we first construct a forward curve of the price and of the wind energy from periods t through T (each forward curve consists of expected values conditional on the current state variables). Based on these two forward curves, we find the optimal action for the current period by solving a linear program (LP), which is the deterministic version of the MDP (2.3).

This rolling horizon policy ignores the uncertainty in the optimization, which is different from assuming price and wind energy are deterministic: we still model the uncertainty in the evolution of these variables, but we make decisions in each stage and state as if the future were certain.

Naïve policy. If the conditional expected price for this period is positive, this policy generates and sells as much as possible and stores as much leftover electricity as possible; if this expected price is negative, this policy generates and stores as much as possible.

2.4.4 Comparison of the computational requirements of different policies

To compute an optimal policy for the MDP (2.3) we use backward dynamic programming. For every discrete modified state $(x_{t-1}, w_t, \mathbf{p}_{t-1})$ of period t, we search for all feasible decision pairs (a_t, g_t) to find an optimal action. Thus, the computation required for each period is on a discretized grid of $4 + d$ dimensions: There is one dimension for each of x_{t-1}, w_t, a_t, and g_t; and d is the dimension of our price model ($d = 2$ in our price model; see §2.6).

To solve for the triple-threshold policy for (2.4), for every (w_t, $\mathbf{p}_{t-1}$) (note that the state variable x_{t-1} is excluded) of each period t, we compute an optimal inventory action in two steps: step 1) is to find the three critical inventory levels $\underline{X}_t^1$, $\underline{X}_t^2$, and $\overline{X}_t$; step 2) is to compute the value function of each modified state $(x_{t-1}, w_t, \mathbf{p}_{t-1})$ using Proposition 2.2. In step 1), we also use exhaustive search, but we do *not* need to search for g_t, as it is given in closed-form. Thus, the computation required for each period is only a discretization grid of 2 + d dimensions. In step 2), we use Proposition 2.2 to find the optimal action (a_t, g_t) without exhaustive search, thus the computation required is only on a grid of $2 + d$ dimensions as well. As a result, the total computational effort for both steps is still $2 + d$ dimensional. We compute the dual-threshold policy similarly. Therefore, the triple-threshold and dual-threshold policies require two fewer dimensions of computation than an optimal policy.

Compared to an optimal policy, the other heuristics that we consider are also easier to compute. The two-period policy solves for optimal actions only for two periods rather than for the entire horizon; the rolling horizon policy is determined by repeatedly solving an LP, which is more efficient to solve than the MDP (2.3); and the naïve policy is trivial to compute.

We compare the numerical and computational performance of these heuristics against those of an optimal policy, based on price and wind energy models calibrated to real data, in §2.8.2.

2.5 Storage valuation

The value that storage provides for a WST system can be three-fold:

- Storage can reduce wind energy curtailed due to the transmission capacity constraint;
- Storage enables the wind farm to time-shift generation to periods of more favorable prices;
- Storage enables the wind farm to buy electricity from the market for future resale.

For these reasons, the value of storage can be measured both financially, as the increase in the total value of the system; or with respect to energy, as the decrease in the wind energy curtailed, or the increase in energy or wind energy sold. We compute these values in §2.8.3.

2.5.1 Monetary value of storage

We quantify the monetary value of storage as the percentage increase in the value of the system with storage under the triple-threshold policy compared to that of the system without storage. (We use the triple-threshold policy as it is both efficient to calculate and near-optimal, as shown in §2.8.2.) Specifically, the value of storage is

$$\frac{V_0^{H1} - V_0^{NS}}{V_0^{NS}} \times 100 = \left(\frac{V_0^{H1} - V_0^{H2}}{V_0^{NS}} + \frac{V_0^{H2} - V_0^{H3}}{V_0^{NS}} + \frac{V_0^{H3} - V_0^{NS}}{V_0^{NS}} \right) \times 100, \qquad (2.5)$$

where V_0^{H1}, V_0^{H2}, and V_0^{H3} are the values of the system with storage at the initial stage and state using the triple-threshold policy, the dual-threshold policy, and the naïve policy (denote by $H3$), respectively; and V_0^{NS} is the optimal value of the system without storage (the arguments of all V_0's are removed for simplicity). Using (2.5), we can interpret the value of storage as the sum of the following three components:

- $(V_0^{H1} - V_0^{H2})/V_0^{NS}$: the value of storage due to arbitrage, as $V_0^{H1} - V_0^{H2}$ is the difference between the value of the system with storage under the triple-threshold policy and the value of the same system under the dual-threshold policy (which does not buy).
- $(V_0^{H2} - V_0^{H3})/V_0^{NS}$: the value of storage due to time-shifting generation, as $V_0^{H2} - V_0^{H3}$ is the difference between the value of the system with storage under the dual-threshold policy and the naïve policy (which sells as much as possible when conditional expected prices are positive).
- $(V_0^{H3} - V_0^{NS})/V_0^{NS}$: the value of storage due to reduced curtailment, as $V_0^{H3} - V_0^{NS}$ is the difference between the value of the WST system under the naïve policy and that of the system without storage.

2.5.2 Energy value of storage

To measure the energy value of storage we again use the triple-threshold policy. We will compare—for the cases with and without storage—the following three average quantities: (i) The average wind energy curtailed: the average wind energy available minus the average wind

energy generated; (ii) The average energy sold: the average energy sold to the market, from generation and inventory; and (iii) The average wind energy sold: the difference between the average energy sold and the average energy bought from the market. These quantities are the sum of the expected corresponding quantities for all stages starting in the initial stage and state at inventory level zero, divided by the number of periods.

To provide a basis for evaluating the performance of different policies and computing the values of storage, we need a price and a wind energy model.

2.6 Price model

In this section we specify the price model that is used in our numerical study in §2.8. We describe the price data that we use in §2.6.1, review the literature on commodity price models in §2.6.2 and discuss the price model that we use in §2.6.3. We discuss how we calibrate this model to this data in §2.6.4, and how we discretize this model in §2.6.5.

2.6.1 Price data

We use price data from NYISO to carry out our experiments; NYISO is among the largest and most liquid electricity markets (NYISO 2011). For each of its fifteen zones, NYISO (2011) reports the real-time price for every five minutes from 1999 until the present. We choose a single zone (New York City), and focus on data from 2005-2008, as this time span is recent and long enough for calibration. We take the average real-time price of every hour, and use this as the original price series for calibrating our model. In §2.8 we use one hour as the stage length of our MDPs. We chose an hourly decision frequency because most real-time markets, including NYISO, run on a hourly interval, at which time transactions for five-minute subintervals are decided.

We plot this hourly price series in Figure 2.6. This figure shows that these prices exhibit mean reversion, a tendency to revert back to the mean price level (approximately \$75/MWh, where MWh represents megawatt hour); and seasonality, a term we use to describe any repeated pattern on any time scale, such as hourly, daily, weekly, monthly, and yearly. Furthermore, these prices show a slight upward trend. The most prominent feature, however, is the variability, with a substantial number of positive and negative price jumps. The maximum price is $\$1,943.5$/MWh; the minimum is $\$-300.3$/MWh. Another important feature is the

Figure 2.6 The average hourly real-time price in New York City from 2005-2008 in NYISO

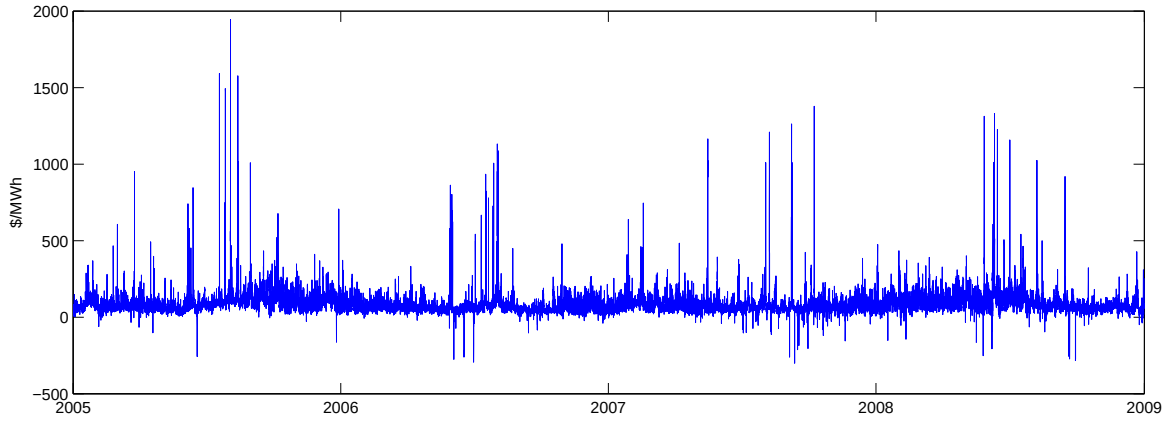

existence of negative prices (166 instances), most of which result from negative jumps. Thus, a reasonable price model for this data should capture mean reversion, seasonality, a long-term trend, and both positive and negative jumps.

2.6.2 Electricity price models

In this subsection we review the literature on electricity price models. Since electricity is a commodity, its price models are mostly based on those of general commodities from the field of financial engineering (such as Schwartz and Smith 2000, and references therein). Most of these commodity price models (mainly reduced-form, see Seppi 2002) capture mean reversion and a long-term trend, and can be tailored to describe special features of electricity prices, such as seasonality (Lucia and Schwartz 2002). Apart from reduced-form price models, there are also equilibrium models to describe the evolution of electricity prices, such as those of Barlow (2002) and Benth and Koekebakker (2008). Other models, commonly used in the electrical engineering literature, include input/output hidden Markov models (Gonzalez et al. 2005) and artificial neural networks (Szkuta et al. 1999). A comprehensive review of electricity price models in the engineering field can be found in Bunn (2004).

To fully describing the features of electricity prices also requires one to capture extreme price variability (a feature contributed to by the current difficulty in economically storing electricity on a large scale). For example, on June 25, 1998, the electricity price in the Midwest region jumped to $7,500/MWh (FERC 1998), compared to around $40/MWh on average in that year. This type of extreme variability cannot be modeled by pure Gaussian price models.

To capture it, alternatives include

- Adding a jump process where the jump size is modeled as a normal distribution (Cartea and Figueroa 2005), or an affine jump diffusion (Villaplana 2005) in which the jump size and intensity are affine functions of the state variables.
- Modeling volatility as a stochastic process, for instance, a GARCH model (Escribano et al. 2002, Garcia et al. 2005), or a Lévy process (Benth et al. 2007).
- Specifying—on top of "normal" regimes—regimes of "abnormal" states, a method often called regime-switching, such as in Deng (2000), Rambharat et al. (2005), Huisman and Mahieu (2003), De Jong (2006), Geman and Roncoroni (2006), and Seifert and Uhrig-Homburg (2007). Variants of this approach differ in modeling the transitions between regimes.

2.6.3 Our price model

To obtain a price model that describes all the features of electricity prices discussed in §2.6.1, we modify one of the models in Lucia and Schwartz (2002) by generalizing its seasonality component and adding a jump component. Specifically, in our reduced-form model, the electricity price p_t for period t is

$$p_t = \xi_t + f(t) + J_t,$$

where ξ_t is a mean reverting process; $f(t)$ a deterministic seasonality function; and J_t a jump process. A mean-reverting process is commonly used in energy price models, such as in Smith and McCardle (1999), Seppi (2002), Jaillet et al. (2004), Secomandi (2010a,b), and Devalkar et al. (2011). As in one of the models in Lucia and Schwartz (2002), we use the following mean reverting model with zero mean-reversion level:

$$d\xi_t = -\kappa\xi_t dt + \sigma dZ_t,$$

where κ is the mean-reverting rate; σ the constant volatility; and dZ_t a standard Brownian motion increment. We use this spot price model rather than a log-spot price model because of the existence of negative electricity prices. The mean price level in the data is captured by the seasonality function of our model.

To obtain the seasonality function $f(t)$, we generalize one from Lucia and Schwartz (2002),

which consists of three terms: a constant level; a term to describe the effect of a non-business day; and a cosine function to capture daily differences, which in effect captures monthly and yearly seasonality as well. To capture the non-business day effect, they use the term $B \cdot D_t$, where B is the magnitude of this effect, and D_t equals 1 if period t belongs to a holiday or a weekend, and 0 otherwise.

We add another two terms to this seasonality function: a linear term to describe any general trend of electricity prices, and a cosine function to capture hourly "seasonality." To summarize, we use the following seasonality model:

$$f(t) = A + B \cdot D_t + \gamma_1 \cos\left((t + \omega_1)\frac{2\pi}{365 \cdot 24}\right) + \mu \cdot t + \gamma_2 \cos\left((t + \omega_2)\frac{2\pi}{24}\right),$$

where A is the constant level; γ_1 and ω_1 are the magnitude and the phase shift of daily seasonality, respectively; μ is the long-term trend; and γ_2 and ω_2 are the magnitude and the phase shift of the hourly seasonality, respectively.

We model the jump component J_t as an arrival process with the arrival rate λ and the jump size following an empirical distribution, derived from our data:

$$J_t = \text{jump size} \cdot \{1, \text{ if there is a jump; } 0, \text{ if there is no jump}\}.$$

We use an empirical distribution because it is the easiest distribution to use to solve our MDPs *numerically*. We incorporate negative jumps to model the sudden large negative prices in our data, which the mean reversion model cannot produce.

2.6.4 Price model calibration

We calibrate our price model to the hourly price series described in §2.6.1. To estimate the model parameters, we first separate the jump component from this hourly price series, and estimate the parameters related to jumps. Then from the resulting series we estimate the parameters related to mean-reversion and seasonality.

We regard any price as including a (positive or negative) jump if either the difference between this price and its predecessor price is an "outlier," or its absolute value is an "outlier" (we define "outlier" in Appendix A.8). Cartea and Figueroa (2005) use only the former qualification, but we find the latter useful because of the jump clumping in our data: there

Table 2.1 Empirical jump size distribution

Size	−1200	−1100	−1000	−900	−800	−700	−600	−500
Probability	0.0004	0.0004	0.0004	0.0007	0.0011	0.0007	0.0026	0.0015
Size	−400	−300	−200	−100	0	100	200	300
Probability	0.0022	0.0126	0.0167	0.1746	0.3079	0.4097	0.0383	0.0123
size	400	500	600	700	800	900	1000	1100
Probability	0.0071	0.0022	0.0030	0.0015	0.0015	0.0004	0.0007	0.0015

Table 2.2 Estimated parameters for each component of the price model (MAE = \$12.50/MWh)

Mean Reversion		Seasonality							Jump
κ	σ	A	B	γ_1	ω_1	γ_2	ω_2	μ	λ
0.1924	17.3215	74.9985	−1.3769	2.9681	164.8868	−18.3058	−4.4985	0.00034	0.0768

are a number of visually apparent jumps that are adjacent to each other in Figure 2.6, but their individual differences are not large enough to be detected by the method of Cartea and Figueroa (2005). To identify outliers, we use steps standard in statistical quality control (Montgomery 2008), as detailed in Appendix A.8.

For any price tagged as an outlier in the above steps, we set the jump size equal to the difference between this price and its predecessor. We then bin these jumps to construct an empirical distribution, and estimate the jump arrival rate λ as the number of jump occurrences divided by the number of periods (Table 2.1). This method, though simple, extracts almost all jumps that are visually apparent. More sophisticated methods could also be applied, see for example Klüppelberg et al. (2010) and Fanone and Prokopczuk (2010).

We perform a nonlinear regression, similar to Lucia and Schwartz (2002), on the hourly price series with jumps removed. This yields the estimated parameters displayed in Table 2.2. The mean absolute error (MAE) from this regression is 12.5 (\$/MWh), while the mean of this price series is 76.21 (\$/MWh). We assume the market price of risk (Duffie 1992) is zero, because we do not have futures prices to calibrate it. If one had such data, one could estimate the market price of risk accordingly (Lucia and Schwartz 2002).

2.6.5 Discretization

To numerically solve our MDPs we discretize the mean reverting process to a lattice: A tree with discrete time steps that specifies attainable price levels and their probabilities for each period. Based on the estimated parameters for the mean reversion model, we use the method in Hull and White (1993) to construct a trinomial price lattice, with each time step equal to

an hour. This discretized mean reverting process and the discrete jump process comprise the two-dimensional price vector in the state of our MDPs.

Even though in §2.3 we assume that each component of the price vector is unknown before the operator makes a decision, in the numerical study we assume that before decision-making the operator does not know the mean reversion component, but knows the jump component; otherwise we do not need to keep the jump component in the state, because jumps are independently and identically distributed.

2.7 Wind energy model

In this section we specify the wind energy model that is used in our numerical study in §2.8. We describe the data and our model in §2.7.1, and the calibration and discretization of our model in §2.7.2 and §2.7.3, respectively.

2.7.1 Data and model

We use hourly wind speed data of the Central Park weather station in New York City, the same location from which we draw our price data. We obtain these data from NOAA (2010), and focus on 2001-2008, as this time span is long enough for calibration.

The wind speed obtained was recorded at 10 meters above ground, and we need to convert it to wind speed at the hub height of a wind turbine. We accomplish this by using the model from Heier (2006):

$$\text{Wind speed at height } h = \text{Wind speed at 10 meters} \cdot (h/10)^{\text{constant}},$$

where this constant depends on conditions such as air and ground. We set $h = 80$ meters, the height for the General Electric (GE) turbine model 1.5-77, because the GE has the largest share of the U.S. wind turbine market and its 1.5 MW series is among the best selling turbines in the U.S. (Wiser and Bolinger 2010). We choose the constant to be 0.38 so that our wind data's capacity factor (the ratio of actual energy output over a long period versus nameplate capacity) is 32%, in the range of capacity factors of wind farms in New York state[1]. We convert

[1] www.windpoweringamerica.gov/pdfs/wind_maps/ny_wind_potential_chart.pdf

Table 2.3 Production Curve of GE1.5MW

Speed (m/s)	0	1	2	3	4	5	6	7	8	9	10	11	12
Power (MW)	0	0	0	0	0.043	0.131	0.25	0.416	0.64	0.924	1.181	1.359	1.436
Speed (m/s)	13	14	15	16	17	18	19	20	21	22	23	24	25
Power (MW)	1.481	1.494	1.5	1.5	1.5	1.5	1.5	1.5	1.5	1.5	1.5	1.5	1.5

wind speed to wind energy through the production curve of GE1.5-77 (see Table 2.3), which specifies the amount of wind energy produced by such a turbine for any given wind speed.

We model the wind speed process Q_t as the sum of an autoregressive (AR) process ξ'_t and a seasonality function $f'(t)$:

$$Q_t = \xi'_t + f'(t).$$

Specifically, ξ'_t is an AR(1) (an AR process of order 1) as follows:

$$\xi'_t = \phi\xi'_{t-1} + \sigma'\epsilon_t,$$

where ϕ and σ' are scalars, and each $\epsilon_t \sim N(0,1)$ is an i.i.d. error term. The seasonality component $f'(t)$ is

$$f'(t) = A' + \gamma_3 \cos((t+\omega_3)\cdot 2\pi/(24\cdot 365)) + \gamma_4 \cos((t+\omega_4)\cdot 2\pi/24),$$

where A' is a constant level; γ_3 and ω_3 are the magnitude and the phase shift of daily seasonality, respectively; and γ_4 and ω_4 are the magnitude and the phase shift of the hourly seasonality, respectively.

2.7.2 Calibration

Since the AR(1) model is a discrete-time version of a mean reverting model, we calibrate the wind speed model using the same method used to calibrate the mean reverting component of our price model. The estimated parameters are shown in Table 2.4. We test the fitness of this calibration by computing MAE in terms of power: We first compute the series of energy of the actual wind speed and that of the estimated wind speed, then sum up the difference between these two energy series, and finally divide it by the number of periods. The MAE is 0.2715 MW; the turbine generation capacity is 1.5 MW. We also experimented with an AR(2) model,

[2] www.inl.gov/wind/software/powercurves/pc_ge_wind.xls

Table 2.4 Estimated parameters for the wind speed model (MAE = 0.2715 MW)

ϕ	A'	σ'	γ_3	γ_4	ω_3	ω_4
0.6398	6.4690	2.9522	1.4811	0.1028	−53.1759	−16.4796

and found that it does not fit the data any better than the AR(1) model in terms of MAE.

Even though in our analytical model we allow price and wind processes to be correlated, statistical analysis shows that the *stochastic* component of our price series is uncorrelated with the *stochastic* component of the wind data. (The *deterministic* seasonality components of wind and price capture the fact that wind tends to blow most strongly at night, when prices tend to be low.) This lack of correlation is not surprising, because for the considered time period wind energy consisted of only a small proportion of the electricity generation in NYISO.

2.7.3 Discretization

In order to use the continuous-space wind speed process in our MDPs, we discretize this process into a grid, which specifies the wind speed levels and transition probabilities among all levels. We choose a grid rather than a trinomial tree as we have a natural set of wind speed levels: the positive integers that do not exceed 25 (meters/second), which comprises the production curve of the GE15-77 turbine. We denote this set as $\mathscr{M}$. To find the transition probability from any level $i \in \mathscr{M}$ to any level $j \in \mathscr{M}$, ρ_{ij}, we try to match the first two moments of the discretized wind speed model at level i and its continuous counterpart as follows:

$$\min_{\rho_{ij}, \forall j \in \mathscr{M}} \quad \sum_{j \in \mathscr{M}} (\rho_{ij} \cdot j - \phi \cdot i)^2 + \sum_{j \in \mathscr{M}} \left[\rho_{ij} \cdot j^2 - (\phi \cdot i)^2 - \sigma'^2 \right]^2, \forall i \in \mathscr{M},$$

where the first (second) summation is the difference of the first (second) moment matching: the first moment of the continuous wind speed model for each $i \in \mathscr{M}$ is $\phi \cdot i$; the second moment is $(\phi \cdot i)^2 + \sigma'^2$. We give equal weights to these moment matchings for simplicity; one can easily specify different weights. Likewise, other methods of estimating the transition probabilities can be applied, for example, those in Hoyland and Wallace (2001).

2.8 Numerical study

In this section we discuss the setup of our numerical study in §2.8.1, compare the performance of all the heuristic policies and an optimal policy in §2.8.2, and quantify the monetary and energy values of storage in §2.8.3.

2.8.1 Setup

We study a wind farm that includes 120 GE1.5-77 turbines, so its total generation capacity is 120×1.5 MW= 180 MW (MW represents megawatt; 1 watt = 1 joule/ second). This wind farm is remote and connected to a wholesale market via a transmission line that has a loss of 3%, that is, $\tau = 3\%$ (DukeEnergy 2011). We vary the wind farm's transmission capacity (in MW) from 80 MW to 180 MW in steps of 20 MW. (This transmission capacity could be leased from a transmission company, so the capacity of the entire transmission line can be larger.) Co-located with the wind farm is an industrial battery, which can be charged or discharged fully in ten hours (EPRI 2004). We vary its energy capacity (in MWh; 1 megawatt hour = 3.6 Giga joules) from 200 MWh to 1200 MWh in steps of 200 MWh. The relative size of the WST system is consistent with Denholm and Sioshansi (2009) and Pattanariyankool and Lave (2010). We also vary the round-trip efficiency of this industrial battery, and find that our qualitative managerial insights to be consistent. Therefore in the results we report, the storage efficiency parameters are fixed at $\alpha = 0.85$, $\beta = 1$, and $\eta = 1$.

As mentioned in §2.6.1, we assume each period is one hour. We use a time horizon of one month, so the total number of periods is $31 \times 24 = 744$. The discount factor δ for each stage (period) is 0.999999, corresponding to an annual risk-free interest rate of 1% with continuous compounding (recall that we use risk-neutral valuation).

We numerically evaluate an optimal policy to (2.3), along with all the heuristics of §2.4. For all policies, we discretize the inventory set evenly to 301 levels (beyond this level of discretization the results vary little). The value of each policy is the value of the objective function in (2.2) evaluated at initial inventory zero using the action of this policy for each stage and state. We find the actions of each policy using dynamic programming to solve each corresponding MDP, based on steps specified in §2.4.3 and §2.4.4.

Figure 2.7 Value of heuristics versus that of an optimal policy: storage energy capacity equals 600 MWh

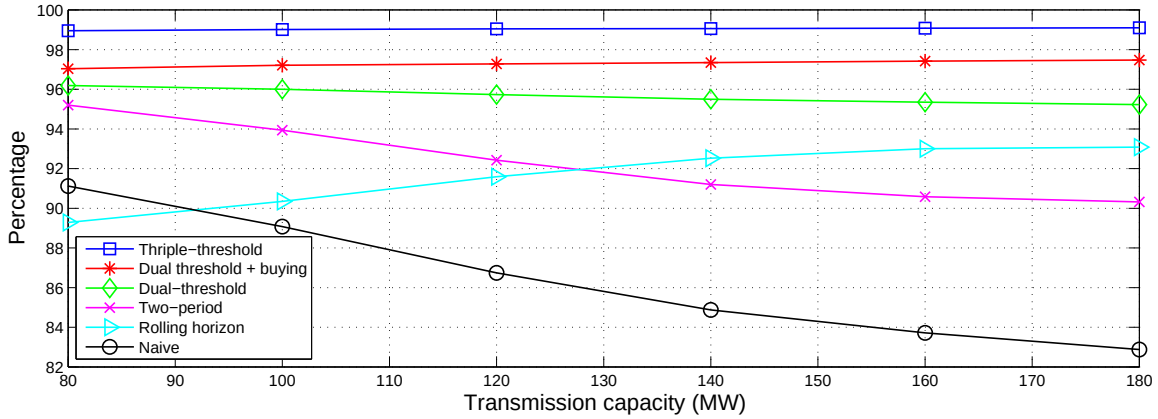

2.8.2 The performance of all the policies

We report here the performance of all policies not only in terms of their relative values, but also in their computation time. We carry out all experiments on a computer with Intel(R) Core(TM) i7-2600K CPU of 3.40GHz with 8 MB cache.

On average, for a given WST configuration, computing an optimal policy takes around 11 hours, which exceeds the decision frequency of every hour; in contrast, the triple-threshold policy and dual-threshold policy (and its variant) take around 30 and 20 minutes, respectively, which is within hourly decision frequency. All other heuristics can be computed within seconds.

For each heuristic, we compute the percentage of its value relative to that of an optimal policy. Figure 2.7 reports these results for a range of transmission capacity levels given a storage energy capacity of 600 MWh (this corresponds to the proportions of storage energy capacity to generation capacity used in Denholm and Sioshansi 2009). As seen in this figure, the problem of managing a WST system is non-trivial: using the naïve policy can result in a significant loss of optimality, from 9% at 80 MW of transmission capacity to 17% at 180 MW of transmission capacity. In contrast, almost all the optimal value is captured by the triple-threshold policy: it achieves about 99% of the optimal value over all the transmission capacity levels. The sub-optimality of the other heuristic policies is more pronounced: from 95% to 96.4% for the dual-threshold policy, from 97% to 97.5% for the dual-threshold policy augmented with buying, from 90.5% to 95% for the two-period policy, and from 89% to 93% for the rolling horizon policy. Therefore, the triple-threshold policy is practical *and* near optimal, while other heuristic policies, though practical, do not perform as well.

Figure 2.8 Effect of storage energy capacity and transmission capacity on the value of the triple-threshold policy: each curve represents one storage energy capacity level

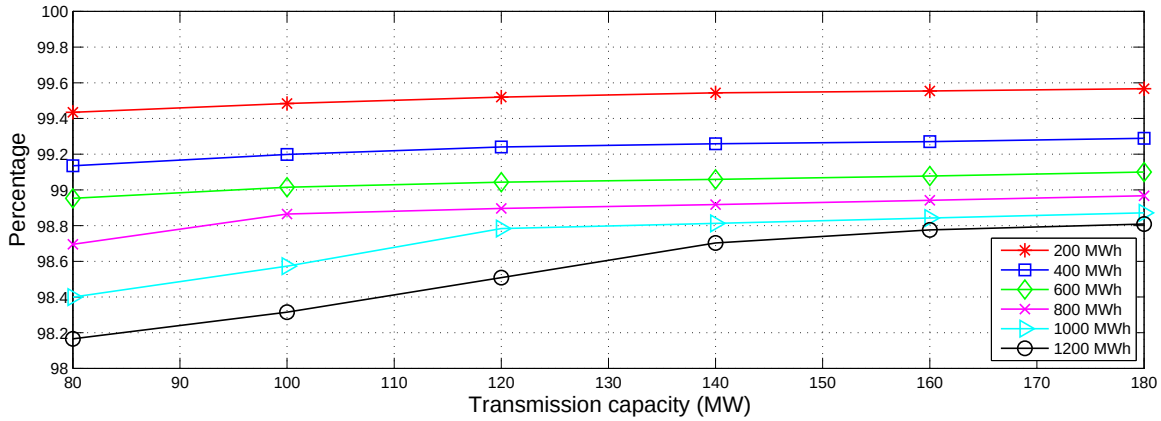

Next we further examine the performance of the triple-threshold policy. Figure 2.8 plots the performance of this policy relative to the optimal policy that we obtain (the optimal policy may not be unique), over a range of storage energy capacity and transmission capacity levels. The triple-threshold policy consistently performs well for all the parameters considered, achieving at least 98% of the optimal value. Given any transmission capacity, the performance of our heuristic policy deteriorates as the storage energy capacity increases: with larger storage energy capacities our computed optimal policy can buy much more than the triple-threshold policy (which thinks any negative expected price is zero). Moreover, given any storage energy capacity, the performance of this triple-threshold policy improves as the transmission capacity increases: as this transmission capacity becomes less constraining, the difference in the quantity purchased by our optimal policy and the triple-threshold policy diminishes because storage energy capacity becomes binding.

2.8.3 The value of storage

We now analyze the monetary and energy values of storage under the triple-threshold policy.

2.8.3.1 The monetary value of storage. We present the monetary value of storage and the breakdown into its three components (defined in §2.5) for a range of storage and transmission capacity levels in Figure 2.9. Storage can substantially increase the monetary value of a WST system: for a typical setting when the transmission capacity is 120 MW, and the storage energy capacity is 600 MWh (the relative size of a WST system in Denholm and

Figure 2.9 Breakdown of the monetary value of storage under the triple-threshold policy given 600 MWh of storage energy capacity (left) and 120 MW of transmission capacity (right)

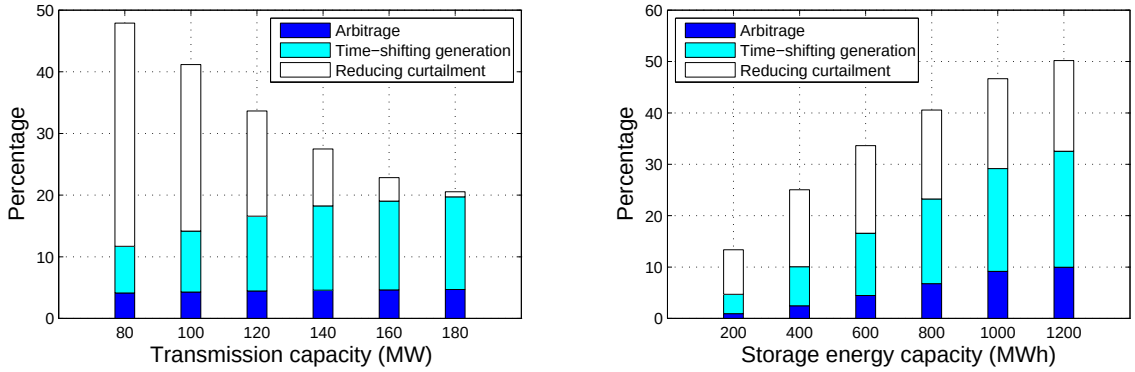

Sioshansi 2009 and Pattanariyankool and Lave 2010), the monetary value of storage is around 33.5%, of which 4.5% is from arbitrage, 12% from time-shifting generation, and 17% from reducing curtailment.

Given a storage energy capacity level of 600 MWh (Figure 2.9 Left), the monetary value of storage decreases with more transmission capacity, because the value of reducing curtailment plummets as the transmission capacity increases, even though both the value of arbitrage and the value of time-shifting generation increase with more transmission capacity (see expression (2.5) in §5). In addition, when the transmission is tight, the majority of the monetary value of storage is due to reducing curtailment; with ample transmission capacity, the majority of this value is attributable to time-shifting generation and arbitrage.

Given a transmission capacity level of 120 MW (Figure 2.9 Right), the monetary value of storage is increasing concave with more storage energy capacity. This is because for any given transmission capacity, the value of the system without storage is constant when changing the storage energy capacity, while all three monetary values of storage (from reducing curtailment, time-shifting, and arbitrage) increase with the storage energy capacity until they level out because of the bottleneck in transmission capacity (see expression (2.5) in §5).

2.8.3.2 The energy value of storage. We next examine the energy value of storage. Figure 2.10 (Left) shows that using storage can substantially reduce curtailment. For instance, when the storage energy capacity is 600 MWh and the transmission capacity is 120 MW, the average curtailment per period (i.e., per hour) is reduced by around 87% compared to the system without storage: if lack of transmission is leading to curtailment, 87% of the wind

Figure 2.10 Curtailment per hour (left) and energy sold per hour (right) under the triple-threshold policy for different storage energy capacity levels

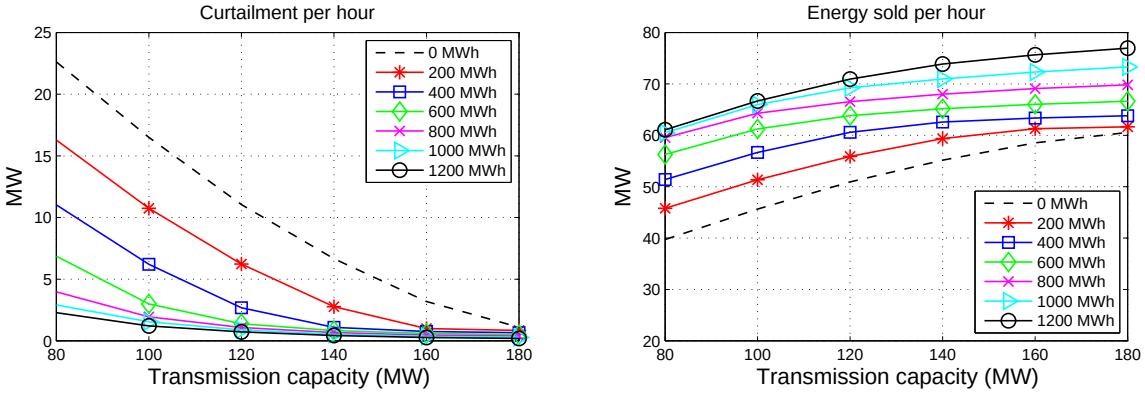

Note: Each curve corresponds to a storage energy capacity level; 0 MWh corresponds to no storage

Figure 2.11 Wind energy sold per hour for different storage energy capacity levels under the triple-threshold policy (left) and the naive policy (right)

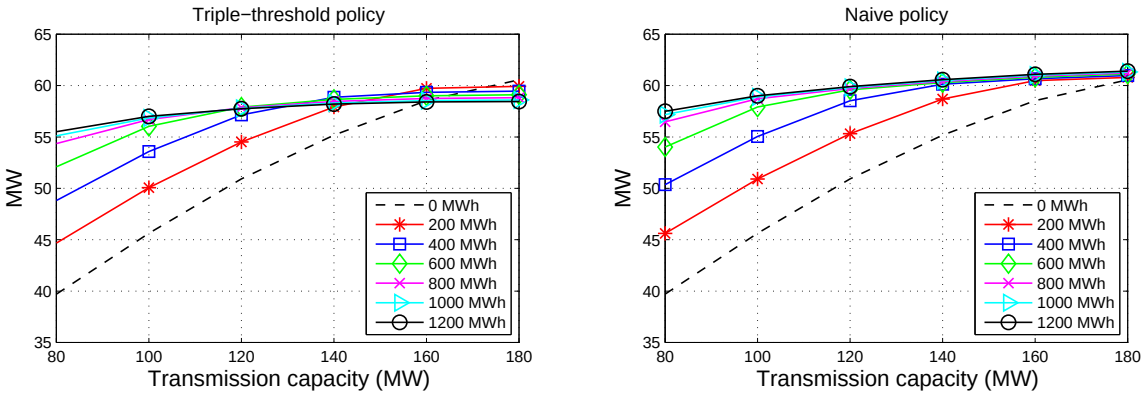

Note: Each curve corresponds to a storage energy capacity level; 0 MWh corresponds to no storage.

energy curtailed can be recouped through use of storage under our triple-threshold policy. Given any storage energy capacity (including the no-storage case), the curtailment shrinks with more transmission capacity; and given any transmission capacity, the curtailment shrinks with more storage energy capacity.

Figure 2.10 (Right) indicates that storage can greatly increase the average energy sold per period. For instance, when the storage energy capacity is 600 MWh and the transmission capacity is 120 MW, storage increases the average energy sold by about 26% compared to the no-storage case: 14% is due to more wind energy sold (less curtailed); and 12% due to reselling electricity bought from the market.

However, under the triple-threshold policy, storage does not necessarily increase the average

wind energy sold per period. As seen from Figure 2.11 (Left), when the transmission capacity is low, more storage energy capacity indeed increases the average wind energy sold; however, when the transmission capacity is high, more storage can actually slightly reduce average wind energy sold. This is because at high transmission capacity there is very limited curtailment for the system without storage; the benefit of reducing curtailment with storage decreases to such an extent that this benefit is surpassed by the conversion loss in the storage facility. In contrast, if the naïve policy is used, then more storage energy capacity does increase the average wind energy sold (see Figure 2.11 right). This observation implies that a policy that strives to maximize revenue (such as the triple-threshold policy) does not also maximize the average wind energy sold.

2.9 Conclusions and future work

We consider the problem of managing a WST system that trades electricity in an electricity market. We demonstrate that computing an optimal policy does not have any simple structure, while overly simple policies may sacrifice significant value. We thus develop a triple-threshold heuristic policy, which generalizes policy structures that are known in the commodity storage literature. This structure enables us to reduce the computation significantly compared to an optimal policy.

We investigate the performance of this triple-threshold policy and other heuristics relative to that of an optimal policy. We do so using price and wind energy models calibrated to real data for a range of round-trip efficiency, transmission capacity, and storage energy capacity levels. We find that while other heuristics are inferior, the triple-threshold policy is within 2% of optimality on a set of realistic instances. This implies that in practice the optimal policy may resemble a triple-threshold policy.

Our experiments show that storage can substantially increase the monetary value of the system: when the transmission capacity is tight, the majority of this value comes from reducing curtailment and time-shifting generation; when the transmission capacity is abundant, the majority arises from time-shifting generation and arbitrage. The substantial monetary value of storage—combined with the fact its cost is dropping rapidly (AquionEnergy 2011)—makes investing in storage potentially appealing. We also find that although storage can substantially reduce curtailment and increase the average energy sold, more storage energy capacity may

actually decrease the average wind energy sold if a revenue-maximizing policy is used.

Our work can be extended in several directions. First, one could include bidding in a forward market, in addition to the spot market considered in this chapter. Second, one could investigate the collective effect of multiple wind farms and storage facilities on electricity prices, at high levels of wind energy penetration, such as 20% of the total electricity generation in the U.S. (DOE 2008).

Chapter 3

Is It More Valuable to Store or Destroy Electricity Surpluses?

3.1 Introduction

In a commodity market, storage is useful to match supply and demand: when supply outstrips demand, any surpluses can be stored for future sale. Thus, storing surpluses is a natural strategy for dealing with electricity surpluses for a merchant that trades electricity in a market, particularly because electricity supply and demand must be matched in real time to ensure the integrity of the electrical grid. However, another potential strategy for dealing with electricity surpluses is to destroy and dispose of them. This strategy is potentially appealing for a merchant because of the existence of negative electricity prices, as mentioned in Chapter 2, or, equivalently, because of periods in which buyers are paid to buy electricity.

Negative prices are caused by various factors, as mentioned in Chapter 2. Other than those reasons, in recent years, negative prices in the U.S. may also have been caused by Renewable Energy Credits traded in the market, or the federal Production Tax Credit received by wind-based electricity generators (Fink et al. 2009): Production Tax Credit is currently valued at $22/MWh (DSIRE 2011); thus wind generators may bid a negative price and still

This chapter is a joint work with Alan Scheller-Wolf, Nicola Secomandi, and Stephen Smith; it is under the first round revision for *Management Science*.

generate positive revenue from the sale, as long as the price is higher than -$22/MWh. With the increased use of wind power, negative prices may become more frequent and larger in magnitude in the future (Brandstätt et al. 2011, Genoese et al. 2010, Nicolosi 2010).

It is not clear which—storage or disposal—strategy for managing electricity surpluses is more valuable for a merchant. We investigate this question by considering a merchant's problem of managing a storage facility at different *round-trip efficiencies*. As mentioned in Chapter 2, the round-trip efficiency of an electricity storage facility represents the ratio of the quantity of electricity withdrawn to that injected (EPRI 2004). By varying this efficiency, our model encompasses both the case when electricity surpluses are stored and the case when they are destroyed: a high round-trip efficiency represents the storage strategy and a low round-trip efficiency the disposal strategy (as the majority of the electricity is lost during the conversion process).

We model this problem of managing a storage facility with prices that are potentially negative as an MDP. The round-trip efficiency and the physical constraint on the energy capacity of the storage facility make our electricity storage problem similar to that of other commodities, such as natural gas or oil. However, our problem differs from these due to the existence of negative prices; negative prices have not been observed in these markets, and there is no known optimal policy structure for this case in the literature. Therefore, we derive our model's optimal policy: We show that for every state and stage, the inventory domain can be divided into three regions, one region in which it is optimal to empty the facility, one in which it is optimal to fill up the facility, and one in which it is optimal to do nothing. This policy structure subsumes the optimal policy structure for managing storage in Charnes et al. (1966); when price can be only positive, our policy simplifies to theirs. This structure facilitates computing the values of the storage and disposal strategies for managing electricity surpluses.

We compare the values of these two strategies using the same financial engineering price model in Chapter 2. We vary the round-trip efficiency of the storage facility over a range that includes both low and high values, to model both disposal and storage strategies. Our numerical results show that the disposal strategy is even more valuable than the storage strategy. They also suggest that the value of the storage strategy originates from using an efficient storage facility to store electricity purchased mainly at low but *positive* prices for resale at high positive prices. This is in contrast to the disposal strategy, whose value arises

from using an inefficient storage facility to destroy surpluses purchased at *negative* prices. These findings are potentially relevant to electricity merchants, and also may inform policy makers who might be interested in assessing the potential impact of the disposal and storage strategies on consumer surpluses and social welfare.

The rest of this chapter is organized as follows: we review the extant literature in §3.2; we present our MDP in §3.3 and our structural analysis of its optimal policy in §3.4; we carry out our numerical analysis in §3.5; we conclude in §3.6.

3.2 Literature Review

Our work is related to the commodity and energy storage literature. One problem studied in this literature is the classical warehouse problem introduced by Cahn (1948): given a warehouse with limited space, what is the optimal inventory trading policy in the face of variability in the commodity price? Charnes et al. (1966) show that if this price is stochastic and positive, for a given time and spot price the optimal inventory trading decisions are the same for any inventory level: either fill up the warehouse, empty it, or do nothing. The warehouse in this chapter is an electricity storage facility. We show that the presence of negative prices can dramatically alter the optimal policy structure of Charnes et al. (1966): for a given time and commodity price, different types of actions can be optimal at different inventory levels. Also, in our model it can be optimal to fully charge the storage facility at low inventory levels and fully discharge it at high inventory levels, which is not optimal in the models considered by Charnes et al. (1966). Other related work can be found in the literature on commodity and energy real option (see, e.g., Smith and McCardle 1999, Geman 2005), which we have mentioned in Chapter 2. However, all of these papers assume that the commodity price is positive.

Most of the extant literature on electricity storage assumes perfect information on future electricity prices, including Graves et al. (1999), Figueiredo et al. (2006), Walawalkar et al. (2007), and Sioshansi et al. (2009). These authors use historical price data to examine the value of storage in various electricity markets: they assume that one has the ability to foresee future prices, and find the optimal policy for a given price path by solving a linear programming problem. In contrast, we model prices as a stochastic process, and derive the optimal policy in the face of price uncertainty. Two papers on electricity storage that do model price as a stochastic process are Mokrian and Stephen (2006) and Xi et al. (2011): Mokrian and Stephen

(2006) assess the value of different electricity storage facilities in an electricity market; Xi et al. (2011) co-optimize multiple usages of storage, including energy usage and backup service. However, neither of these papers considers the case when price can be negative, nor do they derive the optimal policy structure.

This chapter is also related to Chapter 2 on managing wind-based electricity generation with storage: Although Chapter 2 also considers the possibility of negative prices, it does not quantify the relative values of the storage strategy and the disposal strategy, which we do in this chapter. And, unlike Chapter 2's finding that negative prices can be ignored when managing a remote wind farm with storage and transmission capacity, we find in this chapter that negative prices are significant enough to make the disposal strategy even more valuable than the storage strategy for managing a standalone storage facility located at a market.

3.3 Model

We consider a merchant's problem of managing electricity storage in an electricity wholesale market, specifically in a real-time market. (Consistent with the literature on valuing electricity storage mentioned in §3.2, we do not consider bidding in a forward market.) Note that the model in this section is a subset of the model in §2.3: excluding from §2.3 all the modeling elements (states, actions, and constraints) related to wind, transmission capacity, and power capacity gives the model in this section, except some differences in conventions as we explain later on. However, for the sake of concreteness, we define the model completely in this section. We assume that the merchant is a price taker, and thus his trading decisions do not affect the market price. The merchant trades electricity in a finite horizon at each period t from a set $\mathscr{T} := \{1, \cdots, T\}$; at the terminal period $T+1$, any electricity left is worthless. Different from Chapter 2, this chapter does not define *period* as the interval between two *time* epochs; furthermore, this chapter does not even introduce the concept of *time*, but uses only *period*, because this chapter does not have wind energy as in Chapter 2, which is revealed *gradually* over a period. Chapter 4 is the same as Chapter 3 in this regard.

The source of uncertainty in the model of this chapter is only the evolution of electricity price $\{\mathbf{P}_t, t \in \{0\} \cup \mathscr{T}\}$; $\mathbf{P}_t$ is a random variable with the support $\mathscr{P} \subseteq \mathbb{R}^n$, where n is the number of components in $\mathbf{P}_t$. As in Chapter 2, $\mathbf{P}_t$ is a vector of price components. Note that in this chapter, the convention of denoting a random variable is different from Chapter

2: in Chapter 2, a random variable is always denoted in lower case, and a random variable with subscript t is unknown or random before *time* t, but is known or realized at *time* t; in this chapter, a variable is random if it is denoted in upper case, and it is known if it is denoted in lower case. We use the same convention in Chapter 4 as well. This section and the next are *independent* of any specific price model, except for the requirement that prices be Markovian and not affected by the merchant's decisions. We use the same price model as in Chapter 2, but calibrate it to different input data for estimating model parameters, which we mention in §3.5.1. At the beginning of every period $t \in \mathscr{T}$, the merchant knows the price of the previous period $\mathbf{p}_{t-1}$ (\$/MWh, where MWh represents megawatts hour), which gives the conditional probability distribution of the price in the current period, $\mathbf{P}_t$. The market price is unknown *before* each market player's decision to be consistent with the operation of an electricity market, which clears after all players' decisions.

The merchant's storage facility is finite in energy capacity; without loss of generality, we normalize the available energy capacity to be one (MWh). The storage facility's round-trip efficiency equals $\alpha \cdot \beta \cdot \eta$, where α, β and η (all in $(0, 1]$) represent the efficiency in charging, discharging, and storing over one period (storage facilities may lose electricity by self-discharging when on standby). Most of the literature models round-trip efficiency as a single number in between 0 and 1, irrespective of how long electricity has been stored. Our model allows the possibility of asymmetric charging and discharging efficiencies, and η allows the storage loss to depend on time.

We denote the inventory (electricity) in the merchant's facility at the beginning of each period t by x_t, where x_t has the domain $\mathscr{X} := [0, 1 \cdot \eta]$. (The maximum inventory level is η because we assume that the storage loss occurs at the end of each period.) The decision for each period t is denoted by a_t: if $a_t < 0$, a_t is the quantity of inventory decrease due to selling, so the actual quantity sold to the market is a_t multiplied by the discharging efficiency, that is $a_t \cdot \beta$; if $a_t \geq 0$, a_t is the quantity of the inventory increase due to buying, so the actual quantity bought from the market is a_t divided by the charging efficiency, that is a_t/α. For any given initial inventory level x_t, the feasible action set for a_t is $[-x_t, 1 - x_t] =: \Psi(x_t)$.

For each period $t \in \mathscr{T}$, let $R(a_t, p_t)$ denote the immediate payoff function, which is the

[3]Chapter 2 differs in this convention due to a referee's suggestion on the journal version of Chapter 2.

purchasing cost if $a_t \geq 0$ and the selling revenue if $a_t < 0$, specifically

$$R(a_t, p_t) := \begin{cases} -\frac{1}{\alpha} a_t \cdot p_t, & \text{if } a_t \geq 0, \\ -\beta a_t \cdot p_t, & \text{if } a_t < 0, \end{cases} . \tag{3.1}$$

For each period $t \in \mathscr{T}$, the sequence of events is as follows:

(i) At the beginning of period t, based on x_t and $\mathbf{p}_{t-1}$, the merchant decides on a_t.

(ii) The physical transfer of electricity follows, either from the merchant to the market in the case of selling or vice versa in the case of buying. With the physical transfer, there occurs a loss in discharging (selling) or charging (buying).

(iii) The market price $\mathbf{p}_t$ is revealed, and the associated financial settlement is completed.

(iv) At the end of period t, the inventory decreases by $(1-\eta) \times 100$ percent, thus $x_{t+1} = \eta(x_t + a_t)$.

We formulate the merchant's problem as a finite-horizon MDP. Each stage of the MDP corresponds to one time period. The state variables in stage t are x_t and $\mathbf{p}_{t-1}$. The objective is to maximize the total expected discounted market value of the cash flows over the horizon.

For period $t \in \mathscr{T} \cup \{T+1\}$, let $V_t(x_t, \mathbf{p}_{t-1})$ denote the value function from period t onward given x_t and $\mathbf{p}_{t-1}$; if $t = T+1$, the value function is $V_{T+1}(x_{T+1}, p_T) := 0$. Let $\mathbb{E}_t[\cdot]$ be a shorthand notation for $\mathbb{E}_{\mathbf{P}_t}[\cdot|\mathbf{p}_{t-1}]$. For any period $t \in \mathscr{T}$, the value function $V_t(x_t, \mathbf{p}_{t-1})$ is the expected sum—given $\mathbf{p}_{t-1}$—of the optimal immediate payoff function and the discounted resulting value function for the next period, and thus satisfies the following recursion:

$$\begin{aligned} V_t(x_t, \mathbf{p}_{t-1}) &= \max_{a_t \in \Psi(x_t)} \mathbb{E}_t \left[R(a_t, P_t) + \delta V_{t+1} \left(\eta(x_t + a_t), \mathbf{P}_t \right) \right] \\ &= \max_{a_t \in \Psi(x_t)} \left\{ R(a_t, \mathbb{E}_t[P_t]) + \delta \mathbb{E}_t[V_{t+1} \left(\eta(x_t + a_t), \mathbf{P}_t \right)] \right\}, \end{aligned} \tag{3.2}$$

where $\delta \in (0, 1]$ is the one-period risk-free discount factor. The second equality follows because $R(a_t, \cdot)$ is linear. This model is consistent with a market value maximization formulation (Seppi 2002), i.e., we use risk-neutral probability measures, and use a constant risk-free rate to determine the discount factor.

3.4 Analysis

In this section, we derive the optimal policy structure of model (3.2). Define $y_t := \eta(x_t + a_t)$ as the ending inventory level in period t, thus $y_t \in [0, \eta]$ since $a_t \in [-x_t, 1 - x_t]$. Substituting $a_t = y_t/\eta - x_t$ into (3.2), for every period $t \in \mathscr{T}$ we obtain

$$\begin{aligned} V_t(x_t, \mathbf{p}_{t-1}) &= \max_{y_t \in [0,\eta]} R(y_t/\eta - x_t, \mathbb{E}_t[P_t]) + \delta \mathbb{E}_t \left[V_{t+1}\left(y_t, \mathbf{P}_t\right) \right] \\ &= \max\left\{ V_t^S(x_t, \mathbf{p}_{t-1}), V_t^B(x_t, \mathbf{p}_{t-1}) \right\}, \end{aligned} \tag{3.3}$$

where $V_t^S(x_t, \mathbf{p}_{t-1})$ is the optimal value function attainable by selling, and $V_t^B(x_t, \mathbf{p}_{t-1})$ by buying:

$$V_t^S(x_t, \mathbf{p}_{t-1}) := \max_{y_t \in [0, \eta x_t]} \left\{ -y_t \beta \mathbb{E}_t[P_t]/\eta + \delta \mathbb{E}_t[V_{t+1}\left(y_t, \mathbf{P}_t\right)] + x_t \beta \mathbb{E}_t[P_t] \right\}, \tag{3.4}$$

$$V_t^B(x_t, \mathbf{p}_{t-1}) := \max_{y_t \in [\eta x_t, \eta]} \left\{ -y_t \mathbb{E}_t[P_t]/(\alpha\eta) + \delta \mathbb{E}_t[V_{t+1}\left(y_t, \mathbf{P}_t\right)] + x_t \mathbb{E}_t[P_t]/\alpha \right\}. \tag{3.5}$$

To avoid trivial cases, we make the following standard assumption about price (Assumption 3.1). We then establish the convexity of our value functions in Proposition 3.1 (see Appendix B.1 for its proof).

Assumption 3.1. *For any $t \in \mathscr{T}$, $\mathbb{E}_t[|P_t|] < \infty$.*

Proposition 3.1. *For any $t \in \mathscr{T} \cup \{T+1\}$, it holds that $|V_t(x_t, \mathbf{p}_{t-1})| < \infty$ and $V_t(x_t, \mathbf{p}_{t-1})$ is convex in $x_t \in \mathscr{X}$ given any $\mathbf{p}_{t-1} \in \mathscr{P}$.*

For any period $t \in \mathscr{T}$, we can solve the original maximization problem in (3.2) by solving the two equivalent problems in (3.4) and (3.5). In each of the two objective functions, the last term is independent of the decision variable y_t, and hence can be omitted from the optimization, so (3.4) and (3.5) reduce to

$$W_t^S(x_t, \mathbf{p}_{t-1}) := \max_{y_t \in [0, \eta x_t]} -y_t \beta \mathbb{E}_t[P_t]/\eta + \delta \mathbb{E}_t[V_{t+1}\left(y_t, \mathbf{P}_t\right)], \tag{3.6}$$

$$W_t^B(x_t, \mathbf{p}_{t-1}) := \max_{y_t \in [\eta x_t, \eta]} -y_t \mathbb{E}_t[P_t]/(\alpha\eta) + \delta \mathbb{E}_t[V_{t+1}\left(y_t, \mathbf{P}_t\right)]. \tag{3.7}$$

Denote $y_t^{S*}(x_t)$ and $y_t^{B*}(x_t)$ as the optimal solution to (3.6) and (3.7), respectively. We characterize these optimal solutions in the following lemma.

Lemma 3.1. *$y_t^{S*}(x_t)$ can be either 0 or ηx_t; $y_t^{B*}(x_t)$ can be either ηx_t or η.*

Proof: Following from Proposition 3.1, $V_{t+1}(y_t, p_t)$ is finite and convex in y_t given any p_t. Thus as shown in the proof of Proposition 3.1, $\mathbb{E}_t[V_{t+1}(y_t, \mathbf{P}_t)]$ is finite because $\mathbb{E}_t[|P_t|]$ is finite, and $\mathbb{E}_t[V_{t+1}(y_t, \mathbf{P}_t)]$ is convex in y_t given any $\mathbf{p}_{t-1}$ as expectation preserves convexity. Adding finite linear terms does not alter the finiteness and convexity, thus both objective functions in (3.6) and (3.7) are finite and convex in y_t given any $\mathbf{p}_{t-1}$. Therefore, the maximizers of both objective functions can occur at only their corresponding end points, that is, $y_t^{S*}(x_t)$ can be either 0 or ηx_t; $y_t^{B*}(x_t)$ either ηx_t or η. □

Define $Y_t^S := y_t^{S*}(\eta)$ and $Y_t^B := y_t^{B*}(0)$, thus it follows directly from Lemma 3.1 that Y_t^S can be either 0 or $\eta \cdot \eta = \eta^2$, and Y_t^B can be either 0 or η. Relax (3.6) and (3.7) by setting $x_t = \eta$ and $x_t = 0$, respectively; define $\overline{w}_t^S(y_t, \mathbf{p}_{t-1})$ and $\overline{w}_t^B(y_t, \mathbf{p}_{t-1})$ as the objective functions of these two relaxed problems, respectively.

We next prove the existence of two critical thresholds using $y_t^{S*}(x_t)$ and $y_t^{B*}(x_t)$, and characterize these two thresholds using Y_t^S and Y_t^B. Then we will use these two thresholds to characterize the optimal policy structure of (3.4) and (3.5), and correspondingly the optimal policy for (3.2).

Lemma 3.2. *For any $t \in \mathscr{T}$ and $\mathbf{p}_{t-1} \in \mathscr{P}$, there exist feasible inventory levels $X_t^S(\mathbf{p}_{t-1})$ and $X_t^B(\mathbf{p}_{t-1})$ (simplified to X_t^S and X_t^B, respectively) such that*

$$\begin{cases} y_t^{S*}(x_t) = 0, & \text{if } x_t \in [0, X_t^S), \\ y_t^{S*}(x_t) = \eta x_t, & \text{if } x_t \in [X_t^S, \eta]; \end{cases} \qquad \begin{cases} y_t^{B*}(x_t) = \eta x_t, & \text{if } x_t \in [0, X_t^B], \\ y_t^{B*}(x_t) = \eta, & \text{if } x_t \in (X_t^B, \eta]. \end{cases}$$

Specifically, X_t^S and X_t^B can be computed by considering different values for Y_t^S and Y_t^B, respectively:

$$X_t^S = \begin{cases} \eta, & \text{if } Y_t^S = 0, \\ \max\ y_t/\eta \text{ s.t. } \overline{w}_t^S(y_t, \mathbf{p}_{t-1}) = \overline{w}_t^S(0, \mathbf{p}_{t-1}) & \text{if } Y_t^S = \eta^2; \end{cases} \tag{3.8}$$

$$X_t^B = \begin{cases} 0, & \text{if } Y_t^B = \eta, \\ \min\ y_t/\eta \text{ s.t. } \overline{w}_t^B(y_t, \mathbf{p}_{t-1}) = \overline{w}_t^B(\eta, \mathbf{p}_{t-1}), & \text{if } Y_t^B = 0. \end{cases} \tag{3.9}$$

Proof: According to Lemma 3.1, $y_t^{S*}(x_t)$ can be either 0 or ηx_t. Since the objective

Figure 3.1 Illustration of the inventory level X_t^S

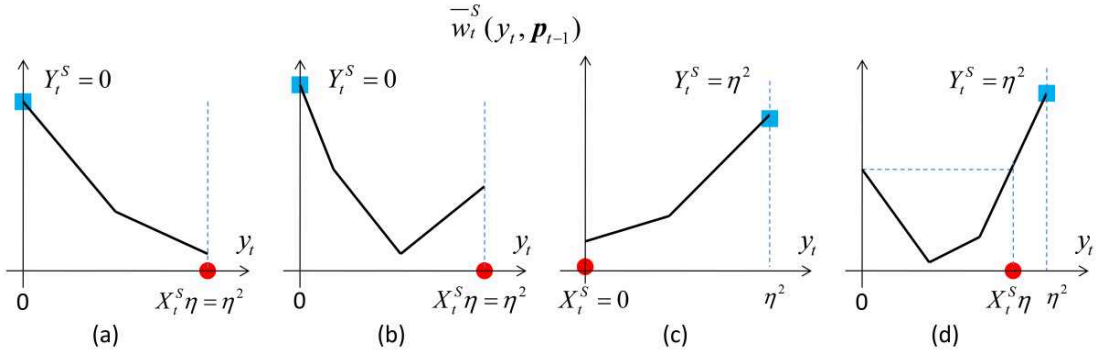

Note: The squares represent the global maximum for each figure, which correspond to the two different cases in (3.8); the dots represent the corresponding X_t^S for each case.

function in (3.6) is convex in y_t for any $x_t \in [0, \eta]$ (similar to the proof in Lemma 3.1), it follows that as x_t increases from 0 to η, there exists *one and only one* inventory level (denoted by X_t^S) below which $y_t^{S*}(x_t) = 0$ (sell down to zero), and above which $y_t^{S*}(x_t) = \eta x_t$ (do nothing). We can characterize X_t^S by considering the two different values of Y_t^S:

- If $Y_t^S = 0$ (either $\overline{w}_t^S(y_t, \mathbf{p}_{t-1})$ is non-increasing as in Figure 3.1(a), or it is not monotonic as in Figure 3.1(b)), then $X_t^S = \eta$, since $y_t^{S*}(x_t) = 0$ for all x_t.
- If $Y_t^S = \eta^2$ (either $\overline{w}_t^S(y_t, \mathbf{p}_{t-1})$ is non-decreasing as in Figure 3.1(c), or it is not monotonic as in Figure 3.1(d)), then X_t^S is the maximum value of y_t/η in the interval $[0, \eta x_t]$ such that $\overline{w}_t^S(y_t, \mathbf{p}_{t-1}) = \overline{w}_t^S(0, \mathbf{p}_{t-1})$. In this case, X_t^S can be either zero as in Figure 3.1(c), or nonzero as in Figure 3.1(d).

Similarly, for (3.7), since the objective function in (3.7) is convex in y_t for any x_t, then as x_t increases from 0 to η, there exists *one and only one* inventory level (denoted by X_t^B) *below* which $y_t^{B*}(x_t) = \eta x_t$ (do nothing), and above which $y_t^{B*}(x_t) = \eta$ (fill up). We can then define X_t^B as stated. □

The inventory level X_t^S splits the feasible inventory domain into two regions: a sell-all region on the left, and a do-nothing region on the right (see Figure 3.2). Likewise, X_t^B splits the inventory domain into two regions: a do-nothing region on the left, and a fill-up region on the right (see Figure 3.2). The value of X_t^S can be smaller than, equal to, or larger than the value of X_t^B; we characterize them in detail in Lemma 3.3.

Lemma 3.3. *For each period $t \in \mathcal{T}$, (i) both X_t^S and X_t^B change from 0 to η, as $\mathbb{E}_t[P_t]$ changes from $-\infty$ to ∞; (ii) if $\mathbb{E}_t[P_t] < 0$, then $X_t^S \geq X_t^B$; if $\mathbb{E}_t[P_t] \geq 0$, then it is possible that either $X_t^S > X_t^B$ or $X_t^S \leq X_t^B$.*

To prove the optimal structure in Proposition 3.2, we need the following Lemma 3.4 (see Appendix B.3 for its proof).

Lemma 3.4. *For any $t \in \mathscr{T}$, if $X_t^S > X_t^B$, the graphs of $V_t^S(\cdot, \mathbf{p}_{t-1})$ and $V_t^B(\cdot, \mathbf{p}_{t-1})$ cross at most once over $\mathscr{X}$. When they do cross, either one of the following conditions holds:*

- *If $X_t^S = \eta$, $X_t^B = 0$, and $\mathbb{E}[P_t] < 0$, then $V_t^S(\eta, \mathbf{p}_{t-1}) \geq V_t^B(\eta, \mathbf{p}_{t-1})$;*
- *Otherwise, $V_t^S(\eta, \mathbf{p}_{t-1}) \leq V_t^B(\eta, \mathbf{p}_{t-1})$.*

Remark: Note that by *crossing at most once*, we meant $V_t^S(\cdot, \mathbf{p}_{t-1})$ and $V_t^B(\cdot, \mathbf{p}_{t-1})$ have the same value at most once over the interval $\mathscr{X}$ excluding the two end points, that is, over the interval $(0, \eta)$. The above two conditions hold *only* when $V_t^S(\cdot, \mathbf{p}_{t-1})$ and $V_t^B(\cdot, \mathbf{p}_{t-1})$ do cross; they do not need to hold when $V_t^S(\cdot, \mathbf{p}_{t-1})$ and $V_t^B(\cdot, \mathbf{p}_{t-1})$ do not cross.

With Lemma 3.4, we can establish the optimal policy structure in the following proposition.

Proposition 3.2. *For each period $t \in \mathscr{T}$, the feasible inventory set $\mathscr{X}$ can be divided into at most three non-overlapping regions: a region where it is optimal to empty the storage facility, one where it is optimal to fill up the facility, and one to do nothing. Specifically,*

Case 1: *If $X_t^S \leq X_t^B$, the optimal action in stage t and state $(x_t, \mathbf{p}_{t-1})$ for model (3.2) is*

$$a_t^*(x_t, \mathbf{p}_{t-1}) = \begin{cases} -x_t, & \text{if } x_t \in [0, X_t^S), \\ 0, & \text{if } x_t \in [X_t^S, X_t^B], \\ 1 - x_t, & \text{if } x_t \in (X_t^B, \eta]. \end{cases} \tag{3.10}$$

Case 2: *If $X_t^S = \eta$, $X_t^B = 0$ and $\mathbb{E}[P_t] < 0$, when x_t varies from 0 to η in set $\mathscr{X}$, the optimal action in stage t and state $(x_t, \mathbf{p}_{t-1})$ for model (3.2) changes from filling up the facility to selling all the available inventory.*

Case 3: *If $X_t^S > X_t^B$ except under the condition in Case 2, when x_t varies from 0 to η in set $\mathscr{X}$, the optimal action in stage t and state $(x_t, \mathbf{p}_{t-1})$ for model (3.2) changes from selling all the available inventory to filling up the facility.*

Proof: ***Case 1:*** $X_t^S \leq X_t^B$

We will examine the optimal action in stage t and state $(x_t, \mathbf{p}_{t-1})$ for model (3.2), denoted by a_t^* for simplicity, in three regions separately:

i) For $x_t \in [0, X_t^S)$, as seen from Figure 3.2(a), the optimal decision for (3.6) is $y_t = 0$ (to

Figure 3.2 Illustration of Case 1, 2 and 3 in Proposition 3.2

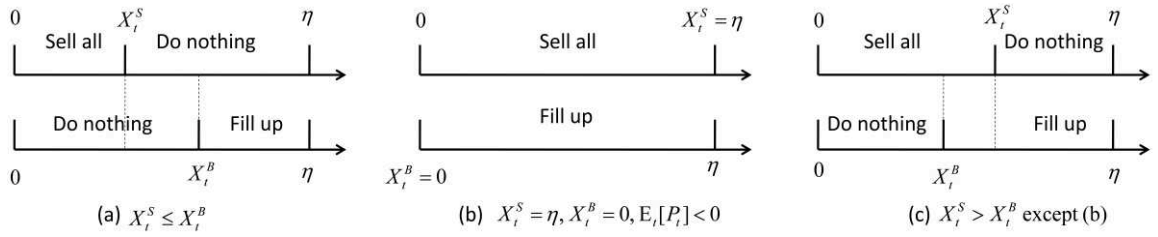

sell everything), and the optimal decision for (3.7) is to do nothing, which is also a feasible solution to (3.6). Thus, the optimal decision for (3.3) is $y_t = 0$, or, equivalently, $a_t^* = -x_t$.

ii) Similar to i), for $x_t \in (X_t^B, \eta]$, the optimal decision for (3.7) is to fill up, while for (3.6) is to do nothing, which is also a feasible action for (3.7). Thus, the optimal decision for (3.3) is $y_t = \eta$, or, equivalently, $a_t^* = 1 - x_t$.

iii) For $x_t \in [X_t^S, X_t^B]$, the optimal decisions for both (3.6) and (3.7) are to do nothing. Thus, the optimal decision for (3.3) is to do nothing.

Case 2 and Case 3: $X_t^S > X_t^B$

If $X_t^S > X_t^B$, for $x_t \in [0, X_t^B)$ the optimal decision is to sell all the available inventory, and for $x_t \in (X_t^S, \eta]$ the optimal decision is to fill up the facility. The interval $[X_t^B, X_t^S]$ requires further consideration, since the optimal decision for (3.6) is to sell all the available inventory while for (3.7) it is to fill up the facility.

To prove the optimal structure for this region, we use Lemma 3.4, which implies that when x_t varies over $\mathscr{X}$ the optimal action can change at most once. (Note that this property holds not only for region $[X_t^B, X_t^S]$, but for the entire $\mathscr{X}$.) Thus the set $\mathscr{X}$ can be partitioned into two regions: in each region, any inventory level has the same optimal ending inventory level, or, equivalently, optimal action.

However, to determine whether as x_t increase the optimal action would change from selling all to filling up, or vice versa, we need to consider the following two cases separately:

Case 2: $X_t^S = \eta$, $X_t^B = 0$ *and* $\mathbb{E}[P_t] < 0$.

In this case, it follows from Lemma 3.4 that when $V_t^S(\cdot, \mathbf{p}_{t-1})$ and $V_t^B(\cdot, \mathbf{p}_{t-1})$ do cross, we have $V_t^S(\eta, \mathbf{p}_{t-1}) \ge V_t^B(\eta, \mathbf{p}_{t-1})$, which means that when they cross, $V_t^S(\cdot, \mathbf{p}_{t-1})$ ends at a point no lower than that for $V_t^B(\cdot, \mathbf{p}_{t-1})$. Thus, the optimal structure can be only of the form in Figure 3.3(b), that is, as x_t increase, the optimal action changes from filling up to selling

Figure 3.3 The optimal policy structure for case 1 (panel a), case 2 (panel b), and case 3 (panel c) in Proposition 3.2

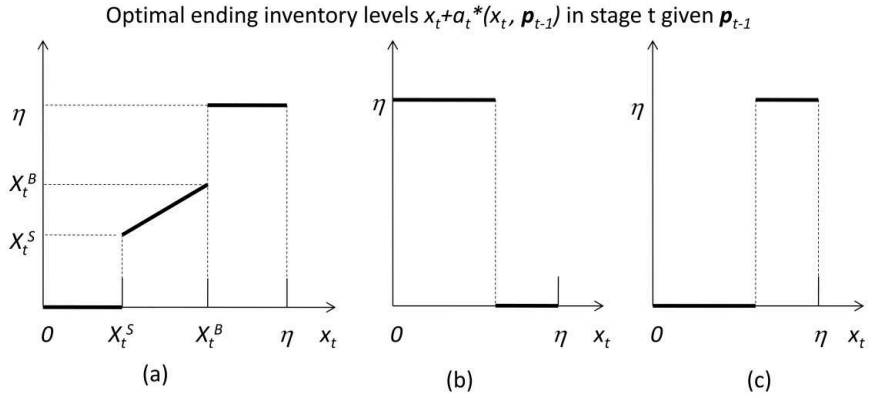

all. This structure includes two degenerated cases when these functions do not cross: for all $x_t \in \mathscr{X}$, the optimal action is to fill up; or for all $x_t \in \mathscr{X}$, the optimal action is to sell down to zero.

Case 3: $X_t^S > X_t^B$ *except the scenario in Case 2*

Similar to Case 2, it follows from Lemma 3.4 that when $V_t^S(\cdot, \mathbf{p}_{t-1})$ and $V_t^B(\cdot, \mathbf{p}_{t-1})$ do cross, we have $V_t^S(\eta, \mathbf{p}_{t-1}) \leq V_t^B(\eta, \mathbf{p}_{t-1})$; thus the optimal structure can be only of the form in Figure 3.3(c), that is, as x_t increase, the optimal action changes from selling all to filling up. When these functions do not cross, this structure includes the same two degenerated cases as in Case 2. □

Figure 3.3(a) shows the optimal policy structure for Case 1: it consists of three ordered regions corresponding to the optimal action of discharging, doing-nothing, and charging, but some regions may be empty. For instance, it is possible that $X_t^S = X_t^B = \eta$, in which case the optimal decision is to sell down to zero at all initial inventory levels, i.e., all of $\mathscr{X}$ is a discharging region, and the other two regions are empty.

For Case 2 and 3, $\mathscr{X}$ is divided into two regions: discharging and charging; the do-nothing region is reduced to a single point. Again one region can be empty.

Lemma 3.3 complements Proposition 3.2 in illustrating the price regions for which the optimal policy structure of Case 1, 2 and 3 would occur, that is if $\mathbb{E}_t[P_t] < 0$, the optimal structure can be from either Figure 3.3(b) or (c); when $\mathbb{E}_t[P_t] \geq 0$, the optimal structure can be from either 3.3(a) or (b).

We next examine how $V_t(x_t, \mathbf{p}_{t-1})$ changes with different parameters. Specifically, the

Figure 3.4 The optimal policy structure by Charnes et al. (1966) when prices are positive

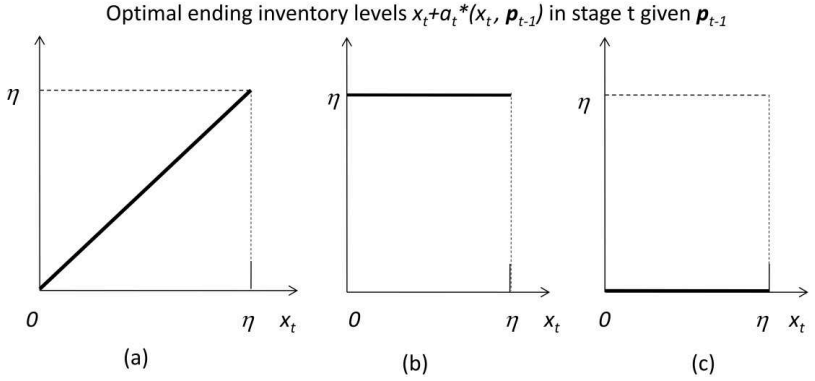

following proposition illustrates how $V_t(x_t, \mathbf{p}_{t-1})$ changes with α. We elaborate on this in the numerical analysis.

Proposition 3.3. *For each period $t \in \mathscr{T}$, if $\mathbb{E}_t[P_t] < 0$, there always exists an $\bar{\alpha}$ such that if $\alpha \leq \bar{\alpha}$, $V_t(x_t, \mathbf{p}_{t-1})$ increases when α decreases.*

We have shown that the three patterns in Figure 3.3 characterize the optimal structure of our MDP. This structure generalizes the optimal structure established by Charnes et al. (1966) when the commodity price can be only positive: In this case the optimal action in a given stage and state is the same for all inventory levels: either do nothing, fill up the facility, or empty it, as in Figure 3.4(a), (b) and (c), respectively. Each pattern in Figure 3.4 is a special case of a pattern in Figure 3.3. Note that the optimal ending inventory levels in the structure of Charnes et al. (1966) are monotone in inventory; however, this is not always true in our structure (see Figure 3.3).

Mathematically, this difference is due to the *linearity* in inventory of the value functions of the model of Charnes et al. (1966), and the *convexity* in inventory of the value functions of our model, as shown in Proposition 3.1. This disparity in value functions is remarkable, as the value functions of other storage models (see, e.g., Secomandi 2010b) are concave rather than convex in inventory. In the following example, we demonstrate how negative prices together with the effect of a round-trip efficiency less than one give rise to a value function that is convex in inventory. This example also illustrates Proposition 3.2.

Example 3.1. *For simplicity, we assume no loss in charging or storing over time ($\alpha = \eta = 1$). However, half of the electricity will be lost in discharging ($\beta = 0.5$). The time horizon consists of three periods, thus $T = 3$; their prices are deterministic and equal to -4, -3, and*

Figure 3.5 The optimal value function and optimal ending inventory level in stage 1 for Example 3.1

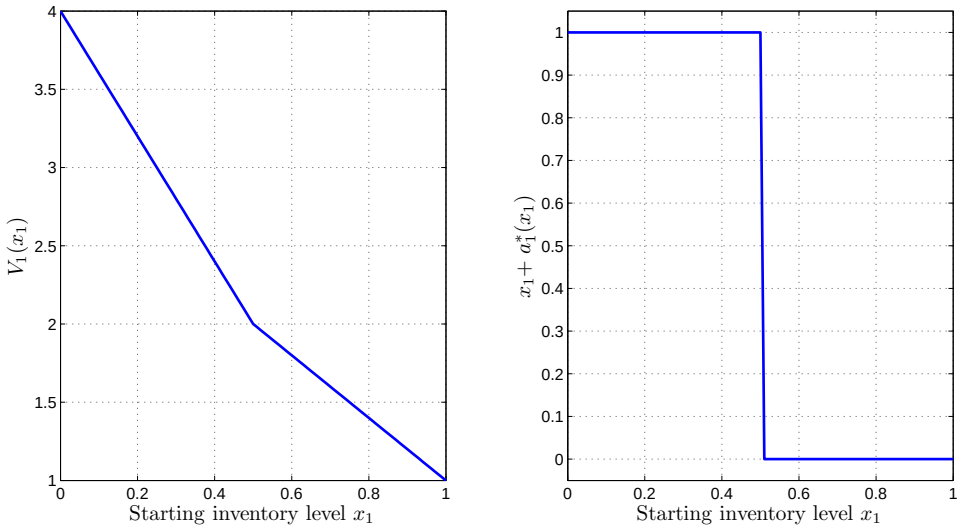

0 respectively. The value function for the second period is (we omit the price argument as it is obvious from the example setup)

$$V_2(x_2) = \max\left\{ \max_{-x_2 \le a_2 \le 0} \{-a_2 \cdot (-3) \cdot 0.5 + 0\}, \max_{0 \le a_2 \le 1-x_2} \{-a_2 \cdot (-3) + 0\} \right\} = 3(1 - x_2).$$

The value function for the first period is

$$\begin{aligned} & V_1(x_1) \\ =& \max\left\{ \max_{-x_1 \le a_1 \le 0} \{-a_1 \cdot (-4) \cdot 0.5 + 3(1 - x_1 - a_1)\}, \max_{0 \le a_1 \le 1-x_1} \{-a_1 \cdot (-4) + 3(1 - x_1 - a_1)\} \right\} \\ =& \max\left\{ \max_{-x_1 \le a_1 \le 0} \{-a_1 + 3 - 3x_1\}, \max_{0 \le a_1 \le 1-x_1} \{a_1 + 3 - 3x_1\} \right\} \\ =& (4 - 4x_1) \cdot \mathbf{1}(0 \le x_1 \le 0.5) + (3 - 2x_1) \cdot \mathbf{1}(0.5 \le x_1 \le 1), \end{aligned}$$

where $\mathbf{1}(\cdot)$ *is an indicator function: one if the inequalities in the parenthesis are satisfied; zero otherwise.*

Thus $V_1(x_1)$ *is convex in* x_1 *(see the left panel of Figure 3.5). The optimal inventory decision is to fill up the storage facility when* x_1 *is less than a half, and to sell all the available inventory otherwise (see the right panel of Figure 3.5), which is an example of the structure in Figure 3.3(b). It is easy to show that* $X_1^S = \eta$ *and* $X_1^B = 0$*: Defining* $y_1 := x_1 + a_1$*, we obtain that* $y_1^S(\eta) = Y_t^S = 0$ *and* $y_1^B(0) = Y_t^B = \eta$*, then apply Lemma 3.2.* □

The intuition for Example 3.1 is as follows: Since the price trajectory is -4, -3, 0, filling up the storage facility in period 1 is always better than filling it up in period 2, and in period 2 selling any inventory level is never optimal. The only issue is then whether it may be optimal to empty the storage facility in period 1 and to fill it up in period 2, rather than filling it up in period 1 and doing nothing in period 2. The payoff of the first strategy is $3 - 2x_1$; the payoff of the second strategy is $4 - 4x_1$. The first strategy is better than the second one if and only if $3 - 2x_1 > 4 - 4x_1$, that is, $x_1 > 0.5$. This means that in period 1 it is optimal to empty when the inventory level exceeds 0.5, and it is optimal to fill up when the inventory level is less than or equal to 0.5. This illustrates how an efficiency loss (in this example 50% for charging) combined with negative prices can induce a nontrivial relationship between inventory availability and an optimal action; that is, emptying the storage facility at high inventory levels (above 0.5) and filling it up at low inventory levels (at or below 0.5). This nontrivial relationship manifests itself in the convexity of the optimal value function in inventory in period 1.

Example 3.2. *This example has the same efficiency as Example 3.1, but it has four periods. In the first period, the price is deterministic: 4; the price of the last three periods is stochastic, with equal probability to be either of the following three paths:* $(-12, -10.8, 0)$, $(-12, -7.5, 0)$, *and* $(54, 0, 0)$.

Using the same method in Example 3.1, we can compute—for each of the three price paths—the value function of the second stage. We then combine these three price paths to obtain the expected value function for stage two, which is the continuation valuation function for stage 1. Similarly, we compute the value function for stage 1 and its optimal ending inventory level versus the starting inventory level, which we plot in Figure 3.6. (Detailed derivation is available upon request.) This demonstrates an example of the optimal structure in Figure 3.3 (a).

3.5 Numerical analysis

In this section, we examine the market value of an electricity storage facility by applying the optimal policy established in §3.4, in conjunction with an electricity price model from Chapter 2. We first discuss the numerical setup in §3.5.1; we then discuss our numerical results on

Figure 3.6 The optimal value function and optimal ending inventory level in stage 1 for Example 3.2

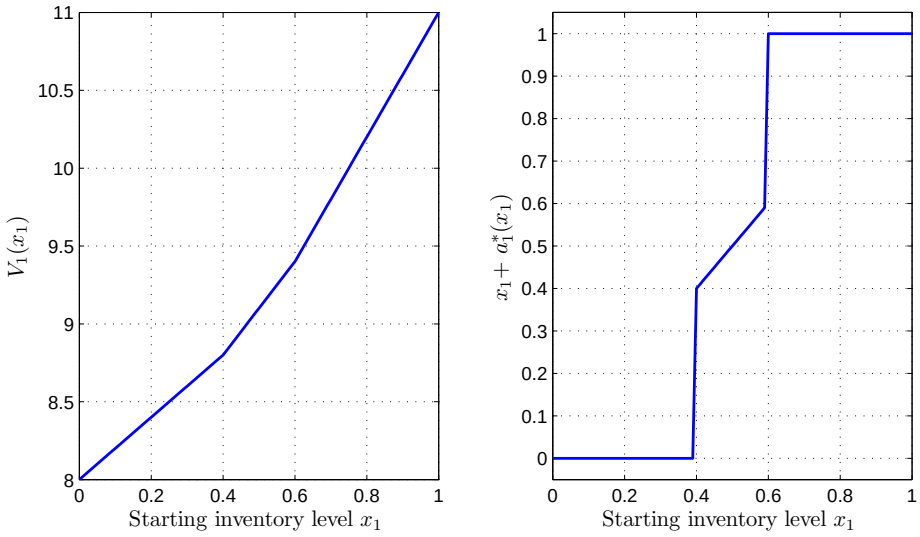

Table 3.1 Estimated parameters for the mean reversion, seasonality, and jump model for every eighth hours (MAE = \$14.32/MWh)

Mean Reversion		Seasonality							Jumps
κ	σ	A	B	γ_1	ω_1	γ_2	ω_2	μ	λ
0.2736	18.7771	77.1156	−0.6235	4.4012	−161.7086	−18.5844	1.9777	0.0032	0.0459

comparing the two strategies of dealing with surpluses in §3.5.2, and on the value lost by ignoring negative prices in §3.5.3.

3.5.1 Setup

In the ensuing analysis, we focus on one specific type of storage technology, and choose its parameters from the standard range in Eyer and Corey (2010): a battery that has an energy capacity of 8 MWh and can be fully charged/discharged within eight hours. Thus we set eight hours as the length of each period, which is also the period length in the price model.

We use the same price model and the same calibration method as in Chapter 2, but the input data for calibration is the average price of every eight hour block (three blocks of each day: 00:00-8:00, 8:00-16:00, 16:00-24:00) of the data used in Chapter 2. We show the calibration result for all the three components of the price model in Table 3.1, and the jump size distribution in Table 3.2.

To solve our MDP, we use backward dynamic programming. To compute the optimal action for each state in each period t, we leverage the optimal policy structure obtained in §4.

Table 3.2 Jump size distribution

Size	-300	-250	−200	−150	−100	−50	0	50	100
Probability	0.005	0.0100	0.0149	0.0249	0.0647	0.0498	0.1343	0.2338	0.2338
Size	150	200	250	300	350	400	450	500	
Probability	0.0846	0.0796	0.0299	0.0050	0.0100	0.0100	0.0050	0.0050	

Assuming that the battery starts empty, according to Proposition 3.2, the possible inventory levels visited by an optimal policy in period t is 0, η, ..., η^{t-1}. Thus, for each period t we only need to compute the value functions at these inventory levels. In addition, as in Chapter 2, we discretize the mean reversion process as a trinomial lattice based on the method in Jaillet et al. (2004). In summary, the state variable for each stage in our MDP is the discretized triple (inventory level, mean reversion level, jump size).

We solve the MDP in (3.2) for a horizon of one year, so the total number of periods (stages) is the product of the number of days in a year and the number of periods per day: $365 \cdot 3 = 1,095$ periods. The discount factor δ for each stage (period) is 0.99999, corresponding to an annual risk-free interest rate of 1% with continuous compounding (recall that we use risk-neutral valuation, but we assume a zero market price of risk). In the following experiments, we vary the round-trip efficiency, denoted by r, by varying α, β, and η: α and β can be any number in (0,1]; η is chosen from the set $\{1, 0.9997, 0.9983, 0.9962\}$, which corresponds to the self-discharge rate over a month of 0% for a sodium sulfur, 3% for a lead acid, 15% for a NiCad, and 20% for a NiMH (EPRI 2004, Linden and Reddy 2002).

3.5.2 Comparison of the value of destroying and storing surpluses

Recall that our goal is to assess the relative merits of two strategies for dealing with surpluses, storing or destroying them. To do this, we compare the total expected discounted values of our MDP for different round-trip efficiencies r ranging from 0.01 to 1. For each round-trip efficiency, this total value is the value function at zero inventory level in the initial stage. (Note that these values do not include capital costs, as our model assumes that the battery already exists.) We model the disposal and storage strategies by setting $r = 0.01$ and $r = 1$, respectively. The other considered values for the parameter r correspond to intermediate strategies.

If the electricity price is strictly positive, then we would expect the total value to increase when the storage facility becomes more efficient, that is, as the round-trip efficiency parameter

Figure 3.7 Total value in a year for different round-trip efficiencies

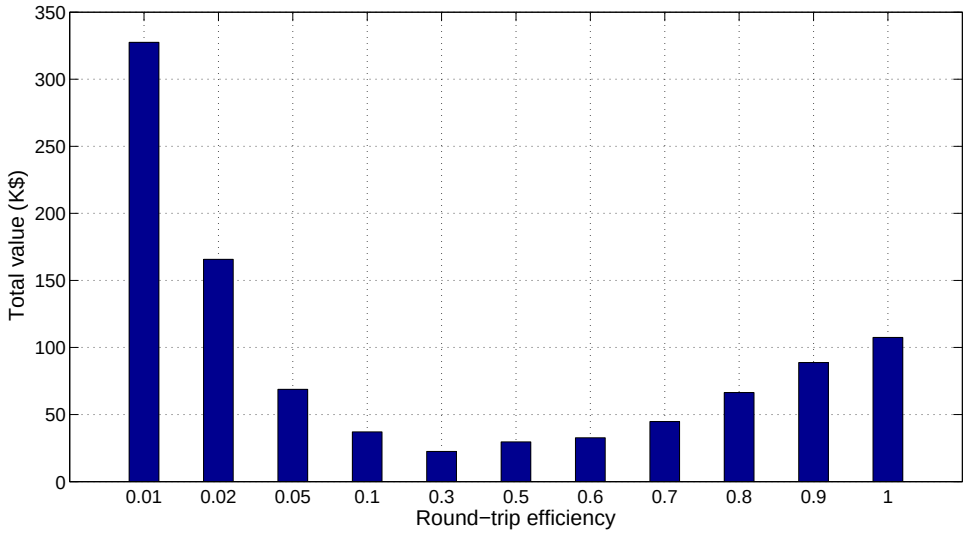

Note: The x-axis values are not evenly spaced.

r becomes larger. However, due to the possibility of negative electricity prices, this is *not* true in general. As seen in Figure 3.7, as the round-trip efficiency increases from 0.01 to 1, the total value of the facility first decreases, and then increases after 0.3. In Figure 3.7, we assume $\beta = \eta = 1$ and vary α, so the round-trip efficiency r equals α. The value of $\$66,403$ for a battery with round-trip efficiency 0.8 in Figure 3.7 is consistent with the range of values for comparable batteries reported by Denholm et al. (2010). We repeated this experiment for a range of different β and η values, and found the same non-monotonic phenomenon as we vary α. (This non-monotonicity illustrates Proposition 3.3.)

This non-monotonicity results from negative prices combined with low round-trip efficiencies: The greater the loss in charging, the more electricity is needed to fill up a battery, and the more value the merchant can obtain by buying electricity at a negative price. Thus, an inefficient battery creates market value primarily by destroying electricity surpluses when purchasing them at negative prices. This is in stark contrast to an efficient one, which creates market value by storing electricity surpluses: purchasing them at low, mainly positive, prices and reselling them at higher prices. Next we further explore this difference.

We compare the value breakdown of a perfect battery ($r = 1$, solid bars) and an inefficient one ($r = 0.01$, grey bars) over different price intervals in Figure 3.8. In this figure, each bar within each price interval represents the total expected discounted cash flow in this price interval over the entire horizon. For a perfect battery, most of the notably positive bars

Figure 3.8 Value for $r = 1$ and $r = 0.01$ at different price intervals

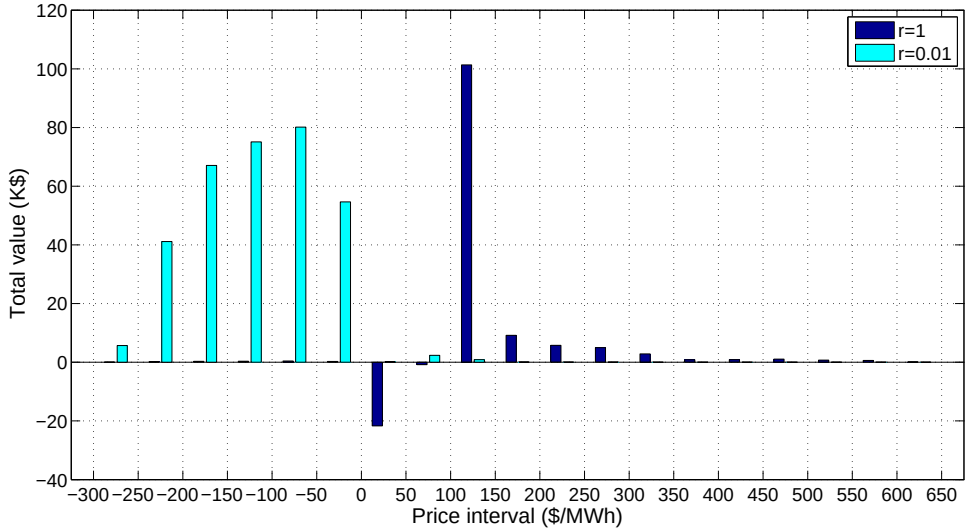

are above \$100/MWh, with the highest value in the interval [100\$/MWh, 150\$/MWh]; the most notable negative value, which denotes purchasing costs, is in the interval [0\$/MWh, 50\$/MWh]. So if $r = 1$, most of the value comes from buying at low positive prices and selling at high positive prices. This contrasts with the graph for an inefficient battery, for which most of the positive bars spread over the negative price range: The majority of the market value of such a battery comes from buying and burning electricity when price is negative. Thus, setting $r = 0.01$ is a fairly accurate model of the disposal strategy.

To further demonstrate the different approaches of optimally managing a perfect battery and an inefficient one, we plot the total quantity sold and bought at different price intervals in Figures 3.9 and 3.10, respectively. These figures indicate that a perfect battery sells much more than an inefficient one;the former typically buys at low positive price intervals, from [0\$/MWh, 100\$/MWh] (it also infrequently buys at negative prices, though this is not apparent from Figure 3.10), and the latter buys predominately at negative prices (it also buys at extremely low positive prices, though almost never and thus apparent from Figure 3.10).

Our experiments shows that the value of a battery with round-trip efficiency 0.01 exceeds that of a perfect battery, suggesting that the disposal strategy is even more valuable than the storage strategy. This superiority implies that destroying electricity surpluses with an extremely inefficient storage facility, or even a load bank (a device that acts as an electricity load to consume power) is likely to be more valuable than storing surpluses using a battery with high performance. The advantage of the disposal strategy over the storage strategy may

Figure 3.9 Total quantity sold for $r = 1$ and $r = 0.01$ at different price intervals

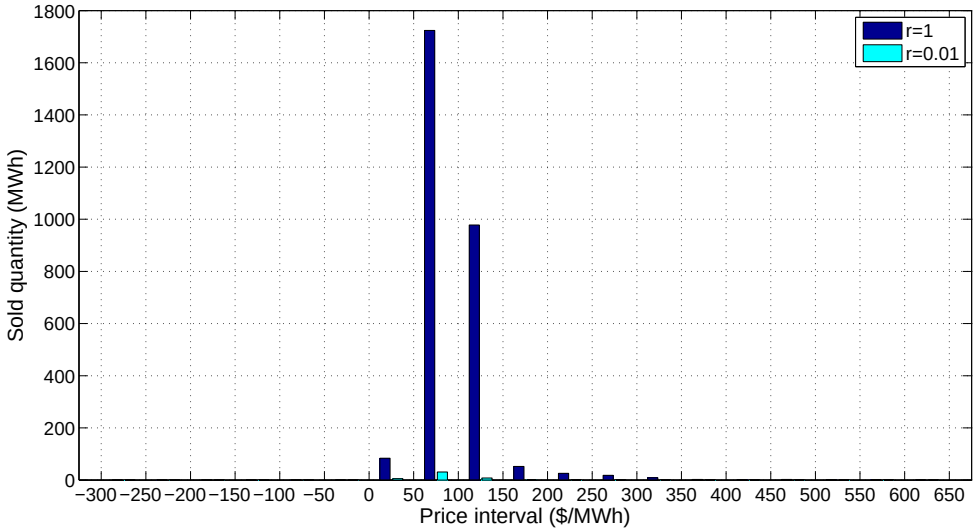

Figure 3.10 Total quantity bought for $r = 1$ and $r = 0.01$ at different price intervals

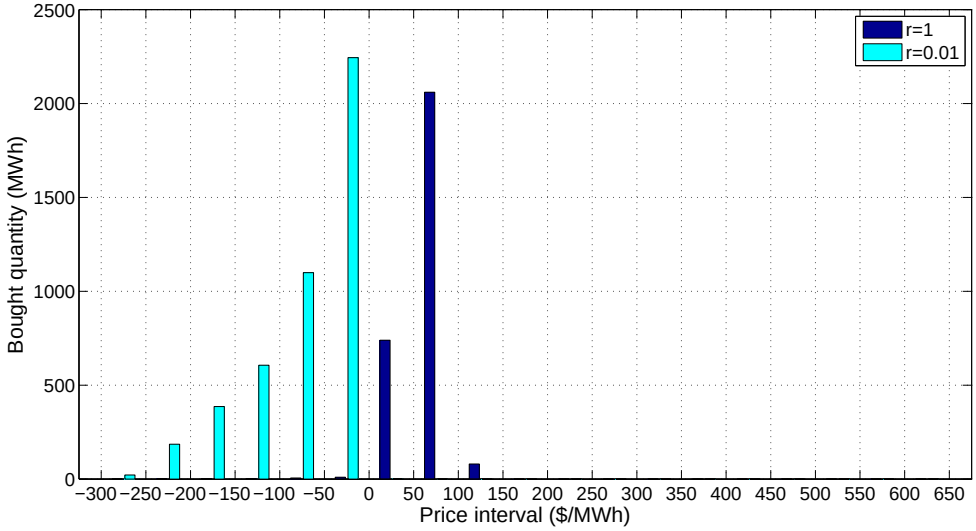

Figure 3.11 Comparing the values at different round-trip efficiencies for both the cases considering and ignoring negative prices

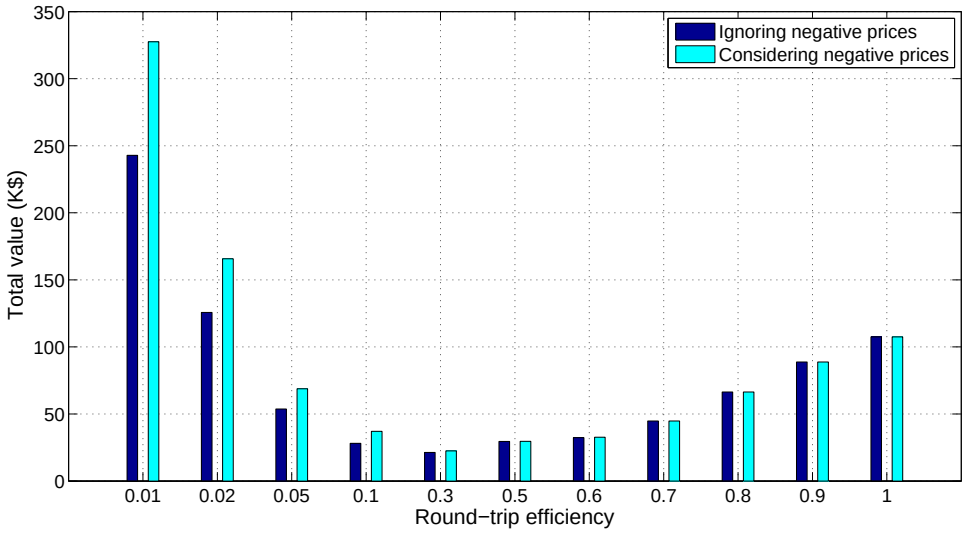

be even more substantial in the Electric Reliability Council of Texas (ERCOT 2008) and the European Energy Exchange (Brandstätt et al. 2011, Nicolosi 2010) as compared to our experiments using NYISO data, because these two markets exhibit larger and more frequent negative prices.

3.5.3 Value lost in ignoring negative prices

We have illustrated in §3.4 that the existence of negative prices can change the optimal inventory policy from Charnes et al. (1966) to that shown in Proposition 3.2. We now illustrate how much value is lost for both the storage and disposal strategy if one ignores negative prices and assumes the policy from Charnes et al. (1966) is optimal. To do so, for each round-trip efficiency we compare the optimal value obtained in Figure 3.7 with the value for the case in which we ignore negative prices in determining our operating strategy. To compute the latter, we first construct a price model that ignores negative prices, then obtain its corresponding optimal action, and finally apply these actions in the original price model. We construct a price model that ignores negative prices based on the original price model by truncating any negative $\mathbb{E}_t[P_t]$ in the immediate payoff function in the MDP (3.2) to zero. We chose not to truncate any negative p_t to zero because the underlying price distribution is inflated, and it is hard to isolate the effect of a wrong price distribution from the effect of ignoring negative prices.

Figure 3.12 Value breakdown into different price intervals when $r = 0.01$

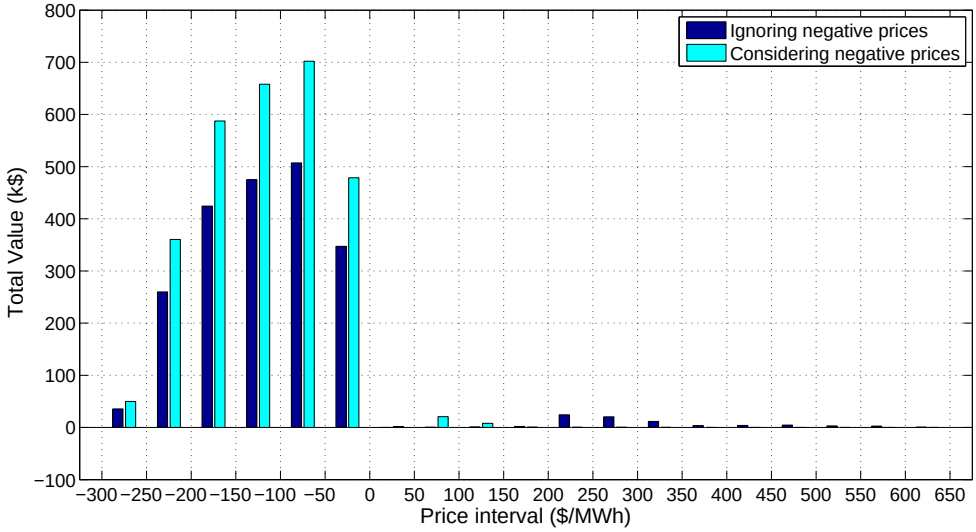

We compare these two sets of value for different round-trip efficiencies in Figure 3.11: the value considering negative expected prices and the value ignoring them. We can see from this figure that the value of the storage strategy ($r = 1$) does not change much if we ignore negative conditional expected prices. However, the value of the disposal strategy ($r = 0.01$) decreases significantly: from $\$327,511$ to $\$242,861$, a decrease of around 25.9%. This is not surprising given the findings of Figure 3.9 and 3.10: since the value of the storage strategy stems mainly from sales at positive prices, this value would not be far off even if negative expected prices are ignored; since the value of the disposal strategy comes mainly from purchases at negative prices, this value may drop considerably if we ignore negative expected prices.

We investigate this difference further in Figure 3.12, which shows the value breakdown into price intervals for considering and ignoring negative prices when $r = 0.01$. Figure 3.12 shows that if we ignore negative prices, we hold the electricity longer hoping for a good positive price to sell; if we do consider the negative prices, we sell as soon as possible if price is positive so that the battery is ready to absorb more negative prices, the major source of earnings. As a result, for the negative price brackets, the values for considering negative prices are higher than those ignoring these negative prices.

3.6 Conclusions

Motivated by the empirical observation that electricity prices can be negative, we investigate whether it is more valuable for merchants to manage electricity surpluses by storing them or destroying them. We evaluate these two strategies by considering a storage facility with different round-trip efficiencies: a high round-trip efficiency corresponds to the storage strategy; a low round-trip efficiency to the disposal strategy. We model this problem as an MDP and derive its optimal policy structure, which generalizes a classic result by Charnes et al. (1966). We apply this optimal policy to data and find that the disposal strategy has even more value for a merchant than the storage strategy. In addition, we find that the value of the storage strategy arises from purchasing electricity primarily at low *positive* prices and reselling the stored electricity at higher prices, whereas the disposal strategy generates value primarily by buying electricity at negative prices and destroying it.

Our model and conclusions are intriguing, but they are also limited in the following ways. First, we assume that the merchant makes a decision every eight hours, a period long enough to fully charge/discharge a storage facility without significantly shortening its life expectancy. In reality, however, these trading decisions can be made more frequently, for instance every hour, during which charging/discharging may not have been completed. If such decisions are permitted, flow rate constraints would have to be added to our model, such as in Chapter 2. Second, since we assume the merchant is a price taker, our model does not capture the equilibrium behavior of all players in the market. Third, in comparing the values of the disposal and storage strategies we assume that the facilities (including power electronics) associated with these two strategies already exist, and we thus ignore their capital costs. If these facilities need to be developed, then these costs would have to be included in our analysis. The main difficulty here would be gathering data on the cost of a device to destroy electricity, such as an extremely inefficient battery or, alternatively, a load bank. It is unclear how our conclusions might change when relaxing these limitations, which could be addressed by future research.

Chapter 4

Combining Operations Management and Engineering Models to Effectively Manage Electricity Storage

4.1 Introduction

Electricity storage has the potential to play an important role in many aspects of the global economy: grid-level electricity storage can help match electricity supply and demand in a market (as in Chapter 3); it can support the growth of renewable energy, such as wind and solar energy, mitigating their variability and intermittence (as in Chapter 2); and electricity storage such as car batteries can enable the development of Plug-in Hybrid Electric Vehicles (PHEVs) or Battery Electric Vehicles (BEVs). California is in the process of enacting laws to mandate a minimum amount of electricity storage for 2015 and 2020 (CPUC 2012). Thus, it is crucial to manage electricity storage properly and value storage correctly.

When electricity storage is managed or valued (say in an electricity market), it is often implicitly assumed that characteristics such as energy capacity and round-trip efficiency are

This chapter is a joint work with Jay Apt, Alan Scheller-Wolf, Nicola Secomandi, and Stephen Smith.

static. We assumed this in Chapter 2 and 3; similar assumptions are made in Graves et al. (1999), Hittinger et al. (2010), Sioshansi et al. (2009), Walawalkar et al. (2007), Xi et al. (2011), and Hittinger et al. (2012). However, these characteristics are inherently dynamic, being functions of the usage history of the storage facility and the corresponding operating conditions: Energy capacity degrades over time, and may degrade more rapidly with higher discharging speed (EPRI 2004); round-trip efficiency decreases with rapid charging/discharging, according to Peukert's law (Peukert 1897).

It has not been established whether these dynamics materially affect the optimal management, or the valuation of a storage facility. Therefore, we answer the following two sets of questions:

(Q1) What is the effect if we operate a battery as if it did not have these dynamics? For instance, how suboptimal is it to operate a battery as if it did not degrade? As if it were immune to efficiency variation? What about both?

(Q2) What is the effect of modeling these dynamics on valuing a battery? Concretely, if we value an "ideal" battery (everything else being equal except without efficiency variation or energy capacity degradation), how much would we overvalue this battery? What if we ignore both?

The first question addresses the necessity of considering battery dynamics in operating a battery; the second question gives an upper bound on the value of improving a battery's characteristics, and also shows how inaccurate the valuation of a battery can be if we assume that a battery is "perfect" when it is not.

There are two papers that do consider energy capacity degradation in valuing batteries: Jenkins et al. (2008) and Peterson et al. (2010b). However, they do not optimize the operation of the battery: Jenkins et al. (2008) consider how to size a battery by factoring in energy capacity degradation; Peterson et al. (2010b) treat degradation as a fixed cost. Thus, it remains uncertain how the dynamics of energy capacity affect the optimal operating policy, and the ultimate valuation, which depends on this optimal operating policy.

To study the effect of both dynamics in operating and valuing storage, we use a representative setting: operating a battery in an energy arbitrage market. We model this problem as a finite-horizon Markov Decision Process (MDP). Since the dynamics of energy capacity and efficiency are battery specific, we examine three types of batteries: lead acid, the cheapest

and among the most widely-used battery technologies (EPRI 2004); lithium-ion, the most widely-adopted battery technology in the development of new PHEVs and BEVs; and Aqueous Hybrid Ion (AHI), a newly-commercialized battery technology (AquionEnergy 2011). For each type of battery chemistry, we model energy capacity degradation and efficiency variation separately, calibrating them against data from representative manufacturers.

We operate the batteries every hour over a twenty-year horizon—long enough for battery dynamics to be fully exhibited—incorporating the same financial engineering price model as in Chapter 2 calibrated to electricity prices form NYISO. We study the importance of modeling either (i) energy capacity degradation, or (ii) efficiency variation, or (iii) both together, determining answers to both Q1 and Q2.

For each question, we use as a benchmark the value of operating an actual battery with energy capacity 1MWh optimally, taking into account both degradation and efficiency variation. We find these benchmark values to be \$88,000, \$390,000, and \$397,000, for lead acid, lithium-ion, and AHI battery, respectively. These values do not account for capital costs, which are \$300,000, \$600,000, and \$200,000. Our numerical results also show the following:

(i) *Energy capacity degradation*: it is quite suboptimal to operate a battery that degrades as if it did not: sacrificing around 66% of the optimal value for a lead acid battery, around 54% for a lithium-ion battery, and 17% for an AHI battery. This implies that it is imperative to take into account energy capacity degradation when operating a battery. In valuing storage, our analysis shows that if we assume that the battery is free from degradation, we would be too optimistic by a large margin: we may overvalue lead acid by around 135%, lithium-ion by 119%, and AHI by 37%.

(ii) *Efficiency variation*: if we operate a battery as if its efficiency were constant at its rated level, lithium-ion is almost unaffected (within 1% of optimality), but this is not so for lead acid and AHI: they lose around 7% and 9% of their optimal values, respectively. Furthermore, if we value batteries by assuming their efficiencies are fixed at nominal levels, we may overvalue a lead acid battery by 4%, a lithium-ion battery by about 6%, and an AHI battery by about 14%. Thus, accounting for energy capacity degradation in the operation and valuation of a battery is quite important, but accounting for efficiency variation is less so.

(iii) *Both energy capacity degradation and efficiency variation*: if we operate a battery as if it had neither dynamic, the loss of optimal value is even larger than the sum of the

loss of optimality from ignoring either one independently: We may lose 81% of optimality for lead acid, and 65% for lithium-ion, and 47% for AHI. Likewise, if we improve the battery in both features, we may increase the value by 233%, 156%, and 80% for lead acid, lithium-ion, and AHI, respectively. This means that the benefit is greater than the sum of the benefit of improving each feature independently: Accounting for degradation and efficiency variation is complementary.

(iv) *Profitability:* If the capital costs are taken into account, we find that the only battery that can potentially break even through energy arbitrage over a twenty-year horizon is an AHI battery, due to its extremely low energy capacity degradation and next-to-lowest cost among all three types of batteries. These results hold under different salvage values or costs.

The above results can give guidance to managers when operating a storage facility: energy capacity degradation cannot be safely ignored; for efficiency, it depends on the battery chemistry. In addition, our results show that in deciding whether to purchase a battery, if one ignores battery dynamics, one may easily err on the optimistic side, overvaluing the battery. Furthermore, our results shed light on the area of greatest potential for battery engineers to focus on: reducing degradation may be more effective than fighting Peukert's law. These results are potentially relevant for other applications of storage as well: In particular, our modeling of energy capacity degradation and efficiency variation can also be used to value batteries in such applications as operating electric vehicle fleets (Kleindorfer et al. 2012), and coupling with renewable energy.

The rest of this chapter is organized as follows: we introduce our MDP model in §4.2 and characterize and calibrate the dynamics of energy capacity and efficiency in §4.3. We discuss our numerical analysis and report our results in §4.4. We conclude with future work in §4.5.

4.2 Model

We model the problem of managing a battery in an electricity wholesale market (specifically in an energy arbitrage market) over a finite horizon considering the dynamics of energy capacity and efficiency. At the beginning of the finite horizon, the operator buys a battery and incurs a capital cost; at the end of the horizon, the operator either salvages the battery or disposes

[4]This is as opposed to an ancillary market, in which each player provides service such as regulation and spinning reserve. The ancillary market is much smaller than the energy market, and thus can easily be saturated.

of it at a cost. In between, the operator manages the battery periodically in each period $t \in \mathscr{T} = \{1, \cdots, T\}$ according to the following sequence of events:

1) At the beginning of each period t, the operator observes the state variables $S_t := (x_t, M_t, \mathbf{p}_{t-1})$, which are defined as follows (where the initial state variable is $S_1 := (x_1, M_1, \mathbf{p}_0)$):

- x_t, the current inventory level (the quantity of energy stored in the battery; in MWh);
- M_t, the current energy capacity (the maximum amount of energy that the battery can hold). We normalize the maximum energy capacity to be one, so $M_t \in [0, 1]$, and $x_t \in [0, M_t]$.
- $\mathbf{p}_{t-1}$, electricity price in period $t-1$, which gives the conditional probability distribution of $\mathbf{p}_t$, the price for period t. $\mathbf{p}_{t-1}$ and $\mathbf{p}_t$ are vectors, as in Chapter 2 and 3. We discuss $\mathbf{p}_t$ further below.

2) The operator decides the quantity of energy to charge or discharge in this period t, denoted by $a_t \in \mathbb{R}$. Similar to Chapter 2 and 3, if $a_t < 0$, a_t is the quantity of inventory decrease due to selling; if $a_t \geq 0$, a_t is the quantity of inventory increase due to buying.

3) Price $\mathbf{P}_t$ for period t, denoted by $\mathbf{p}_t$, is revealed (as mentioned in Chapter 2, this chapter adopts the same convention as in Chapter 2 to denote a random variable: a random variable is denoted in upper case, and its realization in lower case), and the financial settlement for the trading action a_t is completed. $\mathbf{P}_t$ is the only source of uncertainty in the model; we use the same price transition function as in Chapter 2. As before, P_t and p_t denote the sum of all the components in $\mathbf{P}_t$ and $\mathbf{p}_t$, respectively.

4) At the end of each period t, inventory becomes $(x_t + a_t)\eta$, where η is the self-discharge rate per period, as in Chapter 2 and 3; the energy capacity degrades to $M_t - H(a_t)$, where $H(a_t)$ is the energy capacity degradation in period t due to action a_t, which we specify in §4.3.1.

For each period $t \in \mathscr{T}$, let $R(a_t, p_t)$ denote the immediate payoff function, which is either the purchasing cost if $a_t \geq 0$ or the selling revenue if $a_t < 0$, specifically

$$R(a_t, p_t) := \begin{cases} -\frac{1}{\alpha(a_t)} \cdot a_t \cdot p_t, & \text{if } a_t \geq 0, \\ -\beta(a_t) \cdot a_t \cdot p_t, & \text{if } a_t < 0, \end{cases} \tag{4.1}$$

where $\alpha(a_t)$ and $\beta(a_t)$ are the charging and discharging efficiency given action a_t. We specify them in §4.3.2. Note that here the charging and discharging efficiencies depend on action a_t, while in Chapter 2 and 3 they are constant. Also note that changes of the charging and

discharging efficiency as a function of a_t are not permanent, but changes in M_t are.

The feasible set for an action a_t, denoted by $\Psi(S_t)$, is defined as follows:

$$\begin{aligned} & -x_t \leq a_t \leq M_t - x_t, \\ & K_1 \leq a_t \leq K_2, \\ & M_{t+1} = M_t - H(a_t), \\ & x_{t+1} = (x_t + a_t)\eta, \end{aligned} \tag{4.2}$$

where the first constraint is the energy availability (left) and the remaining storage energy capacity constraint (right); the second constraint is the power capacity constraint for charging and discharging, where K_1 and K_2 are the charging and discharging power capacity (MW) of the battery. Similar to Chapter 2, K_1 and K_2 are implicitly multiplied by one period. The third and forth relations specify the evolution of energy capacity and inventory, respectively.

We formulate the problem of managing the battery as a finite-horizon MDP. Each stage of the MDP corresponds to one time period. Let π denote a policy that maps any state S_t to an action a_t, and denote as $A_t^\pi(S_t)$ the decision rule in stage t under this policy; let Π denote the set of all feasible policies. The objective is to maximize the total expected discounted market value of the cash flows over all feasible policies:

$$\max_{\pi \in \Pi} \sum_{t=1}^{T} \delta^{t-1} \mathbb{E}[R(A_t^\pi(S_t), P_t) | S_1], \tag{4.3}$$

where $\delta \in (0, 1]$ is the discount rate of each stage. Similar to Chapter 2 and 3, we use a risk-neutral framework (Seppi 2002). Note that we omit the constant capital cost in (4.3).

For period t, let $V_t(S_t)$ denote the value function from period t onward given S_t. If $t = T+1$, the value function is $V_t(S_t) := \theta(M_t)$, which reflects salvage value or disposal cost. For any period $t \in \mathscr{T}$, the value function $V_t(S_t)$ is the expected sum of the optimal immediate payoff function and the discounted value function for the next period, and thus satisfies the following recursion:

$$\begin{aligned} V_t(S_t) &= \max_{a_t \in \Psi(S_t)} \mathbb{E}\left[R(a_t, P_t) + \delta V_{t+1}\left(S_{t+1}\right) | \mathbf{p}_{t-1}\right], \\ &= \max_{a_t \in \Psi(S_t)} R(a_t, \mathbb{E}[P_t | \mathbf{p}_{t-1}]) + \delta \mathbb{E}_{t+1}[V_{t+1}\left(S_{t+1}\right) | \mathbf{p}_{t-1}], \end{aligned} \tag{4.4}$$

where the second equality follows as the immediate payoff function is linear in price.

Similar to Chapter 2, we can show that the value function in (4.4) is in general not concave due to negative prices and the power constraint (the power constraint can be viewed as a transmission power capacity constraint as in Chapter 2). It is thus difficult to characterize the optimal policy structure, and we therefore resort to discretizing the continuous-state MDP, and use dynamic programming to solve for the optimal action for each period.

4.3 Dynamics of energy capacity and efficiency

In this section we model how a battery's energy capacity and efficiency change with action a_t. Since these dynamics vary among batteries, we study three different types of batteries: lead acid, lithium-ion, and AHI. To calibrate the model parameters for these three types of batteries we use data sheets from representative manufacturers: for lead acid, we use the sheet from Whisper Power (WhipserPower, 2012); for lithium-ion, the sheet from cell ANR26650M1-B manufactured by A123 systems (A123System, 2012); and for AHI, published data from Aquion Energy (Whitacre et al., 2012).

4.3.1 Dynamics of energy capacity

Different batteries lose their energy capacity according to different mechanisms. In this subsection we briefly discuss the mechanism behind each battery's energy capacity degradation, and then talk about how we model each specifically. Finally, we elaborate on how we calibrate the parameters for each battery.

4.3.1.1 Lead acid and AHI A lead acid battery is believed to degrade at a rate related to its depth of discharge (the energy level to which a lead acid battery is discharged). Data are available describing energy capacity degradation as a function of depth of discharge in experiments with *constant* depth of discharge (EPRI 2004). However, no data are available on how a lead acid battery's energy capacity will evolve over a path with different depths of discharge in different periods.

Nevertheless, the energy throughput of a lead acid battery before failure—the total quantity of energy that a battery can *discharge* over its life time—has been observed to be close to be a

Table 4.1 Parameters used to compute energy capacity degradation and efficiency variation of all three types of batteries

	Characteristics	Lead Acid	Lithium-ion	AHI
1	n_0: maximum number of full cycles	400	2000; not used in experiments, as we use Wang et al. (2011)	5000
2	h_0: rated number of discharging hours	20	1	13
3	β_0: Efficiency at the rated number of hours	85%	90%	88%
4	k: Peukert constant	1.22	1.04	Not Applicable
5	ν_0: Nominal voltage	12.9V	3.25V	Not Applicable
6	m_0: energy capacity for one cell or one module	12.9V× 225 Ah = 2.9 KWh	3.25V × 2.5 Ah =8.125 Wh	1.2V × 0.21 Ah =0.252 Wh; not relevant, as we do not use Peukert's law

Note: Each column is adapted from WhipserPower (2012), A123System (2012), and Whitacre et al. (2012), respectively, unless otherwise cited. Row 1 is for computing the degradation function: the number of cycles for lead acid is adapted from the original data sheet by multiplying the number of cycles given an 80% depth of discharge by 80% to obtain the number of cycles for 100% depth of discharge; Row 2 through Row 6 are for computing the changes in efficiency.

constant (Bindner et al. 2005). Thus we model the effect of lead acid degradation as a constant upper limit on energy discharged; that is we model the energy capacity degraded due to action a_t as a linear function of electricity discharged as follows:

$$H(a_t) = |(a_t)^-|/n_0,$$

where $(a_t)^- := \min\{a_t, 0\}$, as in Chapter 2; n_0 is the commonly-quoted number of cycles before failure: a full cycle is fully charging *and* discharging a battery once (see n_0 in Row 1 of Table 4.1). As we normalize the maximum energy capacity to be one, n_0 should also be interpreted as the maximum energy throughput for this battery. Since we have the same type of data for AHI's energy capacity degradation (Whitacre et al. 2012), we model it similarly.

4.3.1.2 Lithium-ion A lithium-ion battery, specifically the $LiFePO_4$ chemistry, is believed to degrade as a function of the total energy throughput during its life time as well as its discharging rates (Peterson et al. 2010a, Wang et al. 2011). (Please refer to Gang et al. (2003) and Choi and Lim (2002) for other types of lithium-ion battery chemistry.)

Table 4.2 $B(C_{Rate}(a_t))$

$C_{Rate}(a_t)$	0.5	2	6	10
$B(C_{Rate}(a_t))$	31,630	21,681	12,934	15,512

Since in the MDP (4.4) we need to vary discharge rates (the period length is fixed, but the amount of energy to charge or discharge varies, which means that for each period the charging and discharging rates vary), we use the degradation model of Wang et al. (2011), which describes the energy capacity loss of a lithium-ion battery at different discharge rates. Specifically, we use the degradation model in Wang et al. (2011) at room temperature ($25°C$), which expresses the percentage of the energy capacity loss for a lithium-ion battery as a function of ampere-hours and C-Rate (which is the reciprocal of the number of hours to discharge the battery) as follows:

$$H(a_t) = B(C_{Rate}(a_t)) \cdot \exp\left\{\frac{-31,700 + 370.3 \times C_{Rate}(a_t)}{8.314 \times (25 + 273)}\right\} \times (A_h(a_t))^{0.55}, \tag{4.5}$$

where $B(C_{Rate}(a_t))$, unitless, is shown in Table 4.2; $C_{Rate}(a_t)$ represents C-Rate; and $A_h(a_t)$ represents ampere-hours. For any $C_{Rate}(a_t)$ that falls into the range of $C_{Rate}(a_t)$ in Table 4.2, we use linear interpolation; for anything outside of the range, we use the number of its closest neighbor. Please refer to Appendix C.2 for the derivation of $C_{Rate}(a_t)$ and $A_h(a_t)$ as functions of a_t.

Since we model the energy capacity degradation of lithium-ion without using the maximum number of cycles, we do not need to quote a cycle number in Row 1 in Table 4.1 for lithium-ion, but we list it as a ballpark comparison.

4.3.2 Dynamics of efficiency

We next model how the efficiency changes with different action a_t for all three types of batteries.

4.3.2.1 Lead acid and lithium-ion To model how the round-trip efficiency may change with actions a_t, we use Peukert's law (Peukert 1897), which establishes the relationship between the number of hours that a battery takes to discharge and its discharge current.

We derive the discharging efficiency $\beta(a_t)$ for given a_t in any single period with period

Figure 4.1 Discharging voltage versus action a_t for lead acid and lithium-ion

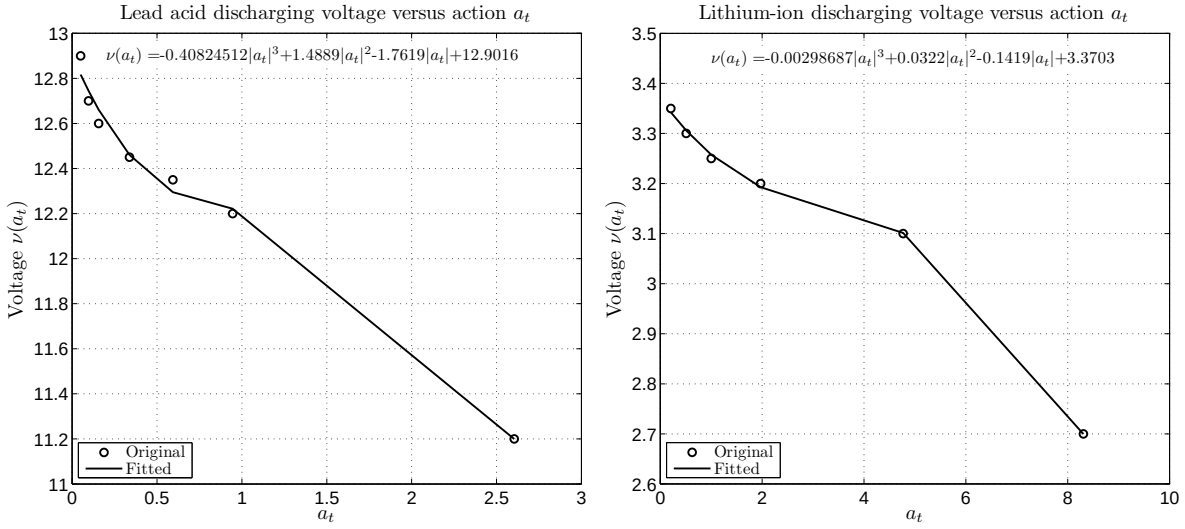

length Δt as follows:

$$\beta(a_t) = \underbrace{\beta_0 \cdot h_0^{\frac{1}{k}-1} \cdot \Delta t \cdot |a_t|^{\frac{1}{k}-1}}_{\text{Current efficiency}} \quad \underbrace{\frac{\nu(a_t)}{\nu_0}}_{\text{Voltage Efficiency}} = \text{Constant} \cdot |a|^{\frac{1}{k}-1} \cdot \nu(a_t), \tag{4.6}$$

where $\beta(a_t)$ can be interpreted as the product of current efficiency (or coulombic efficiency) and voltage efficiency; β_0 is the efficiency at the rated number of hours for a battery to discharge—h_0; k is the Peukert constant: the closer k is to one, the smaller the variation of efficiency is in a_t; and $\nu(a_t)$ captures how the discharging voltage changes with action a_t. Parameters β_0, h_0, and k of lead acid and lithium-ion are listed in Row 3, Row 2, and Row 4 in Table 4.1, respectively. See Appendix C.1 for the derivation of $\beta(a_t)$.

For $\nu(a_t)$, we plot data for lead acid (WhipserPower 2012) and for lithium-ion (A123System 2012) in Figure 4.1 (left) and Figure 4.1 (right), respectively, each of which suggests the fitness of a simple cubic function. We thus use a cubic function for $\nu(a_t)$ as follows: $l_1|a_t|^3 + l_2|a_t|^2 + l_3|a_t| + l_4$, and use nonlinear regression to calibrate it. Because both batteries consist of many identical cells with almost identical physical characteristics, we first calibrate one cell's discharging voltage versus discharging power curve; we then find for action a_t of the entire battery (with normalized maximum energy capacity one) the corresponding power of a single cell: $a_t \cdot m_0/\Delta t$, where m_0 is the energy capacity of a single cell in Row 6 in Table 4.1. Therefore, we convert the curve of discharging voltage versus power to the curve of discharging voltage versus a_t.

Figure 4.2 Efficiency curve for AHI

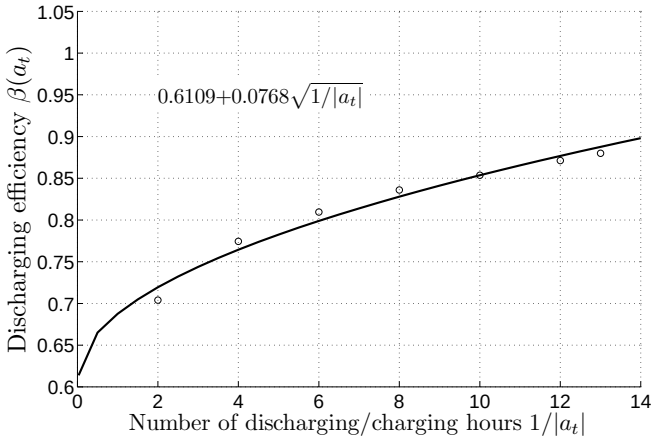

Note: Dots represent data from Whitacre et al. (2012); the line is the calibrated efficiency curve.

Since we could not find similar data for charging, we assume symmetric charging and discharging, that is $\alpha(a_t) = \beta(-a_t)$. This is in line with the standard assumption where the constant charging efficiency is the same as the constant discharging efficiency (Hittinger et al. 2012).

4.3.2.2 AHI As a new battery chemistry, it is not known whether AHI follows Peukert's law or not. However, the efficiency of this battery has been tested, yielding data (Whitacre et al. 2012) shown in dots in Figure 4.2. This data suggests that a simple square root function can capture how the efficiency changes with the number of hour to discharge. Since the number of hours to discharge for given action a_t equals $1/|a_t|$ (recall that the energy capacity is normalized to one), we can characterize the efficiency as a function of a_t. We use nonlinear regression and calibrate the discharging efficiency curve as follows: $\beta(a_t) = 0.6109 + 0.0768/\sqrt{|a_t|}$. As charging and discharging appear symmetric in their current and voltage, we assume symmetric charging and discharging (Whitacre et al. 2012), that is, $\alpha(a_t) = \beta(-a_t)$.

As we model AHI's $\alpha(a_t)$ and $\beta(a_t)$ without using Peukert's law, the numbers in Row 2 through Row 6 in Table 4.1 are not relevant. However, for the sake of comparison, we list those that are applicable for AHI.

We summarize how we model and calibrate the dynamics of energy capacity and efficiency for all three batteries in Table 4.3.

Table 4.3 A summary of models for dynamics of energy capacity and efficiency for all three batteries

	Lead Acid	Lithium-ion	AHI
Degradation	Bindner et al. (2005)	Wang et al. (2011)	Bindner et al. (2005)
Efficiency variation	Peukert's law (Peukert 1897)		Whitacre et al. (2012)
Manufacturer	Whisper Power	A123 Systems	Aquion Energy

Table 4.4 Additional parameters used for all three types of batteries

	Characteristics	Lead Acid	Lithium-ion	AHI
1	Number of modules/cells	345	123,000	4,000,000
2	Maximum C-Rate	0.2	20	10
3	Self-discharging rate	3%/month	5%/month	2%/month
4	Current capital cost	\$200/KWh	\$600/KWh	\$300/KWh
5	Specific energy	2.7KWh/65 kg= 41 Wh/kg	8.25Wh/0.076g = 109 Wh/kg	Not relevant; see below
6	Weight of toxic materials	1MWh/(41Wh/kg) =24,390 kg	1MWh/(109Wh/kg) = 9,174 kg	zero toxic material

Note: Each column is adapted from WhipserPower (2012), A123System (2012), and Whitacre et al. (2012), respectively, unless otherwise cited. Row 1 is the number of cells or modules that are used to assemble a battery of energy capacity 1MWh; Row 2 is also the power capacity K_1 and K_2 (which we assume to be symmetrical) without sign nor units, recalling that C-rate is the reciprocal of number of hours to charge or discharge a battery, and the maximum energy capacity is normalized. (Also observe that because for lead acid $-K_1 = K_2 < 1$, its power constraint is binding, but not for lithium-ion and AHI.) Row 3 is for computing η (EPRI 2004); Row 4 is the capital cost as of the date of writing; and Row 5 and Row 6 are for computing the disposal cost.

4.4 Numerical analysis

In this section we introduce the setup of our numerical analysis, and then discuss how the dynamics of energy capacity and efficiency may affect the operation and valuation of the aforementioned three types of batteries. We fix each battery's energy capacity to be one MWh. Depending on the battery technology, this battery may be made of multiple cells or modules: the number of cells or modules is in Row 1 in Table 4.4, derived from 1MWh divided by the energy capacity of a single cell or module in Row 6 of Table 4.1.

We assume that the period length is one hour, which corresponds to the real-time energy arbitrage market in NYISO. We assume that the decision horizon is 20 years, which means that the number of periods is $24 \times 365 \times 20 = 175,200$ (without accounting for leap years). We use the same price model calibrated to data in NYISO as in Chapter 2, and use the same risk-neutral discounting rate per period (hour): $\delta = 0.999999$, which corresponds to an annual risk-free interest rate of 1% with continuous compounding. η is computed converting

Figure 4.3 Values and profits of three batteries over a twenty-year horizon

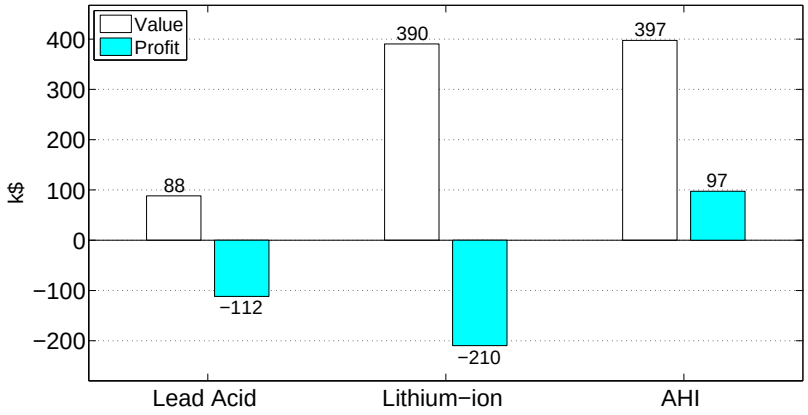

the self-discharge rate per month from Row 3 in Table 4.4 evenly to self-discharge rate per period (hour), which is 0.99996, 0.99993, and 0.99997 for lead acid, lithium-ion, and AHI, respectively.

The current capital cost for each battery is shown in Row 4 in Table 4.4. In the following, we first assume zero salvage value (from §4.4.1 to §4.4.4): $\theta(M_t) = 0$; we later study how the results may change with different salvage values or disposal costs in §4.4.5.

Similar to computing the optimal policy in Chapter 2, we use standard dynamic programming to find the optimal value of each battery. We discretize the inventory and energy capacity to 21 levels each, and discretize the price model in the same way as in Chapter 2.

We study the importance of modeling degradation, modeling efficiency variation, and modeling both together. We first study the value and profit of operating each battery in an energy arbitrage market, considering both degradation and efficiency variation, over the entire horizon in §4.4.1. We then study how these values are affected by ignoring these battery dynamics, in §4.4.2 through §4.4.4. We finally examine how the results may be affected by different salvage values or costs, in §4.4.5.

4.4.1 Value and profit for each battery

The value of managing each battery is the value of $V_1(S_1)$ in the MDP (4.4) evaluated in the initial stage at initial inventory zero and initial energy capacity of 1MWh. The profit of each battery is then its value minus the capital costs (see Row 4 in Table 4.4).

In Figure 4.3 we plot the values and profits of all the three batteries. We can see from

this figure that the values for both lithium-ion and AHI are very close, and are much higher than that of lead acid. However, it is not cost-effective to invest in either lead acid or lithium-ion batteries: their profits are negative. Lead acid, though the cheapest technology, has the shortest life time and lowest efficiency (see Row 1 and Row 3 of Table 4.1), greatly limiting its value; lithium-ion, though possessing the highest efficiency, is still not cost-effective in this application because of its high degradation and high capital cost (see Row 4 of Table 4.4). This lack of profitability is consistent with the existing literature (Peterson et al. 2010b, Sioshansi et al. 2009, Walawalkar et al. 2007). In contrast, the profit of an AHI battery is positive, primarily due to its longer cycle life and next-to-lowest capital cost (see Row 1 in Table 4.1 and Row 4 in Table 4.4, respectively). Nevertheless, the profit of AHI over a twenty-year horizon is merely $\$97,000$, resulting in a return-on-investment of only about 32% over twenty years, and thus an annual return-on-investment of 2.8%.

We next examine, for each battery, the importance of modeling energy capacity degradation in §4.4.2, efficiency variation in §4.4.3, and both in §4.4.4. In each of these three subsections, we study how the optimal value of the MDP (4.4) for each battery is affected by ignoring subsets of these two dynamics. Note that we study the impact on the optimal *value* of the MDP (4.4), rather than its profit; including capital costs would dilute this effect.

4.4.2 The importance of modeling energy capacity degradation

We examine the importance of modeling energy capacity degradation from the following two perspectives:

- How suboptimal is it to operate a battery that degrades as if it did not degrade?
- If we estimate the value of a battery using the value of an ideal battery (operated optimally), by how much do we overestimate the actual value?

The first (second) question is the embodiment of Q1 (Q2) with respect to energy capacity degradation. The answer to the first question demonstrates whether operators can safely ignore degradation when considering operating policies. The answer to the second question determines an upper bound on the ceiling value that the battery can reach if its degradation rate is reduced, or alternatively, whether degradation should be an area of focus for improvement.

For each of these two questions, we compare the optimal case with another case. The optimal case is denoted by (Actual, Actual): the first word represents battery characteristics,

and the second represents the assumptions used in determining the operating policy, as in (4.7). Equivalently, (Actual, Actual) is the case of operating an actual battery optimally, considering both degradation and efficiency variation, as in §4.4.1.

$$\left(\underbrace{\text{Actual}}_{\downarrow} \quad , \quad \underbrace{\text{Actual}}_{\downarrow}\right) \tag{4.7}$$

Battery characteristics Operating policy assumptions

For the first question, we compare the value of (Actual, Actual) with that of (Actual, Ideal): the battery degrades as in (Actual, Actual), but it is operated as if it did not degrade (see Figure 4.4). The difference between the values of (Actual, Actual) and (Actual, Ideal) gives the value lost in operating a battery while ignoring degradation. To compute the value of (Actual, Ideal) for each battery, we modify the MDP (4.4) by removing the energy capacity evolution function (4.2). We compute the action for each stage and each state, and then apply these actions to the MDP (4.4), which includes the battery degradation; the resulting value at the initial state and stage thus gives the value of operating this battery while ignoring degradation. We denote this value by V_1^{AI}, where the superscript AI denotes *Actual* and *Ideal*, respectively. (The state variable in V_1^{AI} is omitted for simplicity.) Thus, the loss of optimality due to ignoring degradation is defined as

$$\frac{V_1 - V_1^{\text{AI}}}{V_1} \times 100\%, \tag{4.8}$$

where V_1 represents the optimal value for the case (Actual, Actual), with its state variable is also omitted for simplicity.

For the second question, we compare the value of (Actual, Actual) with that of (Ideal, Ideal): An ideal battery operated optimally (see Figure 4.4). To compute the value of (Ideal, Ideal) for each battery, we modify the MDP (4.4) by removing the energy capacity evolution function (4.2). The value from this modified MDP is the value of optimally managing an ideal battery, denoted by V_1^{II}, where the superscript II represents *Ideal* and *Ideal*. As before, we omit the state variable. Therefore, we define the upper limit on the value of decreasing

Figure 4.4 Three cases

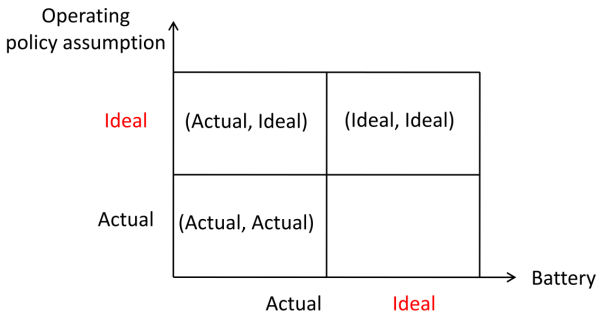

This figure is for §4.4.2, §4.4.3, and §4.4.4; we compare these three cases for the purpose of studying the importance of modeling any combination of features: degradation alone, efficiency variation alone, or both together. When we study the effect of degradation alone, we assume for all three cases that the battery is subject to efficiency variation; vice versa when studying the effect of efficiency variation alone.

Figure 4.5 Effect of energy capacity degradation on managing and valuing a battery

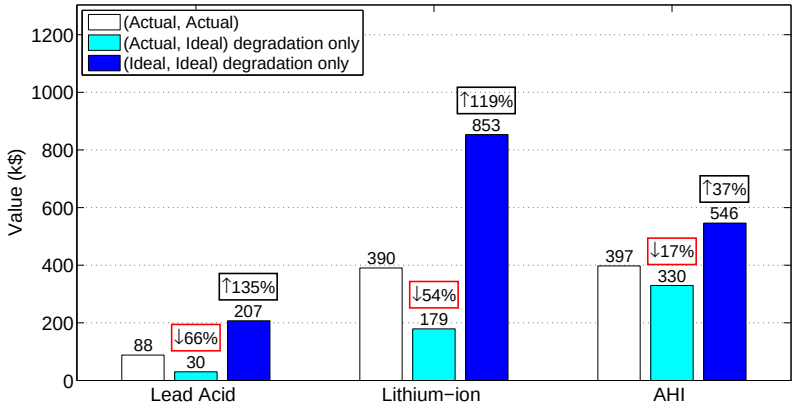

Note: The percentage on each bar for (Actual, Ideal) is computed using (4.8); the percentage on each bar for (Ideal, Ideal) is computed using (4.9).

degradation as

$$\frac{V_1^{\mathrm{II}} - V_1}{V_1} \times 100\%. \tag{4.9}$$

In this subsection, (Actual, Actual), (Actual, Ideal), and (Ideal, Ideal) assume the battery suffers from efficiency loss, and optimize taking this into account. Thus the effect of ignoring capacity degradation is isolated.

Figure 4.5 plots the values of the three cases: (Actual, Actual), (Actual, Ideal), and (Ideal, Ideal). The percentage above each bar of (Actual, Ideal) is computed using (4.8); the percentage above each bar of (Ideal, Ideal) is computed using (4.9).

Figure 4.6 The total expected electricity sold over twenty years for each battery

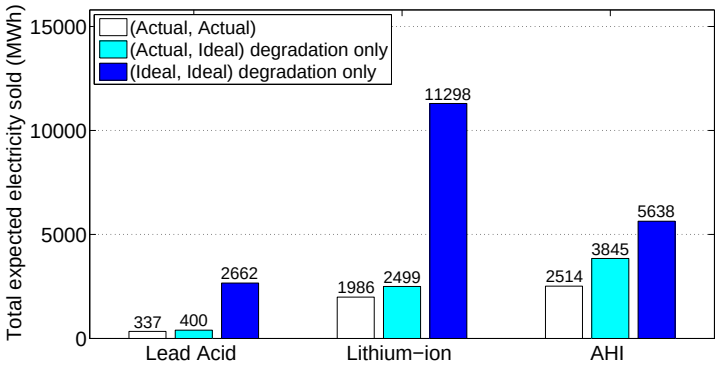

Considering Q1, the batteries that lose the most value if we operate them as if they did not degrade are the lead-acid battery and the lithium-ion battery, decreasing by approximately 66% and 54% of the optimal value, respectively. This is because in (Actual, Ideal), the operator tends to wear the battery out earlier than is optimal—according to (Actual, Actual); even though the total amount of energy sold in (Actual, Ideal) is higher than in (Actual, Actual) (see Figure 4.6), this energy is bought at a higher average price, and sold at a lower average price than under (Actual, Actual), as (Actual, Ideal) does not take into account the opportunity cost of degradation. The least affected battery is the AHI battery: its energy capacity degradation is so low that even though (Actual, Ideal) sells a lot more energy than (Actual, Actual), the energy capacity under (Actual, Ideal) does not degrade much.

To further illustrate this point, we break down the expected electricity sold and the expected cash flows for each battery into each year over the horizon in Figure 4.7. As seen from the left three sub-figures, all three batteries in (Actual, Ideal) buy much more in the early years than in (Actual, Actual). Consequently, since lead acid and lithium-ion degrade fast, they lose most of their energy capacities around midway, resulting in extremely low cash flows in the latter half of the horizon (see Figure 4.7 right). However, since AHI degrades slower than the other two batteries, it still has a reasonable energy capacity for trading in later years.

For the second question, it is thus not surprising that a lead acid and a lithium-ion battery benefit significantly by improving their cycle life: increasing by around 135% and 119%, respectively, if the life time constraint is not binding (seen (Ideal, Ideal) in Figure 4.5). An AHI battery benefits significantly as well, increasing by 37%, but not as dramatically because its degradation rate is already low. These percentage increases give the highest possible value that these batteries can attain if their life time is improved.

Figure 4.7 The expected electricity sold (Left) and expected cash flows (Right) in each year for each battery

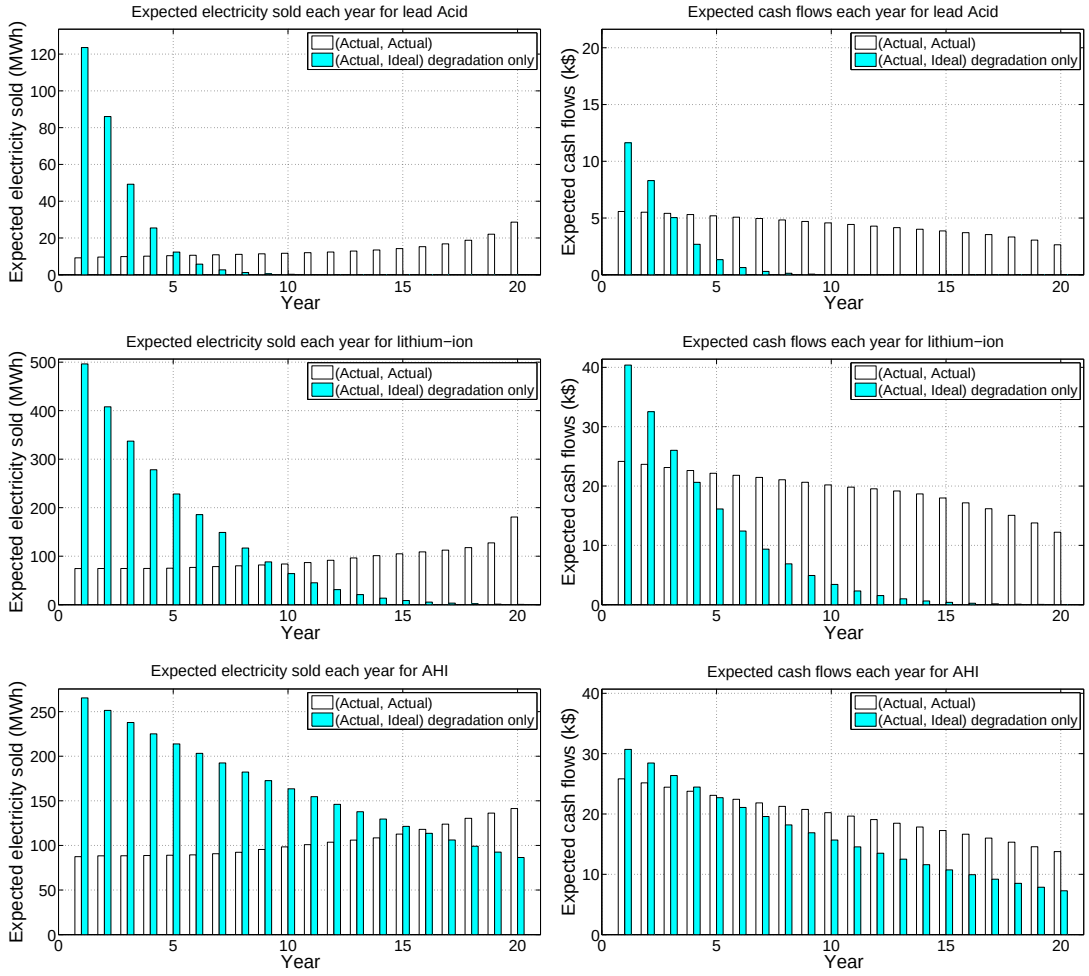

4.4.3 The importance of modeling efficiency variation

Similar to §4.4.2, we consider the importance of modeling efficiency variation by answering two questions: each question is the embodiment of Q1 and Q2 with respect to efficiency variation, respectively. For the first question, we compare the value of the case (Actual, Actual) with that of (Actual, Ideal), where the latter operating policy erroneously assumes the efficiency is constant at the efficiency in Row 3 in Table 4.1. For the second question, we compare the value of the case (Actual, Actual) with that of (Ideal, Ideal), where a battery with constant efficiency at in Row 3 in Table 4.1 is operated optimally.

Also similar to §4.4.2, for all cases in this subsection we assume that the degradation is included in the model—whether Actual or Ideal—and that the optimization takes into this account. We define the loss of optimality due to ignoring efficiency in (4.8) and the value of

Figure 4.8 Effect of efficiency variation on managing and valuing each battery

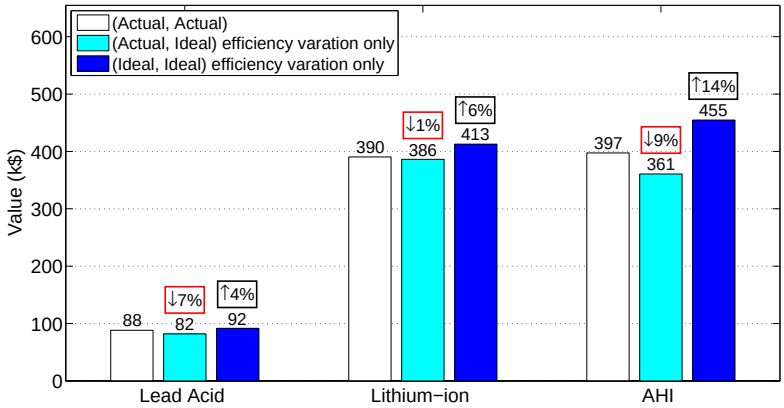

Note: The percentage on each bar for (Actual, Ideal) is computed using (4.8); the percentage on each bar for (Ideal, Ideal) is computed using (4.9).

decreasing efficiency variation in (4.9), respectively.

Figure 4.8 plots the values of all the three cases. If we operate a battery that has *varying* efficiency as if it had *constant* efficiency, the least affected battery is the lithium-ion battery, because its efficiency does not change much with different discharging rates: the Peukert constant is very close to one. Thus even when ignoring changes in efficiency, a lithium-ion battery can still achieve almost all of the optimal value (more than 99%). In contrast, the lead acid and the AHI battery lose value around 7% and 9%, respectively, because the efficiency of these two batteries changes more rapidly than that of lithium-ion.

For all three batteries, if the efficiency is fixed to the rated levels, the battery values would increase by 4% (lead acid), 6% (lithium-ion), and 14% (AHI), respectively, compared to the case of (Actual, Actual). These percentage increases are significantly smaller than those from reducing degradation seen in Figure 4.5, indicating that degradation has a much larger effect than efficiency variation.

4.4.4 The importance of modeling both energy capacity degradation and efficiency variation

In this subsection, we consider the effect of modeling both degradation and efficiency variation together.

We plot the values of all three cases in Figure 4.9. Ignoring both degradation and efficiency variation results in a great loss of optimality: 81% for lead acid, 65% for lithium-ion, and

Figure 4.9 Effect of modeling both degradation and efficiency variation on managing and valuing each battery

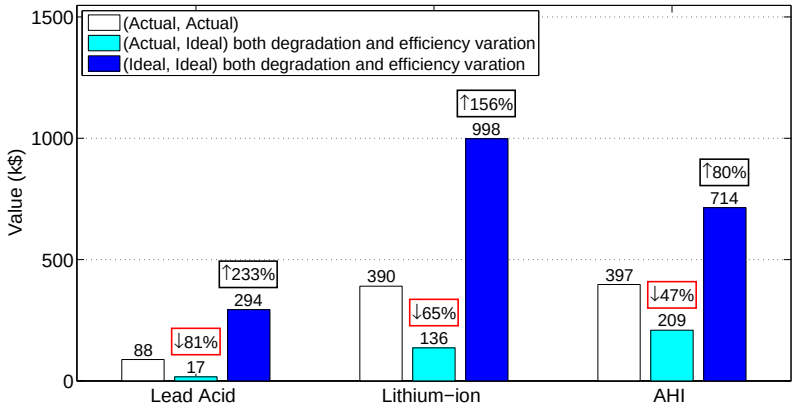

Note: The percentage on each bar for (Actual, Ideal) is computed using (4.8); the percentage on each bar for (Ideal, Ideal) is computed using (4.9).

Figure 4.10 The expected electricity sold for each year for AHI

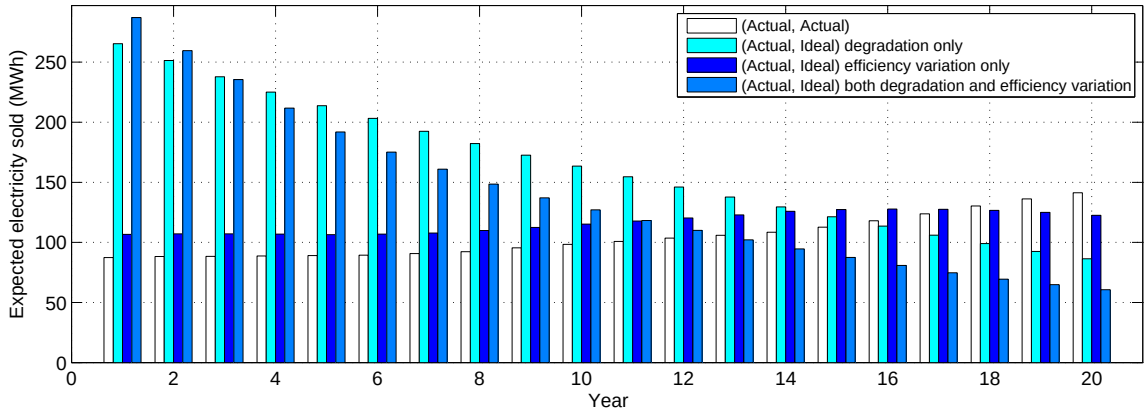

47% for AHI. This loss is greater than the sum of the losses from ignoring each dynamic independently. This is because if the operator uses a model that ignores degradation *and* assumes a fixed higher efficiency than actual, the operator not only trades more often than when ignoring degradation alone, but also trades between prices that are not desirable when ignoring degradation alone. This wears the battery out even earlier than ignoring degradation alone, and earns less value along the way.

We use AHI as an example to demonstrate this point in Figure 4.10 and Figure 4.11, which plot the expected quantity sold and the expected cash flows, respectively, in each year for AHI under four scenarios: (Actual, Actual), (Actual, Ideal) degradation only, (Actual, Ideal) efficiency variation only, and (Actual, Ideal) both degradation and efficiency variation.

As seen from Figure 4.10, in the first two years, the quantity sold when ignoring both

Figure 4.11 The expected cash flows for each year for AHI

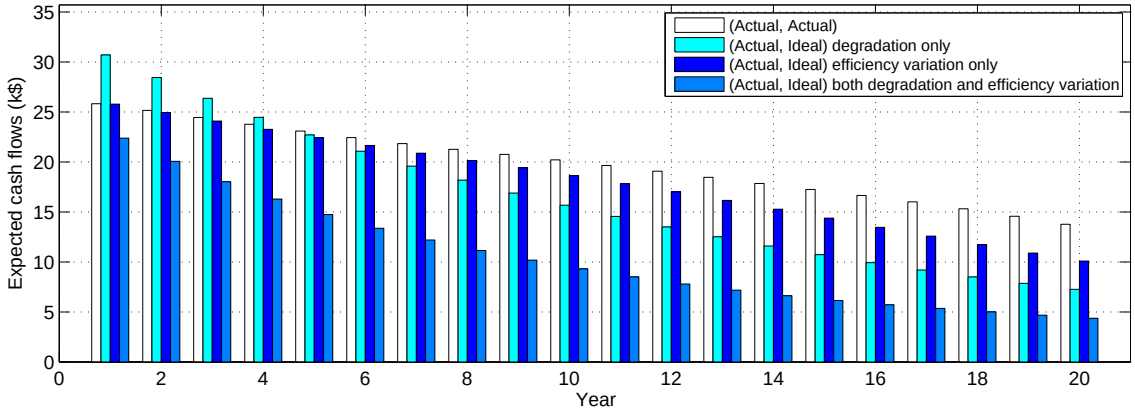

dynamics exceeds that when ignoring degradation alone; however, within the same two years, as seen from Figure 4.11, the order of cash flows is reversed: the cash flow when ignoring both is lower than when ignoring degradation only. This is because while ignoring degradation, assuming that AHI has a higher efficiency than actual would make arbitrage artificially more appealing (higher efficiency indicates lower loss in trading), thus the operator trades more often and at potentially less desirable prices, possibly even resulting in losses. As a consequence, this burns the battery out even earlier, and thus in the latter years the electricity sold when ignoring both dynamics is lower than when ignoring degradation only, and so are the cash flows.

Additionally, seen from the case (Ideal, Ideal) in Figure 4.9, the benefit of reducing degradation and efficiency variation together is greater than the sum of the benefit of reducing one independently: increasing lead acid by 223%, lithium-ion by 156%, and AHI by 80%. This means that reducing degradation and energy variation are complementary. This also implies that if practitioners value these three batteries with the value of their perfect equivalents (with neither degradation nor efficiency variation), they may grossly overestimate the values.

4.4.5 Sensitivity analysis of salvage value or disposal cost

We investigate how the value of each battery is affected by its salvage values or costs. So far, all our results have assumed zero salvage value. We compare the valuation of each battery with those under another two different salvage regimes: (i) disposal cost, the product of the weight of toxic materials in each battery that need to be disposed of and the unit disposal cost per ton, which we set as \$1500 per ton (Buchman 2012, Goonan 2012). The weight of

Figure 4.12 Sensitivity analysis on salvage value (k$)

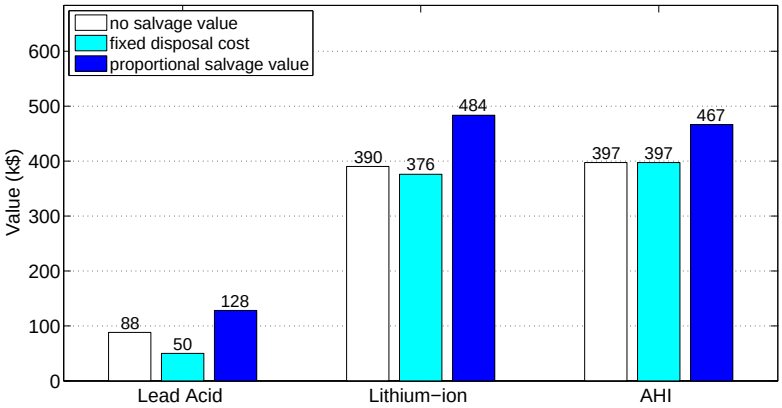

toxic materials to be disposed of are shown in Row 6 in Table 4.4 (note that because an AHI battery does not contain any toxic material, it has zero material to be disposed of). And (ii) a time-dependent proportional salvage value, which is the remaining energy capacity times the forecast unit purchasing cost at the end of the horizon, assuming the capital cost of each battery decreases by 4% every year (see Anderson (2009) for lithium-ion). We also tried an annual decrease of 8% for AHI, as the AHI battery technology is early on the learning curve; however, the qualitative result does not change.

Figure 4.12 compares the values of the MDP (4.4) at zero salvage value, and at salvage values (i) and (ii) above. As expected, an AHI battery is not affected by disposal costs, as it has no toxic materials to dispose of. Compared to a lithium-ion battery, a lead acid battery is strongly adversely affected by the disposal cost, because its specific energy (defined as energy per kg) is lower, indicating that the weight of toxic materials to dispose of for the same energy capacity is higher. Since salvage value (ii) can increase the valuation of each battery almost proportionally to their capital costs, a lithium-ion battery benefits the most, as it is the most expensive, with AHI and lead acid next. In summary, salvage values or costs do not change the above analysis qualitatively: lead acid and lithium-ion remain unprofitable, and AHI remains moderately profitable.

[5]The regulation for disposing of lithium-ion batteries vary between countries (Goonan 2012): We use the one in Europe; lithium-ion batteries in the U.S. can be discarded in landfill without incurring a disposal cost.

4.5 Conclusion and future work

We study how the operation and valuation of electricity batteries are affected by the dynamics of two important features: energy capacity and charging/discharging efficiency. We use a representative setting in which the battery is used for arbitrage in an energy market. We examine three different types of batteries, model the operating dynamics specific to each battery, and calibrate them against specifications from manufactures.

We find that it is quite suboptimal to operate a battery as if its energy capacity did not degrade, particularly for lead acid and lithium-ion batteries. In contrast, operating a battery while ignoring efficiency variation does not matter much for lithium-ion (within 1% of optimality), but matters moderately for lead acid and AHI. Furthermore, if degradation is already ignored when operating a battery, ignoring efficiency variation may greatly amplify the loss in value. Our results also provide guidance for the area of focus for improving a battery: We find for each battery that improving degradation may increase the value of a battery faster than reducing efficiency variation.

To further study whether it is important to model energy capacity degradation and efficiency variation, one could optimize the operation of a battery across multiple markets, such as the regulation market and the spinning reserve market. However, this may suffer from the curse of dimensionality, as one needs to add in the states the price of all other markets. Alternatively, one can also study how energy capacity and efficiency variation may affect the operation of storage facilities that couple with renewable energy, or storage facilities that are used in BEV fleets and BEV battery switching stations (Avci et al. 2012, Taheri et al. 2011, Worley and Klabjan 2011).

Chapter 5

Conclusion and future work

Renewable energy and electricity storage are two potential solutions for the global energy issue. If managed properly, they can contribute to a sustainable energy future. In this thesis, I aim to deepen the understanding of the operational aspect of these two solutions, and hope to inspire more related future research.

In Chapter 2, I consider the problem of managing a wind farm together with an electricity storage facility that sells electricity to a market through a transmission line. I demonstrate that this problem is nontrivial analytically, as the optimal policy does not have any apparent structure, and numerically, as a simple policy may result in a significant loss of value. I then develop a heuristic with a triple-threshold structure which captures almost all the optimal value. This triple-threshold structure also generalizes the policy structure in existing literature. Using a financial engineering price model and calibrating it to real data from NYISO, I examine the value of storage, and find that it is fairly significant. I further find that when transmission is abundant, this value comes mainly from time-shifting generation and arbitrage; while transmission is tight, it comes mainly from time-shifting generation and reducing curtailment. In addition, I find that more storage does not necessarily increase the total *wind* energy sold to the market. The analytical results from this chapter can also be used to the management of other commodity storage with random inflow, such as natural gas storage.

In Chapter 3, I examine how to use electricity storage to implement two different strategies to help match electricity supply and demand. My numerical results, based on real data, show that the new strategy of destroying electricity surpluses because of negative prices may be even more valuable than the conventional strategy of storing surpluses for future sale. Although there may be engineering and policy issues that need to be overcome before implementing this

destruction strategy, it is an opportunity that merits further investigation.

In Chapter 4, I delve into how the operation and valuation of electricity storage can be influenced by whether degradation or efficiency variation are modeled. I study three types of batteries, using real manufacturer data. I demonstrate that though efficiency variation does not matter much in managing and valuing each battery, degradation does play a significant role, particularly for lead acid and lithium-ion batteries. In addition, I find that it is better to reduce degradation together with reducing efficiency variation, because the value of reducing both together is greater than the sum of reducing each one individually. The modeling of battery dynamics in this chapter can be a stepping stone to examine the operation of electric car fleets and battery swapping stations.

Besides the future work mentioned in the conclusion of each chapter, there are other directions toward which this thesis can be extended. First, one can relax the price-taker assumption: Throughout the entire thesis, it is assumed that the operator of either the combined wind-storage system or the storage system alone does not affect market prices. It would be interesting to investigate the effect of this assumption, especially when wind and/or storage makes up a significant portion of an electricity market. Second, as wind power has a strong price-suppressing effect—such as potentially leading to more negative prices—one can investigate how negative prices would evolve with the increased use of wind power, and how these negative prices may in return affect the market valuation of wind power, as well as how all these results may be affected by the introduction of electricity storage on a large scale.

Appendix A

A.1 Non-concavity of the value functions in (2.3)

The non-concavity of the value functions originates from the *convexity* of the immediate payoff function in the decision variable a_t when prices are negative: in (2.1), for any $p_t < 0$, we have $-p_t/(\alpha \cdot \tau) \geq -p_t \cdot \tau/\alpha \geq -p_t \cdot \tau \cdot \beta$. Intuitively, we illustrate the non-concavity of the value function in inventory by showing the case without transmission capacity. When prices are negative, at any low inventory level, the marginal value of increase inventory is the price divided by discharging efficiency; at any high inventory level, the marginal value of decreasing inventory is the price times discharging efficiency. Thus, the marginal value of inventory at a low inventory level is lower than at a high inventory level, resulting in the non-concavity of the value function in inventory.

A.2 Proof of Lemma 2.1

Proof: In period $t = T + 1$ and time $t = T$, we have $V_T^{H1}(x_T, w_T, \mathbf{p}_T) = 0$, $\forall x_T$, thus the hypothesis holds for this case.

Suppose this hypothesis holds for all periods $k+1, \cdots, T$. We next prove that for period $t = k$ and time $t-1$, $V_{k-1}^{H1}(x_{k-1}^1, w_{k-1}, \mathbf{p}_{k-1}) \leq V_{k-1}^{H1}(x_{k-1}^2, w_{k-1}, \mathbf{p}_{k-1})$ for any $0 \leq x_{k-1}^1 < x_{k-1}^2$. We achieve this by proving that for any feasible action (a_k^1, g_k^1) in $\Psi(x_{k-1}^1, w_k)$, we can always find a feasible action (a_k^2, g_k^2) in $\Psi(x_{k-1}^2, w_k)$ such that the objective function in (2.4) at (a_k^2, g_k^2) is no lower than that at (a_k^1, g_k^1).

1) If $a_k^1 < 0$, then $(a_k^2, g_k^2) = (a_k^1, g_k^1)$: (a_k^2, g_k^2) is feasible as (a_k^1, g_k^1) is feasible (it satisfies constraints C1-C6); the immediate payoff function for (a_k^1, g_k^1) and (a_k^2, g_k^2) are the same, but the resulting inventory level from (a_k^2, g_k^2) is higher than that from (a_k^1, g_k^1). Because of

the hypothesis in period $t = k + 1$, the objective function in (2.4) at (a_k^2, g_k^2) is no lower than that at (a_k^1, g_k^1).

2) If $a_k^1 \geq 0$, then $(a_k^2, g_k^2) = (a_k^1 - (x_{k-1}^2 - x_{k-1}^1), [g_k^1 - (x_{k-1}^2 - x_{k-1}^1)/\alpha]^+)$: (a_k^2, g_k^2) is feasible as (a_k^1, g_k^1) is feasible. The resulting inventory level from (a_k^1, g_k^1) and (a_k^2, g_k^2) are the same $(x_{k-1}^2 + a_k^2 = x_{k-1}^2 + a_k^1 - (x_{k-1}^2 - x_{k-1}^1) = x_{k-1}^1 + a_k^1)$, and the immediate payoff function from (a_k^2, g_k^2) is no lower than that at (a_k^1, g_k^1). Thus the objective function in (2.4) at (a_k^2, g_k^2) is no lower than that at (a_k^1, g_k^1). □

A.3 Proof of Lemma 2.2

Proof: For each period t and any given state S_{t-1}, denote the maximum quantity that one can generate by $\bar{g}_t = \min\{w_t, C + \min\{1 - x_{t-1}, K_2\}/\alpha\}$. We prove that $g_t^{H1} = \bar{g}_t$ by showing that for any feasible action (a_t, g_t) such that $g_t < \bar{g}_t$, we can always find a feasible solution $(a_t', g_t + \varepsilon)$, $\varepsilon > 0$, which gives no lower objective value function in (2.4). Denote q_t as the quantity to sell (if $q_t \geq 0$) or buy (if $q_t < 0$) resulting from a feasible action (a_t, g_t). Since $g_t < \bar{g}_t$, it follows that either $q_t < C$ or $x_{t-1} + a_t < \min\{1, x_{t-1} + K_2\}$, thus we consider the following cases:

1) If $q_t < 0$, define $\varepsilon = \min\{w_t - g_t, -q_t\}$. Thus action $(a_t', g_t') = (a_t, g_t + \varepsilon)$ is feasible, and gives $0 \geq q_t' = q_t + \varepsilon \geq q_t$ (buying less) and the same ending inventory. Hence the objective function at (a_t', g_t') is no lower than that at (a_t, g_t).

2) If $0 \leq q_t < C$, define $\varepsilon = \min\{w_t - g_t, C - q_t\}$. Thus action $(a_t', g_t') = (a_t, g_t + \varepsilon)$ is feasible, and gives $q_t' = q_t + \varepsilon > q_t \geq 0$ (selling more) and the same ending inventory. Hence the objective function at (a_t', g_t') is no less than that at (a_t, g_t).

3) If $q_t = C$, then $x_{t-1} + a_t < \min\{1, x_{t-1} + K_2\}$. We consider the following two cases:

   - If $a_t \geq 0$, define $\varepsilon = \min\{w_t - g_t, \min\{1 - x_{t-1} - a_t, K_2 - a_t\}/\alpha\}$, then $a_t' = a_t + \alpha\varepsilon \leq a_t + \alpha \cdot \min\{1 - x_{t-1} - a_t, K_2 - a_t\}/\alpha \leq \min\{1 - x_{t-1}, K_2\}$.
   - If $a_t < 0$, define $\varepsilon = \min\{w_t - g_t, -\beta a_t\}$, then $a_t < a_t' = a_t + \varepsilon/\beta \leq a_t - \beta a_t/\beta = 0$.

   In both cases, $(a_t', g_t + \varepsilon)$ is feasible and gives $q_t' = q_t$ and $a_t' > a_t$, hence it results in no lower objective value than (a_t, g_t) does, due to Lemma 2.1. □

A.4 Proof of Proposition 2.1

Proof: We first prove finiteness. For each stage the quantity sold cannot exceed C. Thus given any S_{t-1}, it holds that $|V_{t-1}^{H1}(S_{t-1})| \leq \sum_{k=t}^{T} |\mathbb{E}[p_k|w_{t-1}, \mathbf{p}_{t-1}]| \cdot C \leq \sum_{k=t}^{T} \mathbb{E}[|p_k||w_{t-1}, \mathbf{p}_{t-1}] \cdot C < \infty$, where the last inequality follows from Assumption 2.1.

We next prove concavity by induction. For period $T+1$ and time T, $V_T^{H1}(S_T) = 0$, so the hypothesis holds. Suppose for all periods $k+1, \cdots, T$, the hypothesis holds. For period $t = k$ and time $k-1$, according to Lemma 2.2, $g_k^{H1} = \min\{w_k, C + \min\{1 - x_{k-1}, K_2\}/\alpha\}$. Substituting g_k^{H1} for g_k in (2.4), we obtain an optimization problem with only one decision variable, a_k, as follows:

$$V_{k-1}^{H1}(S_{k-1}) = \mathbb{E}\Bigg[\max_{a_k \text{ s.t. } (a_k, g_k^{H1}) \in \Psi(x_{k-1}, w_k)} R(a_k, g_k^{H1}, \max\{\mathbb{E}[p_k|w_k, \mathbf{p}_{k-1}], 0\}) \\ + \delta \mathbb{E}\left[V_k^{H1}(S_k)\,|w_k, \mathbf{p}_{k-1}\right] \big|\, w_{k-1}, \mathbf{p}_{k-1}\right]. \qquad \text{(A.4.1)}$$

We next prove that the set $\mathscr{C} := \{(x_{k-1}, a_k) | x_{k-1} \in \mathscr{X}, (a_k, g_k^{H1}) \in \Psi(x_{k-1}, w_k)\}$ is convex: given any (x_{k-1}^1, a_k^1) and (x_{k-1}^2, a_k^2) in $\mathscr{C}$, the linear combination $(x_{k-1}^\lambda, a_k^\lambda) = (\lambda x_{k-1}^1 + (1-\lambda)x_{k-1}^2, \lambda a_k^1 + (1-\lambda)a_k^2)$ is also in $\mathscr{C}$, where $\lambda \in [0,1]$. It is easy to verify that $(x_{k-1}^\lambda, a_k^\lambda)$ is also in $\mathscr{C}$ if: a_k^1 and a_k^2 are both positive ($(x_{k-1}^\lambda, a_k^\lambda)$ satisfies constraints C2-C5-C6, or C3-C5-C6); or both negative ($(x_{k-1}^\lambda, a_k^\lambda)$ satisfies constraint C1-C5-C6). If one is positive and the other negative, we next show that $(x_{k-1}^\lambda, a_k^\lambda)$ is also in $\mathscr{C}$. Without loss of generality, we assume that $a_k^1 < 0 \leq a_k^2$. Clearly, $(x_{k-1}^\lambda, a_k^\lambda)$ satisfies constraint C5 and C6 as (x_{k-1}^1, a_k^1) and (x_{k-1}^2, a_k^2) are in $\mathscr{C}$. If a_k^λ is negative, then $(x_{k-1}^\lambda, a_k^\lambda)$ satisfies C1: $g_k^{H1} - a_k^\lambda \beta \leq g_k^{H1} - a_k^1 \beta \leq C$ (the first equality follows as $0 > a_k^\lambda = \lambda a_k^1 + (1-\lambda)a_k^2 \geq \lambda a_k^1 + (1-\lambda)a_k^1 = a_k^1$). If a_k^λ is nonnegative, then $(x_{k-1}^\lambda, a_k^\lambda)$ satisfies either C2 or C3: if $0 \leq g_t^{H1} - a_k^2/\alpha \leq C$, then $g_k^{H1} - a_k^\lambda/\alpha \leq g_k^{H1} < g_k^{H1} - a_k^1 \beta \leq C$ (the second inequality following from the fact that $a_k^1 < 0$, and the last inequality from the fact that (x_{k-1}^1, a_k^1) is in $\mathscr{C}$), thus C2 is satisfied; if $0 \leq (a_k^2/\alpha - g_k^{H1})/\tau \leq C$, then $(a_k^\lambda/\alpha - g_k^{H1})/\tau \leq (a_k^2/\alpha - g_k^{H1})/\tau \leq C$ (the first inequality following from the fact that $a_k^2 \geq a_k^\lambda$), thus C3 is satisfied. In summary, $\mathscr{C}$ is a convex set.

We now prove that the whole objective function in (A.4.1) is concave on $\mathscr{C}$. Since we have

$$\max\{\mathbb{E}[p_k|w_k, \mathbf{p}_{k-1}], 0\} \geq 0,$$

it follows that

$$-\beta\cdot\tau\cdot\max\{\mathbb{E}[p_k|w_k,\mathbf{p}_{k-1}],0\} \geq -\max\{\mathbb{E}[p_k|w_k,\mathbf{p}_{k-1}],0\}\cdot\tau/\alpha \geq -\max\{\mathbb{E}[p_k|w_k,\mathbf{p}_{k-1}],0\}/(\alpha\cdot\tau),$$

so the immediate payoff function $R(\cdot)$ in (A.4.1) is concave over a_k. As $R(\cdot)$ is constant in x_{k-1} (x_{k-1} does not appear in the function itself), it is jointly concave on $\mathscr{C}$. Furthermore, according to the induction hypothesis, the value function $V_k^{H1}(x_k, w_k, \mathbf{p}_k)$ is concave in $x_k \in \mathscr{X}$ given any w_k and $\mathbf{p}_k$. Since $x_k = (x_{k-1} + a_k)\eta$, $V_k^{H1}(x_k, w_k, \mathbf{p}_k)$ is jointly concave in x_{k-1} and a_k given any w_k and $\mathbf{p}_k$, and thus $\delta\mathbb{E}\left[V_k^{H1}((x_{k-1}+a_k)\eta, w_k, \mathbf{p}_k)\,|w_k, \mathbf{p}_{k-1}\right]$ is also concave on $\mathscr{C}$ given any w_k and $\mathbf{p}_{k-1}$ as expectation preserves concavity. As a result, the objective function in (A.4.1) is concave on $\mathscr{C}$ given any w_{k-1} and $\mathbf{p}_{k-1}$.

Moreover, $\mathscr{X}$ is a convex set, and $\Psi(x_{k-1}, w_k)$ is a nonempty set for any $x_{k-1} \in \mathscr{X}$. Also since $V_{k-1}^{H1}(S_{k-1}) < \infty$, according to Theorem A.4 in Porteus (2002), the expression inside the first expectation in (2.4) is concave on $\mathscr{X}$ given any w_k and $\mathbf{p}_{k-1}$, and thus $V_{k-1}^{H1}(S_{k-1})$ is concave on $\mathscr{X}$ given any w_{k-1} and $\mathbf{p}_{k-1}$.

By the principle of mathematical induction, the hypothesis holds for all periods $t = 1, \cdots, T+1$. □

A.5 Proof of Proposition 2.2

Proof: For each period $t \in \mathscr{T}$, according to Lemma 2.2, $g_t^{H1} = \min\{w_t, C + \min\{1 - x_{t-1}, K_2\}/\alpha\}$. Substituting g_t^{H1} into (2.4) for g_t, we obtain the following optimization problem with only one decision variable, a_t:

$$V_{t-1}^{H1}(S_{t-1}) = \mathbb{E}\left[\max_{a_t \text{ s.t. } (a_t, g_t^{H1})\in\Psi(x_{t-1},w_t)} R(a_t, g_t^{H1}, \max\{\mathbb{E}[p_t|w_t,\mathbf{p}_{t-1}],0\}) \right.$$
$$\left. +\delta\mathbb{E}\left[V_t^{H1}(S_t)\,|w_t,\mathbf{p}_{t-1}\right]\Big|\, w_{t-1},\mathbf{p}_{t-1}\right]. \tag{A.5.1}$$

Define $y_t := x_{t-1} + a_t$ for all a_t such that $(a_t, g_t^{H1}) \in \Psi(x_{t-1}, w_t)$. Let $\underline{\Psi}^1(x_{t-1}, w_t)$ denote the feasible set of y_t for all $a_t \geq g_t^{H1}\cdot\alpha$; $\underline{\Psi}^2(x_{t-1}, w_t)$ the set of y_t for all $0 \leq a_t \leq g_t^{H1}\cdot\alpha$; and $\overline{\Psi}(x_{t-1}, w_t)$ the set of y_t for all $a_t \leq 0$. Note the extra equality signs added to $a_t > g_t^{H1}\cdot\alpha$ and $a_t < 0$, comparing to the cases in (2.1): they do not change the results of the optimal policy,

but facilitate the exposition of the proof later on. We obtain $\underline{\Psi}^1(x_{t-1}, w_t)$, $\underline{\Psi}^2(x_{t-1}, w_t)$, and $\overline{\Psi}(x_{t-1}, w_t)$ by combining constraints C1, C2, C3, C5 and C6 with constraints $a_t \geq g_t^{H1} \cdot \alpha$, $0 \leq a_t \leq g_t^{H1} \cdot \alpha$, and $a_t \leq 0$ respectively:

$$
\begin{aligned}
&\underline{\Psi}^1(x_{t-1}, w_t) \\
=&\{y_t | g_t^{H1} \cdot \alpha + x_{t-1} \leq y_t \leq 1; y_t \leq x_{t-1} + \alpha(C \cdot \tau + g_t^{H1}); K_1 + x_{t-1} \leq y_t \leq K_2 + x_{t-1}\} \\
=&\{y_t | g_t^{H1} \cdot \alpha + x_{t-1} \leq y_t \leq 1; y_t \leq x_{t-1} + \alpha(C \cdot \tau + g_t^{H1}); y_t \leq K_2 + x_{t-1}\}, \qquad \text{(A.5.2)} \\
&\underline{\Psi}^2(x_{t-1}, w_t) \\
=&\{y_t | x_{t-1} \leq y_t \leq 1; y_t \leq g_t^{H1} \cdot \alpha + x_{t-1}; y_t \geq \alpha(g_t^{H1} - C) + x_{t-1}; K_1 + x_{t-1} \leq y_t \leq K_2 + x_{t-1}\} \\
=&\{y_t | y_t \leq 1; y_t \leq g_t^{H1} \cdot \alpha + x_{t-1}; y_t \geq \alpha(g_t^{H1} - C) + x_{t-1}; y_t \leq K_2 + x_{t-1}\}, \qquad \text{(A.5.3)} \\
&\overline{\Psi}(x_{t-1}, w_t) \\
=&\{y_t | 0 \leq y_t \leq x_{t-1}; y_t \geq (g_t^{H1} - C)/\beta + x_{t-1}; K_1 + x_{t-1} \leq y_t \leq K_2 + x_{t-1}\} \\
=&\{y_t | 0 \leq y_t \leq x_{t-1}; y_t \geq (g_t^{H1} - C)/\beta + x_{t-1}; K_1 + x_{t-1} \leq y_t\}. \qquad \text{(A.5.4)}
\end{aligned}
$$

Substituting $a_t = y_t - x_{t-1}$ into (2.4), (2.4) reduces to finding the maximum of the following three:

$$
\begin{aligned}
&\mathbb{E}\Bigg[\max_{y_t \in \underline{\Psi}^1(x_{t-1}, w_t)} \big\{(g_t^{H1} - y_t/\alpha + x_{t-1}/\alpha) \max\{\mathbb{E}[p_t | w_t, \mathbf{p}_{t-1}], 0\}/\tau \\
&\qquad + \delta \mathbb{E}\left[V_t^{H1}\left(y_t \cdot \eta, w_t, \mathbf{p}_t\right) | w_t, \mathbf{p}_{t-1}\right]\big\} \big| \, w_{t-1}, \mathbf{p}_{t-1}\Bigg], \qquad \text{(A.5.5)} \\
&\mathbb{E}\Bigg[\max_{y_t \in \underline{\Psi}^2(x_{t-1}, w_t)} \big\{(g_t^{H1} - y_t/\alpha + x_{t-1}/\alpha) \max\{\mathbb{E}[p_t | w_t, \mathbf{p}_{t-1}], 0\} \cdot \tau \\
&\qquad + \delta \mathbb{E}\left[V_t^{H1}\left(y_t \cdot \eta, w_t, \mathbf{p}_t\right) | w_t, \mathbf{p}_{t-1}\right]\big\} \big| \, w_{t-1}, \mathbf{p}_{t-1}\Bigg], \qquad \text{(A.5.6)} \\
&\mathbb{E}\Bigg[\max_{y_t \in \overline{\Psi}(x_{t-1}, w_t)} \big\{(g_t^{H1} - y_t\beta + x_{t-1}\beta) \max\{\mathbb{E}[p_t | w_t, \mathbf{p}_{t-1}], 0\} \cdot \tau \\
&\qquad + \delta \mathbb{E}\left[V_t^{H1}\left(y_t \cdot \eta, w_t, \mathbf{p}_t\right) | w_t, \mathbf{p}_{t-1}\right]\big\} \big| \, w_{t-1}, \mathbf{p}_{t-1}\Bigg]. \qquad \text{(A.5.7)}
\end{aligned}
$$

These three problems can be thought of as the problem of buying, the problem of generating and storing, and the problem of selling respectively. Next, we relax (A.5.5), (A.5.6) and (A.5.7) by the following three steps:

- removing the last constraint in the feasible set of (A.5.5), (A.5.6) and (A.5.7), which is equivalent to removing the charging and discharging power capacity constraints in C6;

- removing the second to last constraint in the feasible set of (A.5.5), (A.5.6) and (A.5.7), which is equivalent to removing the transmission capacity constraints C3, C2 and C1 respectively;
- in (A.5.5) setting $x_{t-1} = 0$ and $w_t = 0$, so $\underline{\Psi}^1(x_{t-1}, w_t)$ becomes $[0, 1]$;
- in (A.5.6) setting $x_{t-1} = 0$ and setting w_t to be arbitrary large (which means $g_t^{H1} = C + \min\{1 - x_{t-1}, K_2\}/\alpha$), so that $\underline{\Psi}^2(x_{t-1}, w_t)$ becomes $[0, 1]$;
- in (A.5.7) setting $x_{t-1} = 1$, so $\overline{\Psi}(x_{t-1}, w_t)$ becomes $[0, 1]$.

Meanwhile, we remove constant terms from (A.5.5), (A.5.6) and (A.5.7), and obtain the following problems:

$$\mathbb{E}\left[\max_{y_t\in[0,1]}\left\{-y_t\max\{\mathbb{E}[p_t|w_t,\mathbf{p}_{t-1}],0\}/(\alpha\cdot\tau)+\delta\mathbb{E}\left[V_t^{H1}\left(y_t\cdot\eta,w_t,\mathbf{p}_t\right)|w_t,\mathbf{p}_{t-1}\right]\right\}\middle| w_{t-1},\mathbf{p}_{t-1}\right], \tag{A.5.8}$$

$$\mathbb{E}\left[\max_{y_t\in[0,1]}\left\{-y_t\max\{\mathbb{E}[p_t|w_t,\mathbf{p}_{t-1}],0\}\cdot\tau/\alpha+\delta\mathbb{E}\left[V_t^{H1}\left(y_t\cdot\eta,w_t,\mathbf{p}_t\right)|w_t,\mathbf{p}_{t-1}\right]\right\}\middle| w_{t-1},\mathbf{p}_{t-1}\right], \tag{A.5.9}$$

$$\mathbb{E}\left[\max_{y_t\in[0,1]}\left\{-y_t\max\{\mathbb{E}[p_t|w_t,\mathbf{p}_{t-1}],0\}\cdot\tau\cdot\beta+\delta\mathbb{E}\left[V_t^{H1}\left(y_t\cdot\eta,w_t,\mathbf{p}_t\right)|w_t,\mathbf{p}_{t-1}\right]\right\}\middle| w_{t-1},\mathbf{p}_{t-1}\right]. \tag{A.5.10}$$

Denote the optimal solutions to (A.5.8), (A.5.9) and (A.5.10) by $\underline{X}_t^1$, $\underline{X}_t^2$ and $\overline{X}_t$ respectively, which are all in $[0, 1]$. We next show that $\underline{X}_t^1 \le \underline{X}_t^2 \le \overline{X}_t$.

Define $U_t(y_t, w_t, \mathbf{p}_{t-1}) := \delta\mathbb{E}\left[V_t^{H1}\left(y_t\cdot\eta, w_t, \mathbf{p}_t\right)|w_t, \mathbf{p}_{t-1}\right]$ and denote its derivative with respect to y_t over $[0, 1]$ by $U_t'(y_t, w_t, \mathbf{p}_{t-1})$. (In the case when $U_t(y_t, w_t, \mathbf{p}_{t-1})$ is piecewise linear, such as when both the price and wind energy processes follow discrete distributions, define $U_t'(y_t, w_t, \mathbf{p}_{t-1})$ as the right derivative at $y_t = 0$, and the left derivative over $y_t \in (0, 1]$.) According to Proposition 2.1, $V_t^{H1}\left(y_t\cdot\eta, w_t, \mathbf{p}_t\right)$ is concave in $y_t\cdot\eta$ given any w_t and $\mathbf{p}_t$, thus $U_t(y_t, w_t, \mathbf{p}_{t-1})$ is concave in y_t given any w_t and $\mathbf{p}_{t-1}$, and hence $U_t'(y_t, w_t, \mathbf{p}_{t-1})$ is non-increasing in y_t. Since $-\max\{\mathbb{E}[p_t|w_t, \mathbf{p}_{t-1}], 0\}/(\alpha\cdot\tau) \le -\max\{\mathbb{E}[p_t|w_t, \mathbf{p}_{t-1}], 0\}\cdot\tau/\alpha \le -\max\{\mathbb{E}[p_t|w_t, \mathbf{p}_{t-1}], 0\}\cdot\tau\cdot\beta$, it follows that $\underline{X}_t^1 \le \underline{X}_t^2 \le \overline{X}_t$.

These three thresholds characterize the optimal policies for (A.5.5), (A.5.6), and (A.5.7) respectively. The objective functions in (A.5.5), (A.5.6), and (A.5.7) are concave in y_t and their relaxed problems in (A.5.8), (A.5.9), and (A.5.10) achieve their global maxima at $\underline{X}_t^1$,

Figure A.5.1 The proof of Proposition 2.2

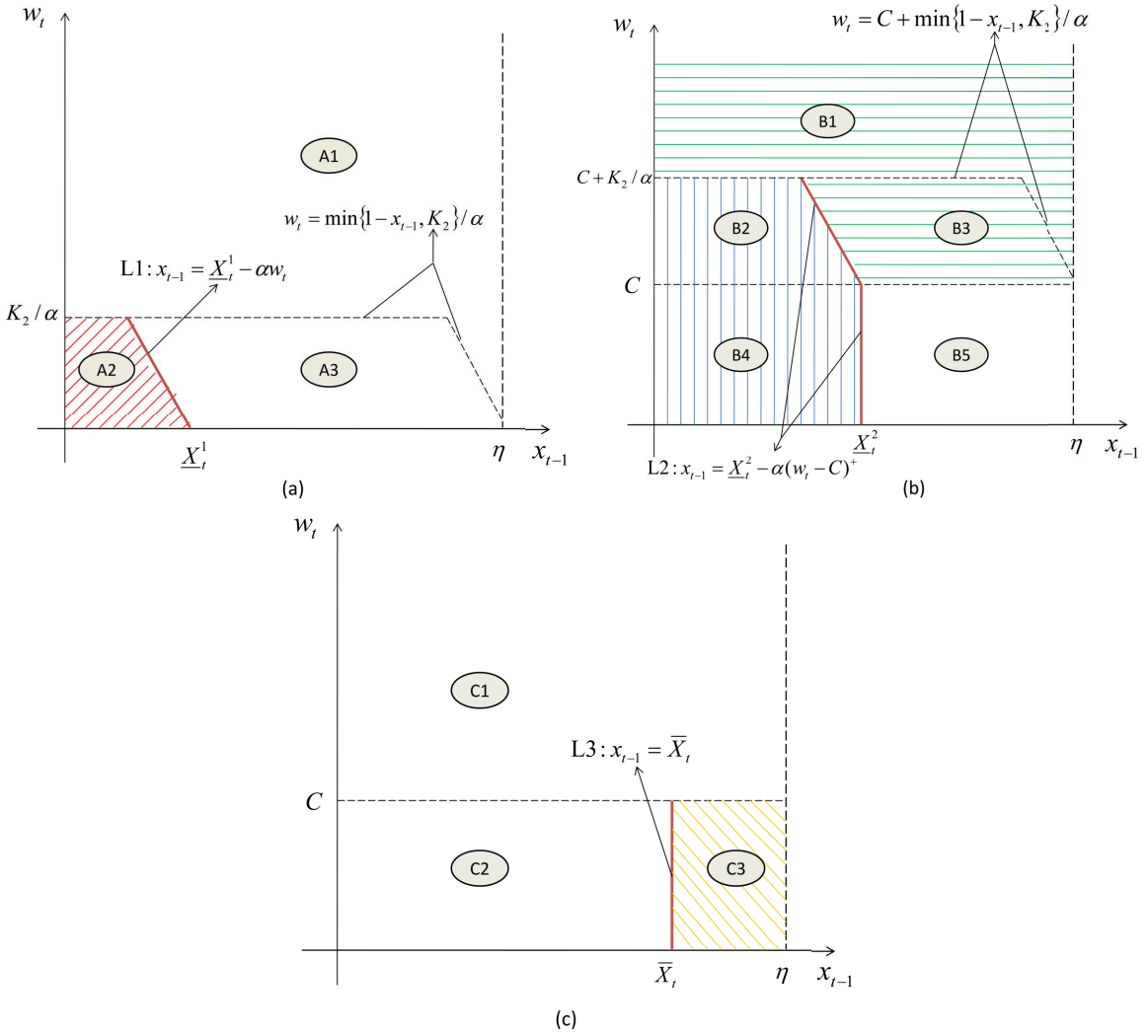

$\underline{X}_t^2$, and $\overline{X}_t$, so the optimal action for (A.5.5), (A.5.6), and (A.5.7) is to move as close as possible to $\underline{X}_t^1$, $\underline{X}_t^2$, and $\overline{X}_t$ in their corresponding feasible set.

We next show the optimal solution for each of the three problems on the (x_{t-1}, w_t) plane, as in Figure A.5.1.

A.5.1 The optimal action for (A.5.5): the problem of buying

For (A.5.5), observe that the feasible set for y_t is $\underline{\Psi}^1(x_{t-1}, w_t) = [x_{t-1} + g_t^{H1} \cdot \alpha, \min\{x_{t-1} + K_2, x_{t-1} + \alpha(C\tau + g_t^{H1}), 1\}]$. This set can be either empty or nonempty in the following two cases:

(i1) if $w_t > \min\{1 - x_{t-1}, K_2\}/\alpha$ (see region A1 in Figure A.5.1(a)): $g_t^{H1} = \min\{w_t, C +$

$\min\{1-x_{t-1}, K_2\}/\alpha\} > \min\{1-x_{t-1}, K_2\}/\alpha$, so the left end of $\underline{\Psi}^1(x_{t-1}, w_t)$ is greater than its right end, indicating that $\underline{\Psi}^1(x_{t-1}, w_t)$ is empty. Intuitively, since the amount generated exceeds what can be stored, the optimal action for (A.5.5) for this case is not to buy.

(i2) if $w_t \leq \min\{1-x_{t-1}, K_2\}/\alpha$: $g_t^{H1} = w_t$, and the feasible set becomes $[x_{t-1} + w_t \cdot \alpha, \min\{x_{t-1}+K_2, x_{t-1}+\alpha(C\tau+w_t), 1\}]$. Relative to the left end point of this feasible set, $\underline{X}_t^1$ can be either to this point's right, or to its left. Recall that the optimal action for (A.5.5) is to bring the inventory level as close as possible to $\underline{X}_t^1$, so for each of these two cases, we can obtain the optimal action for (A.5.5) as follows: on the right ($x_{t-1}+w_t\cdot\alpha \leq \underline{X}_t^1$; see region A2 in Figure A.5.1(a)), the optimal y_t for (A.5.5) equals $\min\{\underline{X}_t^1, x_{t-1}+K_2, x_{t-1}+\alpha(C\tau+w_t), 1\}$, i.e., a_t equals $\min\{\underline{X}_t^1 - x_{t-1}, K_2, \alpha(C\tau+w_t), 1-x_{t-1}\} = \min\{\underline{X}_t^1 - x_{t-1}, K_2, \alpha(C\tau+w_t)\}$. When $\underline{X}_t^1$ is on the left ($\underline{X}_t^1 < x_{t-1} + w_t \cdot \alpha$; see region A3 in Figure A.5.1(a)), the optimal y_t for (A.5.5) equals $x_{t-1} + w_t \cdot \alpha$, i.e., $a_t = w_t \cdot \alpha$;

A.5.2 The optimal action for (A.5.6): the problem of generating and storing

For problem (A.5.6), we consider the following three cases:

(ii1) if $w_t \geq C + \min\{1-x_{t-1}, K_2\}/\alpha$ (see region B1 in Figure A.5.1(b)): $g_t^{H1} = C + \min\{1-x_{t-1}, K_2\}/\alpha$, then it is straightforward that a_t^{H1} is $\alpha(g_t^{H1} - C)^+$, i.e., generate as much electricity as the transmission lines can transport and the storage facility can charge.

(ii2) if $C \leq w_t < C + \min\{1-x_{t-1}, K_2\}/\alpha$: $g_t^{H1} = w_t$. Since the generated amount exceeds the transmission capacity, then the minimum quantity that we have to store in the inventory is the excess $(g_t^{H1} - C)$, thus the optimal a_t for this case is at least $\alpha(g_t^{H1} - C) = \alpha(w_t - C)$. Observe in (A.5.6) that the feasible set for y_t is $[x_{t-1}+\alpha(w_t-C), x_{t-1}+\min\{\alpha\cdot w_t, K_2, 1-x_{t-1}\}]$. Relative to the left end point of this set, $\underline{X}_t^2$ can either lie on its right, or on its left. For each of these two cases, we can obtain the optimal action for (A.5.6) as follows (recall that the optimal action for (A.5.6) is to bring the inventory level as close as possible to $\underline{X}_t^2$): when $\underline{X}_t^2$ is on the right ($x_{t-1} + \alpha(w_t - C) \leq \underline{X}_t^2$; see region B2 in Figure A.5.1(b)), the optimal y_t for (A.5.6) for this case equals $\min\{\underline{X}_t^2, x_{t-1} + \min\{\alpha \cdot w_t, K_2, 1-x_{t-1}\}\}$, so the corresponding a_t equals $\min\{\underline{X}_t^2 - x_{t-1}, \min\{\alpha \cdot w_t, K_2, 1-x_{t-1}\}\} = \min\{\underline{X}_t^2 - x_{t-1}, \alpha \cdot w_t, K_2\}$. When $\underline{X}_t^2$ lies on the left ($\underline{X}_t^2 < x_{t-1} + \alpha(w_t - C)$; see region B3 in Figure A.5.1(b)), the optimal y_t for (A.5.6) for this case equals $x_{t-1} + \alpha(w_t - C)$, i.e., $a_t = \alpha(w_t - C)$.

(ii3) $w_t < C$: $g_t^{H1} = w_t$. The feasible set for y_t is $[x_{t-1}, x_{t-1} + \min\{\alpha \cdot w_t, K_2, 1-x_{t-1}\}]$. Similar to the argument in (ii2), $\underline{X}_t^2$ can fall either on the left or right of the end point of this

set. If $x_{t-1} \in [0, \underline{X}_t^2]$ (see region B4 in Figure A.5.1(b)), then the optimal action for this case is to generate and store as much as possible to reach $\underline{X}_t^2$, i.e., $a_t = \min\{\underline{X}_t^2 - x_{t-1}, \alpha \cdot w_t, K_2\}$; if $x_{t-1} \in (\underline{X}_t^2, \eta]$ (see region B5 in Figure A.5.1(b)), the optimal action is to keep the inventory unchanged by selling all generated electricity, i.e. $a_t = 0$.

Note that the optimal action in B1 and B3 for (A.5.6) are the same: generate as much possible, sell quantity C to the market, and then store the rest. Thus, we combine these two regions and express their unified formula for the optimal action: if (x_{t-1}, w_t) satisfies either of the following two conditions: 1) $w_t \geq C + \min\{1 - x_{t-1}, K_2\}/\alpha$; or 2) $C \leq w_t < C + \min\{1 - x_{t-1}, K_2\}/\alpha$ and $x_{t-1} > \underline{X}_t^2 - \alpha(w_t - C)^+$, then the optimal action a_t for this case equals $\alpha(g_t^{H1} - C)^+$.

Also note that the optimal action in B2 and B4 for (A.5.6) are the same: store generated electricity as much as possible to reach $\underline{X}_t^2$, and sell the rest of the generated electricity. Thus, we can combine these two regions and express their unified formula for the optimal action: if (x_{t-1}, w_t) satisfies the following condition $x_{t-1} + \alpha(w_t - C)^+ \leq \underline{X}_t^2$ and $w_t < C + \min\{1 - x_{t-1}, K_2\}/\alpha$, then the optimal action a_t for this case equals $\min\{\underline{X}_t^2 - x_{t-1}, \alpha \cdot w_t, K_2\}$.

A.5.3 The optimal action for (A.5.7): the problem of selling

For (A.5.7), we consider the following two cases:

(iii1) if $w_t > C$ (see region C1 in Figure A.5.1(c)): $g_t^{H1} = \min\{w_t, C + \min\{1 - x_{t-1}, K_2\}/\alpha\} > C$, the quantity generated exceeds transmission capacity, thus we cannot sell.

(iii2) if $w_t \leq C$: $g_t^{H1} = w_t$. Recall that the optimal action for (A.5.7) is to sell to bring the inventory level as close as possible to $\overline{X}_t$ in its corresponding feasible set, so if $x_{t-1} \in [0, \overline{X}_t)$ (see region C2 in Figure A.5.1(c)), the optimal action for problem (A.5.7) is to sell nothing from inventory. Otherwise, if $x_{t-1} \in [\overline{X}_t, \eta]$ (see region C3 in Figure A.5.1(c)), the optimal action for problem (A.5.7) is to sell down as much as possible to inventory level $\overline{X}_t$, i.e., $a_t = \max\{\overline{X}_t - x_{t-1}, (w_t - C)^-/\beta, K_1\}$.

A.5.4 The optimal action for (A.5.1)

We next find the optimal solution to the original problem (A.5.1) by combining the optimal solution for (A.5.5), (A.5.6), and (A.5.7) for each region mentioned in §A.5.1, §A.5.2, and §A.5.3.

A) If (x_{t-1}, w_t) satisfies either of the following two conditions: 1) $w_t \geq C + \min\{1 - x_{t-1}, K_2\}/\alpha$; or 2) $C \leq w_t < C + \min\{1 - x_{t-1}, K_2\}/\alpha$ and $x_{t-1} > \underline{X}_t^2 - \alpha(w_t - C)^+$ (as in region A in Figure 2.3), then the optimal solution to (A.5.6) is $a_t^{H1} = \alpha(g_t^{H1} - C)^+$, which is also the optimal solution to (A.5.1). This is because the optimal solutions to (A.5.5) and (A.5.7) are also feasible solutions to (A.5.6).

B) If (x_{t-1}, w_t) satisfies the first of the following two conditions, but not the second: 1) $x_{t-1} + \alpha(w_t - C)^+ \leq \underline{X}_t^2, w_t < C + \min\{1 - x_{t-1}, K_2\}/\alpha\}$, but not 2) $w_t \leq \min\{1 - x_{t-1}, K_2\}/\alpha$ and $x_{t-1} + w_t \cdot \alpha \leq \underline{X}_t^1$ (as in region B—excluding C—in Figure 2.3), then the optimal solution to (A.5.6) is $a_t^{H1} = \min\{\underline{X}_t^2 - x_{t-1}, \alpha \cdot w_t, K_2\}$, which is also the optimal solution to (A.5.1). This is because the optimal solutions to (A.5.5) and (A.5.7) are also feasible solutions to (A.5.6).

C) If $w_t \leq \min\{1 - x_{t-1}, K_2\}/\alpha$ and $x_{t-1} + w_t \cdot \alpha \leq \underline{X}_t^1$ (as in region C in Figure 2.3), then the optimal solution to (A.5.5) is $a_t^{H1} = \min\{\underline{X}_t^1 - x_{t-1}, \alpha(C\tau + w_t), K_2\}$, which is also the optimal solution to (A.5.1). This is because the optimal solutions to (A.5.6) and (A.5.7) are also feasible solutions to (A.5.5).

D) If $w_t \leq C$ and $\underline{X}_t^2 \leq x_{t-1} \leq \overline{X}_t$ (as in region D in Figure 2.3), then the optimal solution to (A.5.1) is $a_t^{H1} = 0$, because it is the optimal solution to (A.5.5), (A.5.6), and (A.5.7).

E) If $w_t \leq C$ and $x_{t-1} > \overline{X}_t$ (as in region E in Figure 2.3), then the optimal solution to (A.5.7) is $a_t^{H1} = \max\{\overline{X}_t - x_{t-1}, (w_t - C)^-/\beta, K_1\}$, which is also the optimal solution to (A.5.1). This is because the optimal solution to (A.5.5) and (A.5.6) is also a feasible solution to (A.5.7). □

A.6 Proof of Lemma 2.3

Proof: When $\mathbb{E}[p_t|w_t, \mathbf{p}_{t-1}] \geq 0$, the proof is the same as that for Lemma 2.2. When $\mathbb{E}[p_t|w_t, \mathbf{p}_{t-1}] < 0$, both the immediate payoff function $R(\cdot)$ and the continuation value function in the modified MDP (2.3) (without buying) reach their maxima when the ending inventory level reaches the highest level possible: the immediate payoff function reaches its maximum if the quantity to sell is zero, a decision leaving the highest ending inventory level possible; the continuation value function in modified MDP (2.3) (without buying) is non-decreasing in the ending inventory level because the value function in period t is non-decreasing in inventory level. As a result, the optimal action is to sell nothing and store as much as possible, that is

$a_t^{H2} = g_t^{H2} \cdot \alpha$. Adding these extra two constraints to the feasible set, it is easy to show that $g_t^{H2} = \min\{w_t, (1 - x_{t-1})/\alpha, K_2/\alpha\}$. Note that there may be other optimal solutions, but we focus on the optimal solution that gives the highest ending inventory level.

A.7 Proof of Proposition 2.3

Proof: We prove concavity by induction. For period $T+1$ and time T, $V_T^{H2}(S_T) = 0$, so the hypothesis holds. Suppose for all periods $k+1, \cdots, T$, the hypothesis holds. For period $t = k$ and time $k-1$, if $\mathbb{E}[p_k|w_k, \mathbf{p}_{k-1}] \geq 0$, the proof is a special case of that of Proposition 2.1. If $\mathbb{E}[p_k|w_k, \mathbf{p}_{k-1}] < 0$, according to Lemma 2.3, $g_k^{H2} = \min\{w_k, (1 - x_{k-1})/\alpha, K_2/\alpha\}$, and thus $a_k^{H2} = \alpha \cdot \min\{w_k, (1-x_{k-1})/\alpha, K_2/\alpha\}$. Substituting both a_k^{H2} and g_k^{H2} into (2.3), the objective function is concave in x_{k-1} given $w_{k-1}, \mathbf{p}_{k-1}$: the immediate payoff function is zero and thus concave in x_{k-1}; the continuation value function $\mathbb{E}\left[\delta V_k^{H2}\left((x_{k-1} + a_k^{H2})\eta, w_k, \mathbf{p}_k\right)|w_{k-1}, \mathbf{p}_{k-1}\right]$ is concave in x_{k-1} given any $\mathbf{p}_{k-1}$ and w_k because $V_k^{H2}\left((x_{k-1} + a_k^{H2})\eta, w_k, \mathbf{p}_k\right)$ is concave in $(x_{k-1} + a_k^{H2})\eta$ given any $\mathbf{p}_k$ and w_k according to the hypothesis, and expectation preserves concavity. Therefore, $V_{k-1}^{H2}(x_{k-1}, w_{k-1}, \mathbf{p}_{k-1})$ is concave on $\mathscr{X}$ given any $w_{k-1}, \mathbf{p}_{k-1}$. □

A.8 Procedures to identify jumps

Step 1. For the original price series $\{p_t : 1 \leq t \leq \bar{t}\}$ (where $\bar{t}$ is the last period in this price series), compute its mean $\hat{p}$ and standard deviation $\hat{\sigma''}$. Tag as outliers those prices outside of $\hat{p} \pm 3\hat{\sigma''}$, and remove them from the *original* series.

Step 2. Repeat Step 1 until no more "jumps" can be found.

Step 3. Construct the series $\{\Delta_t : 1 \leq t \leq \bar{t} - 1\}$ by defining Δ_t as $p_{t+1} - p_t$, i.e., the difference between two consecutive prices in the original series. Remove any Δ_t in which p_{t+1} is tagged as an outlier in the previous two steps.

Step 4. Repeat Step 1 and Step 2 for the series $\{\Delta_t : 1 \leq t \leq \bar{t} - 1\}$.

Appendix B

B.1 Proof of Proposition 3.1

Proof: We first prove finiteness. For each period t, the quantity bought cannot exceed $1/\alpha$, and the quantity sold cannot exceed η. Note that $\eta \leq 1 \leq 1/\alpha$, thus for each period t, given any $\mathbf{p}_{t-1}$, it holds that $|V_t(x_t, \mathbf{p}_{t-1})| \leq \sum_{k=t}^{T} |\mathbb{E}_k[P_k|\mathbf{p}_{k-1}]| \cdot (1/\alpha) < \infty$, where the last inequality follows from Assumption 3.1.

We next prove the convexity by induction. For $t = T+1$, $V_{T+1}(x_{T+1}, \mathbf{p}_T) = 0$, so the hypothesis holds. Suppose it holds for any $t = k+1, \cdots, T$, then $V_{k+1}(x_{k+1}, p_k)$ in (3.3) is finite and convex in x_{k+1} given any p_k.

For $t = k$, $\mathbb{E}_k[V_{k+1}(y_k, \mathbf{P}_k)]$ is also finite as $\mathbb{E}_k[|P_k|]$ is finite, and convex in y_k given any x_k and $\mathbf{p}_{k-1}$ as expectation preserves convexity. Therefore given $\mathbf{p}_{k-1}$, the objective function in (3.4) is finite and convex in y_k over $[0, x_k\eta]$, thus the optimal y_k for (3.4) can be either 0 or ηx_k; similarly, the optimal y_k for (3.5) can be either ηx_k or η. So an optimal solution to (3.3) must reside at one of the three candidate points: $0, \eta x_k, \eta$ (define the set of these three points as Y). Denote the objective function in (3.3) by $u_k(x_k, y_k, \mathbf{p}_{k-1})$, thus

$$V_k(x_k, \mathbf{p}_{k-1}) = \max_{y_k \in Y} \{u_k(x_k, y_k, \mathbf{p}_{k-1})\}. \tag{B.1.1}$$

We proceed to show that the functions $u_k(x_k, y_k, \mathbf{p}_{k-1})$ for each $y_k \in Y$ are finite and convex in x_k, for any given $\mathbf{p}_{k-1}$:

(i) $u_k(x_k, 0, \mathbf{p}_{k-1}) = \delta\mathbb{E}_k[V_{k+1}(0, \mathbf{P}_k)] + x_k\beta\mathbb{E}_k[P_k]$, which is finite and linear in x_k given any $\mathbf{p}_{k-1}$.

(ii) $u_k(x_k, x_k\eta, \mathbf{p}_{k-1}) = \delta\mathbb{E}_k[V_{k+1}(\eta x_k, \mathbf{P}_k)]$, which is convex in x_k because $\mathbb{E}_k[V_{k+1}(y_k, \mathbf{P}_k)]$

is convex in y_k for given $\mathbf{p}_{k-1}$ and $x_k = y_k/\eta$.

(iii) $u_k(x_k, \eta, \mathbf{p}_{k-1}) = (x_k - 1) \cdot \mathbb{E}_k[P_k]/\alpha + \delta \mathbb{E}_k[V_{k+1}(\eta, \mathbf{P}_k)]$, finite and linear in x_k given any $\mathbf{p}_{k-1}$.

So $V_k(x_k, \mathbf{p}_{k-1})$ is the maximum of three functions which are convex over a convex set $\mathscr{X}$ for each action in Y given any $\mathbf{p}_{k-1}$. Since Y is a nonempty finite set, by Proposition A-3 in Porteus (2002), $V_k(x_k, \mathbf{p}_{k-1})$ is also convex in x_k given any $\mathbf{p}_{k-1}$. Additionally, $V_k(x_k, \mathbf{p}_{k-1})$ is finite because all three functions are finite.

Therefore, for any $t \in \mathscr{T} \cup \{T+1\}$, $V_t(x_t, \mathbf{p}_{t-1})$ is finite and convex in x_t given any $\mathbf{p}_{t-1} \in \mathscr{P}$. □

B.2 Proof of Lemma 3.3

Proof: (i) As $\mathbb{E}_t[P_t] \to -\infty$, it follows that for all x_t, we have $y_t^{S*}(x_t) \to \eta x_t$ and $y_t^{B*}(x_t) \to \eta$, so $X_t^S = X_t^B = 0$: Intuitively, the optimal action for (3.4) is to sell nothing, and the optimal action to (3.5) is to buy as much as possible. As $\mathbb{E}_t[P_t] \to \infty$, it follows that for all x_t, we have $y_t^{S*}(x_t) \to 0$ and $y_t^{B*}(x_t) \to \eta x_t$, so $X_t^S = X_t^B = \eta$: buy nothing and sell as much as possible.

(ii) We know that $0 \le X_t^S, X_t^B \le \eta$; observe from (3.6) and (3.7) that $\overline{w}_t^S(0, \mathbf{p}_{t-1}) = \overline{w}_t^B(0, \mathbf{p}_{t-1})$. If $\mathbb{E}_t[P_t] < 0$, then $-y_t \beta \mathbb{E}_t[P_t]/\eta \le -y_t \mathbb{E}_t[P_t]/(\alpha\eta)$. Thus for all y_t, we have $\overline{w}_t^S(y_t, \mathbf{p}_{t-1}) \le \overline{w}_t^B(y_t, \mathbf{p}_{t-1})$, which includes $\overline{w}_t^S(\eta, \mathbf{p}_{t-1}) \le \overline{w}_t^B(\eta, \mathbf{p}_{t-1})$. Therefore, we can consider X_t^S and X_t^B in the following two cases:

- If $Y_t^B = 0$, the optimal y_t for $\overline{w}_t^B(y_t, \mathbf{p}_{t-1})$ is 0, thus $\overline{w}_t^B(0, \mathbf{p}_{t-1}) \ge \overline{w}_t^B(\eta, \mathbf{p}_{t-1})$. Therefore, $\overline{w}_t^S(0, \mathbf{p}_{t-1}) = \overline{w}_t^B(0, \mathbf{p}_{t-1}) \ge \overline{w}_t^B(\eta, \mathbf{p}_{t-1}) \ge \overline{w}_t^S(\eta, \mathbf{p}_{t-1})$, so $Y_t^S = 0$. According to (3.8), we have $X_t^S = \eta$, thus $X_t^B \le X_t^S$.
- If $Y_t^B = \eta$, then it follows from (3.9) that $X_t^B = 0$, which means that $X_t^B \le X_t^S$. □

B.3 Proof of Lemma 3.4

Proof: For any $x_t \in [0, X_t^S)$, we have $y_t^{S*}(x_t) = 0$. Substituting $y_t^{S*}(x_t) = 0$ into (3.4) gives $V_t^S(x_t, \mathbf{p}_{t-1}) = \delta \mathbb{E}_t[V_{t+1}(0, \mathbf{P}_t)] + x_t \beta \mathbb{E}_t[P_t]$, which is linear in x_t. Similarly, for any $x_t \in (X_t^B, \eta]$, we have $y_t^{B*}(x_t) = \eta$, and thus $V_t^B(x_t, \mathbf{p}_{t-1}) = -\eta \mathbb{E}_t[P_t]/(\alpha\eta) + \delta \mathbb{E}_t[V_{t+1}(\eta, \mathbf{P}_t)] + x_t \mathbb{E}_t[P_t]/\alpha$, which is also linear in x_t.

Since $0 \leq X_t^B < X_t^S \leq \eta$, then $0 \leq X_t^B < \eta$ and $0 < X_t^S \leq \eta$. Based on the value of X_t^S and X_t^B, we consider the following four cases (a)-(d):

i) $X_t^S = \eta$: This implies that $V_t^S(x_t, \mathbf{p}_{t-1})$ is linear in x_t over the entire $\mathscr{X}$.

(a) If $X_t^B = 0$: Since the plots of $V_t^S(x_t, \mathbf{p}_{t-1})$ and $V_t^B(x_t, \mathbf{p}_{t-1})$ as a function of x_t are both linear in x_t, they can cross at most once. If these two functions ever cross, the linear function with greater coefficient should end at a point no lower than that of the function with smaller coefficient. If $\mathbb{E}_t[P_t] < 0$, the coefficient of x_t in $V_t^S(x_t, \mathbf{p}_{t-1})$ is no less than that in $V_t^B(x_t, \mathbf{p}_{t-1})$ (because $\beta\mathbb{E}_t[P_t] \geq \mathbb{E}_t[P_t]/\alpha$), thus if both functions do cross, we have $V_t^S(\eta, \mathbf{p}_{t-1}) \geq V_t^B(\eta, \mathbf{p}_{t-1})$. Similarly, if $\mathbb{E}_t[P_t] \geq 0$ and both functions cross, then we have $V_t^S(\eta, \mathbf{p}_{t-1}) \leq V_t^B(\eta, \mathbf{p}_{t-1})$.

(b) If $0 < X_t^B < \eta$: In this scenario, $V_t^B(0, \mathbf{p}_{t-1}) = V_t^S(0, \mathbf{p}_{t-1})$, as the optimal action to (3.5) at x_t=0 is to do nothing and the optimal action to (3.4) at x_t=0 is to sell down to zero (effectively to do nothing). Since $V_t^B(x_t, \mathbf{p}_{t-1})$ is convex in x_t according to Proposition 3.1, and starts with the same point as $V_t^S(x_t, \mathbf{p}_{t-1})$, which is a straight line, $V_t^B(x_t, \mathbf{p}_{t-1})$ can cross $V_t^S(x_t, \mathbf{p}_{t-1})$ at most once (see Figure B.3.1 Case (b)) excluding $x_t = 0$. And when these functions do cross, we have $V_t^S(\eta, \mathbf{p}_{t-1}) \leq V_t^B(\eta, \mathbf{p}_{t-1})$: the convex function should end at a point no lower than the straight line.

ii) $0 < X_t^S < \eta$: In this case, $V_t^B(\eta, \mathbf{p}_{t-1}) > V_t^S(\eta, \mathbf{p}_{t-1})$, as the optimal solution to (3.4) at $x_t = \eta$ is to do nothing, which is a feasible , but not optimal, solution to (3.5), as $X_t^B < \eta$. Thus the plot of $V_t^B(x_t, \mathbf{p}_{t-1})$ as a function of x_t ends at a point no lower than the one for $V_t^S(x_t, \mathbf{p}_{t-1})$, which is convex in x_t (Proposition 3.1).

(c) $X_t^B = 0$: As in (a), $V_t^B(x_t, \mathbf{p}_{t-1})$ is a straight line over $\mathscr{X}$. It ends at a point no lower than the one for a convex curve $V_t^S(x_t, \mathbf{p}_{t-1})$ (see Figure B.3.1 Case (c)), so the plots of $V_t^S(x_t, \mathbf{p}_{t-1})$ and $V_t^B(x_t, \mathbf{p}_{t-1})$ as functions of x_t can cross at most once.

(d) $0 < X_t^B < \eta$: Similar to (b), the plots of $V_t^S(x_t, \mathbf{p}_{t-1})$ and $V_t^B(x_t, \mathbf{p}_{t-1})$ cross at most once over $[0, X_t^S)$; and similar to (c), at most once over $(X_t^B, \eta]$. We will consider the following three scenarios separately:

- If there is *one* crossing over $[X_t^B, X_t^S]$ (Figure B.3.1 Case (d1)), then there is no crossing over $[0, X_t^B]$ or $[X_t^S, \eta]$, as there is only one crossing over $[0, X_t^S)$ and $(X_t^B, \eta]$. Observe that the domain $\mathscr{X}$ is covered entirely by $[0, X_t^B]$, $[X_t^B, X_t^S]$ and $[X_t^S, \eta]$, thus the number of times that these plots cross over $\mathscr{X}$ is only once.
- If there is *no* crossing over $[X_t^B, X_t^S]$, then there is at most one crossing over $[0, X_t^B]$.

Figure B.3.1 Cases (b)-(d): case (a) is trivial and not shown.

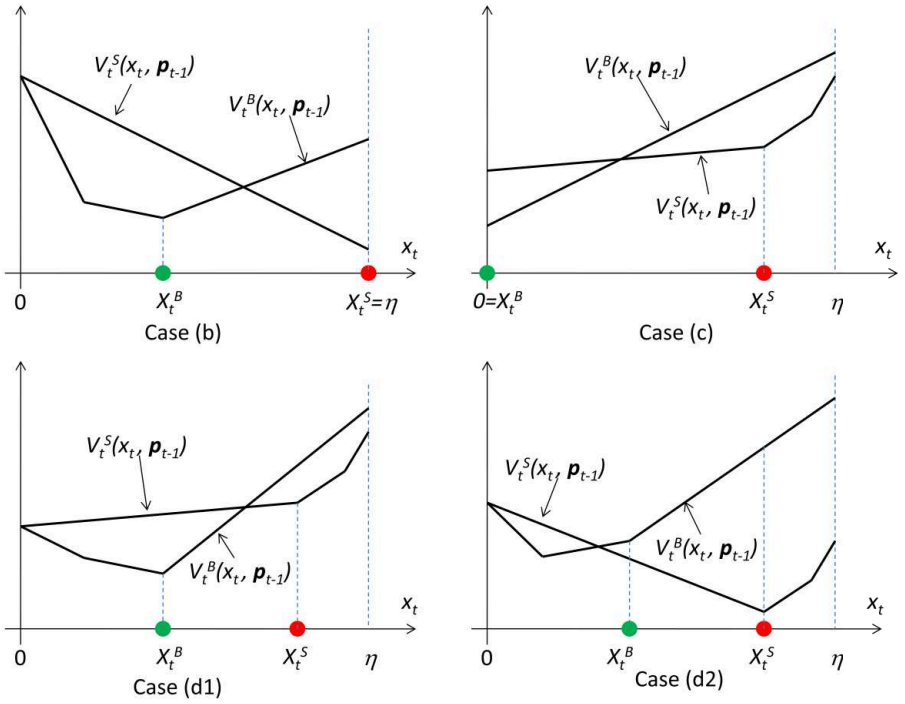

Suppose there is indeed one crossing. Then we apply the same argument in (b) to obtain $V_t^S(0, \mathbf{p}_{t-1}) = V_t^B(0, \mathbf{p}_{t-1})$. Since $V_t^B(x_t, \mathbf{p}_{t-1})$, a convex curve, starts with the same point as another convex curve $V_t^S(x_t, \mathbf{p}_{t-1})$, and ends at a point no lower than the one for $V_t^S(x_t, \mathbf{p}_{t-1})$ (Figure B.3.1 case (d2)), it follows that $V_t^B(X_t^B, \mathbf{p}_{t-1}) \geq V_t^S(X_t^B, \mathbf{p}_{t-1})$. Since $V_t^B(x_t, \mathbf{p}_{t-1})$ is a straight line over $(X_t^B, \eta]$, the plots of $V_t^S(x_t, \mathbf{p}_{t-1})$ and $V_t^B(x_t, \mathbf{p}_{t-1})$ cannot cross over $(X_t^B, \eta]$ as $V_t^B(\eta, \mathbf{p}_{t-1}) > V_t^S(\eta, \mathbf{p}_{t-1})$. Therefore, the plots of $V_t^S(x_t, \mathbf{p}_{t-1})$ and $V_t^B(x_t, \mathbf{p}_{t-1})$ as functions of x_t can cross at most once over $\mathscr{X}$ excluding $x_t = 0$.

- If there is *no* crossing over $[X_t^B, X_t^S]$, there is at most one crossing over $[X_t^S, \eta]$. Suppose there is indeed one crossing, we can likewise prove that the two plots cross at most once over $\mathscr{X}$, in the same manner as above.

Since for cases (c) and (d), it holds that $V_t^B(\eta, \mathbf{p}_{t-1}) \geq V_t^S(\eta, \mathbf{p}_{t-1})$, thus when $V_t^S(\cdot, \mathbf{p}_{t-1})$ and $V_t^B(\cdot, \mathbf{p}_{t-1})$ cross, it still follows that $V_t^B(\eta, \mathbf{p}_{t-1}) \geq V_t^S(\eta, \mathbf{p}_{t-1})$.

From cases (a)-(d), we can summarize that the plots of $V_t^S(x_t, \mathbf{p}_{t-1})$ and $V_t^B(x_t, \mathbf{p}_{t-1})$ as functions of x_t cross at most once over $\mathscr{X}$. When they do cross, if $X_t^S = \eta$, $X_t^B = 0$, and $\mathbb{E}_t[P_t] < 0$, then $V_t^S(\eta, \mathbf{p}_{t-1}) \geq V_t^B(\eta, \mathbf{p}_{t-1})$; otherwise, $V_t^S(\eta, \mathbf{p}_{t-1}) \leq V_t^B(\eta, \mathbf{p}_{t-1})$. □

B.4 Proof of Proposition 3.3

Proof: If $\mathbb{E}_t[P_t] < 0$, the immediate payoff function in (3.2) increases when α decreases: as α approaches zero, the immediate payoff function in (3.2) approaches infinity. Since the second expression is finite according to Proposition 3.1, then there always exists an $\bar{\alpha}$ such that if $\alpha \leq \bar{\alpha}$, the value function increases with decreasing α.

Appendix C

C.1 Deriving the discharging efficiency $\beta(a_t)$

We assume the charging/discharging efficiency is constant over the charging/discharging duration for any given charging/discharging rate. In other words, once the charging and discharging rate is fixed, the efficiency at any time during the charing/discharging process is the same.

We derive the discharging efficiency $\beta(a_t, M_t)$ for given a_t and energy capacity M_t in any single period with period length Δt. We later show that $\beta(a_t, M_t)$ does not depend on M_t. With this rate of discharging (a_t over Δt), the number of hours it takes to discharging the battery, denoted by $h(a_t)$, is $M_t/|a_t|$ (recall that a_t is negative for a discharging action). The corresponding discharge current is $I(a_t) = |a_t| \cdot \beta(a_t)/[\nu(a_t)\Delta t]$, where $\nu(a_t)$ is the discharging voltage for given action a_t, as mentioned in §4.3.2. It follows from Peukert's Law (Peukert 1897) that

$$I^k(a_t)h(a_t) = I_0^k \cdot (h_0 \cdot M_t), \tag{C.1.1}$$

where I_0 is the rated current; $h_0 \cdot M_t$ is the rated number of hours to discharge give energy capacity M_t; and $I_0 = M_t \cdot \beta_0/(\nu_0 \cdot h_0 \cdot M_t) = \beta_0/(\nu_0 \cdot h_0)$. Substituting $h(t) = M_t/|a_t|$, $I(a_t) = |a_t| \cdot \beta(a_t, M_t)/[\nu(a_t)\Delta t]$, and $I_0 = \beta_0/(\nu_0 \cdot h_0)$ into (C.1.1), we obtain

$$\left[\frac{|a_t| \cdot \beta(a_t, M_t)}{\nu(a_t)\Delta t}\right]^k \cdot \frac{M_t}{|a_t|} = \left(\frac{\beta_0}{\nu_0 h_0}\right)^k (h_0 \cdot M_t),$$

which can be simplified to

$$\beta(a_t, M_t) = \beta_0 \cdot h_0^{\frac{1}{k}-1} \cdot \Delta t \cdot |a_t|^{\frac{1}{k}-1} \frac{\nu(a_t)}{\nu_0}. \tag{C.1.2}$$

It can be easily seen from (C.1.2) that $\beta(a_t, M_t)$ does not depend on M_t; thus we write the discharging efficiency as $\beta(a_t)$. This is not surprising because we use Peukert's law to relate discharging efficiency with current, but the corresponding current for given action a_t stays the same irrespective of whether the energy capacity has degraded.

C.2 Deriving $C_{Rate}(a_t)$ and $A_h(a_t)$

For a given a_t, we have

$$C_{Rate}(a_t) = \frac{I(a_t)}{I_0} \cdot C_0 = \frac{I(a_t)}{I_0} \cdot \frac{1}{h_0} = \frac{|a_t| \cdot \beta(a_t)/[\nu(a_t) \cdot \Delta t]}{1 \cdot \beta_0/(\nu_0 \cdot h_0)} \cdot \frac{1}{h_0} = |a_t|^{\frac{1}{k}} h_0^{\frac{1}{k}-1},$$

where $C_0 = M_t/(h_0 \cdot M_t)$ is the rated C-rate for the battery. Similarly, we can derive $A_h(a_t)$ as follows:

$$\begin{aligned} A_h(a_t) = I(a_t) \cdot \Delta t = \frac{|a_t| \cdot \beta(a_t)}{\nu(a_t) \cdot \Delta t} \cdot \Delta t = \frac{|a_t| \cdot \beta(a_t)}{\nu(a_t)} = \frac{|a_t|}{\nu(a_t)} \cdot \beta_0 \cdot h_0^{\frac{1}{k}-1} \cdot \Delta t \cdot |a_t|^{\frac{1}{k}-1} \frac{\nu(a_t)}{\nu_0} \\ = \beta_0 \cdot h_0^{\frac{1}{k}-1} \cdot \Delta t \cdot |a_t|^{\frac{1}{k}} / \nu_0. \end{aligned}$$

References

A123System. 2012. Nanophosphate high power lithium ion cell ANR26650M1-B. Available at: www.a123systems.com/lithium-ion-cells-26650-cylindrical-cell.htm; last retrieved, 09/2012.

Anderson, D. 2009. An evaluation of current and future costs for lithium-ion batteries for use in electrified vehicle powertrains. Tech. rep., Duke University. Master Thesis.

AquionEnergy. 2011. Low cost, aqueous electrolyte sodium ion energy storage. Available at: www.aquionenergy.com/sites/default/files/user_files/news-press/2011_esa_aquion_whitacre.pdf.

Avci, B., K. Girotra, S. Netessine. 2012. Electric vehicles with a battery switching station: Adoption and environmental impact. INSEAD working paper, INSEAD, France.

Barlow, M. T. 2002. A diffusion model for electricity prices. *Mathematical Finance* **12** 287–298.

Bathurst, G.N., G. Strbac. 2003. Value of combining energy storage and wind in short-term energy and balancing markets. *Electric Power Systems Research* **67** 1–8.

Benth, F. E., J. Kallsen, T. Meyer-Brandis. 2007. A non-Gaussian Ornstein-Uhlenbeck process for electricity spot price modeling and derivatives pricing. *Applied Mathematical Finance* **14** 153–169.

Benth, F.E., S. Koekebakker. 2008. Stochastic modeling of financial electricity contracts. *Energy Economics* **30** 1116–1157.

Bindner, H., T. Cronin, P. Lundsager, J.F. Manwell, U. Abdulwahid, I. Baring-Gould. 2005. Lifetime modelling of lead acid batteries. Risø National Laboratory technical report.

Boogert, A., C. de Jong. 2008. Gas storage valuation using a Monte Carlo method. *Journal of Derivatives* **15** 81–98.

Boyabatli, O. 2011. Supply management in multi-product firms with fixed proportions technology. Working paper, Singapore Management University, Singapore.

Boyabatli, O., P. R. Kleindorfer, S. R. Koontz. 2011. Integrating long-term and short-term contracting in beef supply chains. *Management Science* **57** 1771–1787.

Brandstätt, C., K. Brunekreeft, K. Jahnke. 2011. How to deal ith negative power price spikes? Flexible voluntary curtailment agreements for large-scale integration of wind. *Energy Policy* **39** 3732–3740.

Brown, P.D., J.A. Peas Lopes, M.A. Matos. 2008. Optimization of pumped storage capacity in an isolated power system with large renewable penetration. *IEEE Transactions on Power Systems* **23** 523–531.

Buchman, I. 2012. How to recycle batteries. Available at: batteryuniversity.com/learn/article/recycling_batteries; last retrieved, 09/2012.

Bunn, D. 2004. *Modelling Prices in Competitive Electricity Markets*. John Wiley & Sons, England.

Cahn, A. S. 1948. The warehouse problem. *Bulletin of the American Mathematical Society* **54** 1073.

Cartea, A., M. G. Figueroa. 2005. Pricing in electricity markets: A mean reverting jump diffusion model with seasonality. *Applied Mathematical Finance* **12** 313–336.

Castronuovo, E.D., J.A.P. Lopes. 2004. On the optimization of the daily operation of a wind-hydro power plant. *IEEE Transactions on Power Systems* **19** 1599–1606.

Charnes, A., J. Dreze, M. Merton. 1966. Decision and horizon rules for stochastic planning problems: A linear example. *Econometrica* **34** 307–330.

Chen, Z., P. Forsyth. 2007. A semi-Lagrangian approach for natural gas storage valuation and optimal operation. *SIAM Journal on Scientific Computing* **30** 339–368.

Choi, S.S., H.S. Lim. 2002. Factors that affect cycle-life and possible degradation mechanisms of a Li-ion cell based on LiCoO2. *Journal of Power Sources* **111** 130–136.

Costa, L.M., F. Bourry, J. Juban, G. Kariniotakis. 2008. Management of energy storage coordinated with wind power under electricity market conditions. *Probabilistic Methods Applied to Power Systems, 2008. PMAPS '08. Proceedings of the 10th International Conference on*. 1–8.

CPUC. 2012. Decision adopting proposed framework for analyzing energy storage needs, California Public Utilities Commission. Available at: docs.cpuc.ca.gov/published/Final_decision/172201.htm; last retrieved, 09/2012.

De Jong, C. 2006. The nature of power spikes: A regime-switch approach. *Studies in Nonlinear Dynamics & Econometrics* **10**.

Deng, S. 2000. Pricing electricity derivatives under alternative stochastic spot price models. *Hawaii International Conference on System Sciences* **4** 4025.

Denholm, P., E. Ela, B. Kirby, M. Milligan. 2010. The role of energy storage with renewable electricity generation. Tech. rep., National Renewable Energy Laboratory. NREL/TP-6A2-47187.

Denholm, P., R. Sioshansi. 2009. The value of compressed air energy storage with wind in transmission-constrained electric power systems. *Energy Policy* **37** 3149–3158.

Devalkar, S.K., R. Anupindi, A. Sinha. 2011. Integrated optimization of procurement, processing and trade of commodities in a network environment. *Operations Research* **59** 1369–1381.

DOE. 2008. 20 percent wind energy by 2030: Increasing wind energy contribution to U.S. electricity supply. Available at www1.eere.energy.gov/windandhydro/pdfs/41869.pdf.

DSIRE. 2011. Federal incentives/policies for renewables and efficiency. Available at: dsireusa.org/incentives/incentive.cfm?Incentive_Code=US13F, last retrieved Oct, 2011.

DSIRE. 2012a. New york incentives/policies for renewables and efficiency. Availlabe at: www.dsireusa.org/incentives/incentive.cfm?Incentive_Code=NY03R; last retrieved, 10/2012.

DSIRE. 2012b. Renewable portfolio standard policies. Availlabe at: www.dsireusa.org/documents/summarymaps/RPS_map.pdf; last retrieved, 10/2012.

Duffie, D. 1992. *Dynamic Asset Pricing Theory*. Princeton University Press, Princeton, NJ.

DukeEnergy. 2011. Summary of transmission pricing. Available at www.oatioasis.com/PNM/PNMdocs/Pricing_Summary_2011_posted_09-06-11.pdf.

EIA. 2012. Annual energy review. Www.eia.gov/totalenergy/data/annual/pdf/aer.pdf.

EPRI. 2004. EPRI-DOE handbook supplement of energy storage for grid connected wind generation applications. Tech. rep., Electric Power Research Institute. Available at mydocs.epri.com/docs/public/000000000001008703.pdf.

ERCOT. 2008. Balancing energy services market clearing prices for energy annual reports archives. Available at www.ercot.com/mktinfo/prices/mcpea.

Escribano, A, J. I. Pena, P. Villaplana. 2002. Modeling electricity prices: international evidence. Working paper, Universidad Carlos III de Madrid, Madrid, Spain.

Eyer, J., G. Corey. 2010. Energy storage for the electricity grid: Benefits and market potential assessment guide. Tech. rep., Sandia National Laboratories. Available at prod.sandia.gov/techlib/access-control.cgi/2010/100815.pdf.

Fanone, E., M. Prokopczuk. 2010. Modeling positive and negative spikes: A non-Gaussian process for intra-day electricity prices. Working paper, Universitá degli Studi di Trieste, Trieste, Italy.

FERC. 1998. Causes of wholesale electric pricing abnormalities in the Midwest during June 1998. Tech. rep., Federal Energy Regulatory Commission, Washington, DC.

Fertig, E., J. Apt. 2011. Economics of compressed air energy storage to integrate wind power: A case study in ERCOT. *Energy Policy* **39** 2330–2342.

Figueiredo, F. C., P. C. Flynn, E. A. Cabral. 2006. The economics of energy storage in 14 deregulated power markets. *Energy Studies Review* **14** 131–152.

Fink, S., C. Mudd, K. Porter, B. Morgenstern. 2009. Wind energy curtailment case studies. Tech. rep., National Renewable Energy Laboratory. Subcontract Report NREL/SR-550-46716.

Gang, N., B. Haran, B. N. Popov. 2003. Capacity fade study of lithium-ion batteries cycled at high discharge rates. *Journal of Power Sources* **117** 160–169.

Garcia, R.C., J. Contreras, M. van Akkeren, J.B.C. Garcia. 2005. A GARCH forecasting model to predict day-ahead electricity prices. *IEEE Transactions on Power Systems* **20** 867–874.

Geman, H. 2005. *Commodities and Commodity Derivatives: Modeling and Pricing for Agriculturals, Metals and Energy*. John Wiley and Sons, Chichester, UK.

Geman, H., A. Roncoroni. 2006. Understanding the fine structure of electricity prices. *Journal of Business* **79** 1225–1261.

Genoese, F., M. Genoese, M. Wietschel. 2010. Occurrence of negative prices on the German spot market for electricity and their influence on balancing power markets. *Energy Market (EEM), 2010 7th International Conference on the European*. 1–6.

Gonzalez, A.M., A.M.S. Roque, J. Garcia-Gonzalez. 2005. Modeling and forecasting electricity prices with input/output hidden markov models. *IEEE Transactions on Power Systems* **20** 13–24.

Gonzalez, J.G., R. Moraga, L.M. Santos, A.M. Gonzalez. 2008. Stochastic joint optimization of wind generation and pumped-storage units in an electricity market. *IEEE Transaction on Power Systems* **23** 460–468.

Goonan, T. 2012. Lithium use in batteries. Available at: pubs.usgs.gov/circ/1371/pdf/circ1371_508.pdf; last retrieved, 09/2012.

Graves, F., T. Jenkin, D. Murphy. 1999. Opportunities for electricity storage in deregulating markets. *The Electricity Journal* **12** 46–56.

Heier, S. 2006. Grid integration of wind energy conversion systems .

Hittinger, E., J. Whitacre, J. Apt. 2010. Compensating for wind variability using co-located natural gas generation and energy storage. *Energy Systems* **1** 1–23.

Hittinger, E., J.F. Whitacre, J. Apt. 2012. What properties of grid energy storage are most valuable? *Journal of Power Sources* **206** 436–449.

Hoyland, K., S.W. Wallace. 2001. Generating scenario trees for multistage decision problems. *Management Science* **47** 295–307.

Huisman, R., R. Mahieu. 2003. Regime jumps in electricity prices. *Energy Economics* **25** 425–434.

Hull, J., A. White. 1993. One-factor interest-rate models and the valuation of interest-rate derivative securities. *Journal of Financial and Quantitative Analysis* **28** 235–254.

Jaillet, P., E. I. Ronn, S. Tompaidis. 2004. Valuation of commodity-based swing options. *Management Science* **50** 909–921.

Jenkins, D.P., J. Fletcher, D. Kane. 2008. Lifetime prediction and sizing of lead-acid batteries for microgeneration storage applications. *Renewable Power Generation, IET* **2** 191–200.

Kim, J. H., W.B. Powell. 2011. Optimal energy commitments with storage and intermittent supply. *Operations Research* **59** 1526–5463.

Kleindorfer, P. R., A. Neboian, A. Roset, S. Spinler. 2012. Fleet renewal with electric vehicles at La Poste. *Interfaces* **42** 465–477.

Klüppelberg, C., T. Meyer-Brandis, A. Schmidt. 2010. Electricity spot price modelling with a view towards extreme spike risk. *Quantitative Finance* **10** 963–974.

Knittel, K., M. Roberts. 2005. An empirical examination of restructured electricity prices. *Energy Economics* **27** 791–817.

Korpaas, M., A.T. Holen, R. Hildrum. 2003. Operation and sizing of energy storage for wind power plants in a market system. *International Journal of Electrical Power and Energy Systems* **25** 599–606.

Lai, G., F. Margot, N. Secomandi. 2010a. An approximate dynamic programming approach to benchmark practice-based heuristics for natural gas storage valuation. *Operations Research* **58** 564–582.

Lai, G., M. X. Wang, N. Secomandi, S. Kekre, A. Scheller-Wolf. 2010b. Valuation of the real option to store liquefied natural gas at a regasification terminal. *Operations Research* **59** 602–616.

Linden, D., T. B. Reddy. 2002. *Handbook of batteries*. McGraw-Hill.

Löhndorf, N., S. Minner. 2010. Optimal day-ahead trading and storage of renewable energies—an approximate dynamic programming approach. *Energy Systems* **1** 61–77.

Lu, X., M.B. McElroy, J. Kiviluoma. 2009. Global potential for wind-generated electricity. *Proceedings of the National Academy of Sciences* **106**(27) 10933–10938.

Lucia, J., E. Schwartz. 2002. Electricity prices and power derivatives: Evidence from the Nordic Power Exchange. *Review of Derivatives Research* **5** 5–50.

Mokrian, P., M. Stephen. 2006. A stochastic programming framework of the valuations of electricity storage. Working paper, Department of Management Science and Engineering, Stanford University.

Montgomery, D. 2008. *Introduction to Statistical Quality Control*. John Wiley & Sons, NY.

Nasakkala, E., J. Keppo. 2008. Hydropower with financial information. *Applied Mathematical Financ* **15** 1–27.

Nascimento, J., W. Powell. 2010. Dynamic programming models and algorithms for the mutual fund cash balance problem. *Management Science* **56** 801–815.

Nicolosi, M. 2010. Wind power integration and power system flexibility: An empirical analysis of extreme events in Germany under the new negative price regime. *Energy Policy* **38** 7257–7268.

NOAA. 2010. Integrated surface data, hourly, global. Available at: www.ncdc.noaa.gov/oa/mpp/.

NYISO. 2011. NYISO electricty pricing data. Available at www.nyiso.com.

Pattanariyankool, S., L.B. Lave. 2010. Optimizing transmission from distant wind farms. *Energy Policy* **38** 2806–2815.

Peterson, S. B., J. Apt, J.F. Whitacre. 2010a. Lithium-ion battery cell degradation resulting from realistic vehicle and vehicle-to-grid utilization. *Journal of Power Sources* **195** 2385–2392.

Peterson, S.B., J.F. Whitacre, J. Apt. 2010b. The economics of using plug-in hybrid electric vehicle battery packs for grid storage. *Journal of Power Sources* **195** 2377–2384.

Peukert, W. 1897. ber die Abhngigkeit der Kapazitt von der Entladestromstrke bei Bleiakkumulatoren. *Elektrotechnische Zeitschrift* **20**.

Porteus, E. L. 2002. *Foundations of Stochastic Inventory Theory*. Stanford University Press, Palo Alto, CA.

Powell, W.B. 2007. *Approximate Dynamic Programming: Solving the Curses of Dimensionality*. Wiley-Interscience, Hoboken, NJ.

Rambharat, R., A. Brockwell, D. Seppi. 2005. A threshold autoregressive model for wholesale electricity prices. *Journal of the Royal Statistical Society.* **54** 287–299.

Rempala, R. 1994. Optimal strategy in a trading problem with stochastic prices. *System Modelling and Optimization*, *Lecture Notes in Control and Information Sciences*, vol. 197.

REN21. 2010. Renewables 2010 global status report. Available at www.worldwatch.org/node/6481.

Schwartz, E., J. E. Smith. 2000. Short-term variations and long-term dynamics in commodity prices. *Management Science* **46** 893–911.

SECO. 2011. Wind energy transmission. Available at www.seco.cpa.state.tx.us/re_wind-transmission.htm.

Secomandi, N. 2010a. On the pricing of natural gas pipeline capacity. *Manufacturing & Service Operations Management* **12** 393–408.

Secomandi, N. 2010b. Optimal commodity trading with a capacitated storage asset. *Management Science* **56** 449–467.

Seifert, J., M. Uhrig-Homburg. 2007. Modelling jumps in electricity prices: theory and empirical evidence. *Review of Derivatives Research* **10** 59–85.

Seppi, D. J. 2002. Risk-neutral stochastic processes for commodity derivative pricing: An introduction and survey. *E. Ronn, ed. Real Options and Energy Management Using Options Methodology to Enhance Capital Budgeting Decisions*. Risk Publications, London, UK, 3–60.

Sewalt, M., C. de Jong. 2007. Negative prices in electricity markets. Available at www.erasmusenergy.com/articles/91/1/Negative-prices-in-electricity-markets/Page1.html.

Sioshansi, R., P. Denholm, Weiss J. Jenkin, T. 2009. Estimating the value of eletricity storage in PJM: Arbitrage and some welfare effects. *Enegy Economics* **31** 269–277.

Smith, J. E., K. F. McCardle. 1999. Options in the real world: Lessons learned in evaluating oil and gas investments. *Operations Research* **47** 1–15.

Szkuta, B.R., L.A. Sanabria, T.S. Dillon. 1999. Electricity price short-term forecasting using artificial neural networks. *IEEE Transactions on Power Systems* **14** 851–857.

Taheri, N., R. Entriken, Y. Ye. 2011. A dynamic algorithm for facilitated charging of plug-in electric vehicles. Working paper, Stanford University, Stanford, California.

Thompson, M., M. Davison, H. Rasmussen. 2009. Natural gas storage valuation and optimization: A real options application. *Naval Research Logistics* **56** 226–238.

Villaplana, P. 2005. Pricing power derivatives: A two-factor jump-diffusion approach. Working paper, InterMoney Energia, Madrid, Spain.

Walawalkar, R., J. Apt, R. Mancini. 2007. Economics of electric energy storage for energy arbitrage and regulation in new york. *Energy Policy* **35** 2558–2568.

Wang, J., P. Liu, J. Hicks-Garner, E. Sherman, S. Soukiazian, M. Verbrugge, H. Tataria, J. Musser,

P. Finamore. 2011. Cycle-life model for graphite-LiFePO4 cells. *Journal of Power Sources* **196** 3942–3948.

WhipserPower. 2012. Whisper power GEL-power datasheet. Available at: www.whisperpower.nl/images/datasheets/EngDatasheetGEL.pdf; last retrieved, 09/2012.

Whitacre, J.F., T. Wiley, S. Shanbhag, Y. Wenzhuo, A. Mohamed, S.E. Chun, E. Weber, D. Blackwood, E. Lynch-Bell, J. Gulakowski, C. Smith, D. Humphreys. 2012. An aqueous electrolyte, sodium ion functional, large format energy storage device for stationary applications. *Journal of Power Sources* **213** 255–264.

Wiser, R., M. Bolinger. 2010. 2009 wind technologies market report. Tech. rep., Lawrence Berkeley National Laboratory. Available at: eetd.lbl.gov/ea/ems/re-pubs.html.

Worley, O., D. Klabjan. 2011. Optimization of battery charging and purchasing at electric vehicle battery swap stations. *Vehicle Power and Propulsion Conference (VPPC), 2011 IEEE*. 1–4.

Wu, O., R. Kapuscinski. 2012. Curtailing intermittent generation in electrical systems. Working paper, Ross School of Business, University of Michigan, Ann Arbor, MI.

Wu, O., D. Wang, Z. Qin. 2012. Seasonal energy storage operations with limited flexibility: The price-adjusted rolling intrinsic policy. *Manufacturing and Service Operations Management* **14** 449–467.

Xi, X., R. Sioshansi, V. Marano. 2011. A stochastic dynamic programming model for co-optimization of distributed energy storage. Working paper, The Ohio State University.

Zipkin, P. 2000. *Foundations of Inventory Management*. McGraw-Hill, Boston.